ERDC/EL TR-02-15

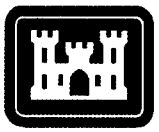

US Army Corps
of Engineers®
Engineer Research and
Development Center

Hydroacoustic Evaluation of a Prototype Surface Collector and In-Turbine Screens at Bonneville Dam Powerhouse 1 in 2000

Gene R. Ploskey, Carl R. Schilt, Michael E. Hanks,
John R. Skalski, William T. Nagy, Peter N. Johnson,
Deborah S. Patterson, Jina Kim, and Larry R. Lawrence

July 2002

Environmental Laboratory

ERDC/EL TR-02-15
July 2002

Hydroacoustic Evaluation of a Prototype Surface Collector and In-Turbine Screens at Bonneville Dam Powerhouse 1 in 2000

by Gene R. Ploskey

Pacific Northwest National Laboratory
902 Battelle Boulevard
Richland, WA 99352

Carl R. Schilt, Michael E. Hanks, Peter N. Johnson, Jina Kim

Mevatec Corporation
1525 Perimeter Parkway
Huntsville, AL 35806

William T. Nagy

U.S. Army Engineer District, Portland
P.O. Box 2946
Portland, OR 97208-2946

Deborah S. Patterson

DynTel Corporation
3530 Manor Drive, Suite 4
Vicksburg, MS 39180

Larry R. Lawrence

Environmental Laboratory
U.S. Army Engineer Research and Development Center
3909 Halls Ferry Road
Vicksburg, MS 39180-6199

John R. Skalski

Skalski Statistical Services
11804-8th Avenue NW
Seattle, WA 98177

Final report

Prepared for U.S. Army Engineer District, Portland
Portland, OR 97208-2946

Contents

List of Figures

List of Tables

Preface

This report was prepared by the Fisheries Engineering Team (FET), Water Quality and Contaminant Modeling Branch (WQCMB), Environmental Processes and Effects Division (EPED), Environmental Laboratory (EL), U.S. Army Engineer Research and Development Center (ERDC), with support from the Pacific Northwest National Laboratory, Richland, WA; Mevatec Corporation, Huntsville, AL; AScI, Inc., McLean, VA; Dyntel Corporation, Vicksburg, MS; the U.S. Army Engineer District, Portland (CENWP), and the University of Washington, Seattle. The research was conducted under the general supervision of Dr. Mark Dortch, Chief, WQCMB; Dr. Richard Price, Chief, EPED; and Dr. Edwin Theriot, Director, EL. Technical oversight was provided by Blaine Ebberts, CENWP.

Many people made valuable contributions to this study. Toni Schneider managed interagency transfers and allocation of funds. Riggers from the Bonneville Project helped with the installation, repair, and removal of hydroacoustic equipment. Schlosser Machine fabricated transducer mounts. A team of AScI, Inc., technicians (Nathan Barret, Kyle Bouchard, Charlie Escher, Theresa Kuhnhausen, Craig Smith, Keri Taylor, Kevin Thornburg, and Erin Wright) deployed hardware, maintained hydroacoustic systems, and aided with data processing. Alan Wirtz and Michael Macaulay of Precision Acoustic Systems in Seattle, WA, supplied and calibrated the hydroacoustic equipment.

At the time of publication of this report, the Commander and Executive Director of ERDC was COL John W. Morris III, EN, and the Director was Dr. James R. Houston.

This report should be cited as follows:

> Ploskey, G. R., Schilt, C. R., Hanks, M. E., Skalski, J. R., Nagy, W. T., Johnson, P. N., Patterson, D. S., Kim, Jina, and Lawrence, L. R. (2002). "Hydroacoustic evaluation of a prototype surface collector and in-turbine screens at Bonneville Dam Powerhouse 1 in 2000," ERDC/EL TR-02-15, U.S. Army Engineer Research and Development Center, Vicksburg, MS.

Conversion Factors, Non-SI to SI Units of Measurement

Non-SI units of measurement used in this report can be converted to SI units as follows:

Multiply	By	To Obtain
degrees (angle)	0.01745329	radians
feet	0.3048	meters
cubic feet / second (cfs)	0.0283	cubic meters / second

Summary

2000 Research

This study was one of many investigations of the U.S. Army Engineer District, Portland (CENWP) to resolve critical uncertainties in the implementation of surface-collector technologies at Bonneville Dam. The program is described in detail in a comprehensive Monitoring and Evaluation Plan developed by the District. Other research efforts in 2000 included a U.S. Geological Survey (USGS) radio-telemetry study of yearling chinook and steelhead passage. The Pacific Northwest National Laboratory (PNNL) evaluated approach behavior and fish distributions using multi-beam and split-beam sonar techniques in front of the Prototype Surface Collector (PSC) entrance at Unit 5. A joint effort by PNNL and USGS investigated behavior of tagged yearling chinook as they approached the project using three-dimensional sonic tag technologies.

Based upon results from 1998 and 1999, the PSC slot configuration for 2000 consisted of a constant 20-ft wide slot width for all six PSC units. The primary effects evaluated in 2000 were weekly changes throughout spring and summer in a variety of fish passage measures, including numbers passing into and under the PSC, efficiency, effectiveness, diel patterns, and horizontal and vertical patterns of distribution.

Goals

The primary goal of this study was to resolve critical uncertainties in the implementation of surface collection at Powerhouse 1 of Bonneville Dam by testing the efficiency of a 6-unit version of the PSC. The secondary goal was to resolve critical uncertainties in the implementation of extended-length submersible bar screens (ESBSs) at Powerhouse 1.

Objectives

a. Estimate the number of fish entering the PSC above the floor elevation at all six PSC slot entrances and the number passing through the PSC based upon in-turbine sampling at all 18 intakes of Units 1-6.

b. Estimate the number of juvenile salmon passing under the PSC and into the 18 intakes of Units 1-6.

c. Test for significant changes in the number of fish entering and passing under the PSC among weeks each season.

d. Estimate fish passage efficiency (FPE) for each of the PSC units and for the entire PSC by season and week, where efficiency is the number of fish passing into the PSC divided by the number entering and passing under the PSC.

e. Estimate fish-passage effectiveness for each of the PSC units and for the entire PSC by season and week, where effectiveness is the ratio of the proportion of fish collected to the proportion of water collected.

f. Compare the number of fish collected by the PSC and prototype FPE with hydroacoustic estimates of fish passage and guidance efficiency in Units 7, 9, and 10 with submerged traveling screens and Unit 8 with an ESBS.

g. Compare estimates of collected fish based upon in-turbine sampling with estimates based upon entrance sampling with split-beam transducers.

h. Describe diel patterns of fish passage, efficiency, and effectiveness for each season and the horizontal distribution of passage among the six PSC slots.

i. Continuously sample numbers of fish passing above and below an ESBS at Unit 8 with fixed-aspect hydroacoustics and estimate fish passage and fish guidance efficiency (FGE) for spring and summer.

j. Compare hydroacoustic and netting estimates of fish passage and FGE in spring and summer.

k. Estimate the vertical distributions of salmon immediately downstream of trash racks and upstream of the ESBS in spring and summer.

l. Compare the vertical distributions and smolt numbers and trajectories immediately downstream of trash racks with vertical distributions sampled upstream of trash racks and FGE estimated by netting.

m. Integrate all findings in an attempt to explain decreasing FGE in late spring and summer.

Materials and Methods

Equipment and calibrations

PSC Units 1-6 and Turbines 7-10 were sampled with nine hydroacoustic systems. Each system consisted of an echosounder, cables, transducers, an oscilloscope, and a computer system. The 420 kHz, circular, single- or split-beam Precision Acoustic Systems (PAS) transducers were controlled by PAS 103 echosounders and Hydroacoustic Assessments' HARP software running on Pentium-class computers.

Before deployment, all hydroacoustic equipment was transported to Seattle, WA, where PAS electronically checked the echosounders and transducers and calibrated the transducers using a standard transducer from the U.S. Navy. After calibration, receiver gains were calculated to equalize the output voltages among transducers for on-axis targets ranging in hydroacoustic size from -56 to -36 dB || $4\pi m^2$. Lengths of fish corresponding to that acoustic size range would be about 3.3 and 38.1 cm long, respectively, for fish insonified within 21° of dorsal aspect (Love 1977).

Sampling the PSC

Two different approaches were used to sample smolt passage at the PSC Units (1-6). The first was based upon in-turbine deployments and sampling with single-beam transducers, and the second relied on split-beam deployments and sampling in the forebay immediately upstream of PSC slot entrances.

In each of 18 intakes downstream of the PSC, one 7° single-beam transducer was mounted at the top of Trash Rack 1 and aimed straight down 11° off the plane of the trash racks. Fish passing through the beam above an elevation 0.5 m below the top of the PSC floor were classified as collected by the PSC, and those passing through the beam at greater ranges were classified as passing under the PSC. The down-looking beams had a blanking distance of 1 m and limited detectability in the first 3 m, and they also could not sample the shallow sluice opening (mean depth = 0.61 m) inside the center slot of every PSC unit. All single-beam transducers had a pulse repetition rate of 14 pings per second and sampled 20 1-minute intervals per hour.

Slot entrances at center intakes of PSC Units 1, 2, 4, 5, and 6 were sampled with 6° split-beam transducers. A team of PNNL researchers sampled the slot entrance at Unit 3. Opposing split-beam transducers were mounted at the top and bottom of a 45-ft tall frame. The lateral position of the transducer pair on the frame was chosen at random so that the pair would sample the north, center, or south third of the 20-ft slot entrance. The frames were deployed by crane and rested on horizontal crossbeams that tied the front of the A and C modules of the PSC together at several elevations. At each slot entrance, the deep transducer was aimed upward 6° upstream off the plane of slot entrance to count fish near the upper half of the slot. The shallow transducer was aimed downward 6° upstream of the plane of the entrance to count fish entering the bottom half of the slot. Fish passage estimates through every slot were based on counts of fish traces with trajectories into the PSC and average displacements ≥ 1 cm / ping.

Counts from the PSC slots were considered to be guided fish as an alternative to the guided counts derived from the upper portion of the single-beam transducers within each PSC turbine intake. Thus, there were two competing estimators of collection efficiency depending on the source of the estimate of guided numbers. Unguided numbers were always obtained from counts of fish passing through the deep portion of the in-turbine beams. Vertical distribution estimates in the forebay were obtained by counting fish within 1-m strata in the upper portion of the up-looking split-beam > 6.5 m from that transducer and in 1-m strata in the down-looking split-beam from 6.5 to 25 m from the down-looking

transducer. All split-beam transducers had a pulse repetition rate of 10 pings per second and sampled 20 1-minute intervals per hour.

Sampling Units 7, 9, and 10

At turbine Units 7, 9, and 10, hydroacoustic sampling was performed within one of three randomly selected intake slots per turbine. In Units 7 and 9, 7° single-beam transducers, one upward- and one downward-angled, were placed in the selected slots to monitor guided and unguided passage, respectively. An identical deployment was made in Unit 10, except that the transducers were 6° split-beams. Sampling was for 20 1-minute intervals per hour per transducer location, and the pulse repetition rate was 14 pings per second for each transducer.

Sampling Unit 8

At Unit 8, the center slot with an ESBS was sampled with an upward- and a downward-angled, 6° split-beam transducer to estimate guided and unguided numbers, respectively. Sampling was continuous, 60 minutes per hour, and the pulse repetition rate was 16.7 pings per second for each transducer.

Fish tracking

Since the hydroacoustic sampling effort on Bonneville Dam was so extensive and generated such a large volume of data (156 Gigabytes) in 2000, it was impossible to manually track enough data to make reliable FPEs with available staff. Therefore, autotracking software developed over the last 3 years by the Fisheries Field Unit and the ERDC/EL was relied on to process raw data into tracked fish observations. Although the autotracker was a very efficient analysis tool, its performance had to be continually verified with respect to trained human trackers. Five human trackers were employed. They received extensive training on raw hydroacoustic data from previous years before the 2000 tracking season began. The autotracker was evaluated by comparing its counts to those of several human trackers who all processed the same sample data sets. This approach was used because fish counts, even for the same files, can vary widely among human trackers.

To evaluate inter-tracker differences, five technicians tracked the same daily samples from every deployment for 3 days in spring and 2 in summer. Human and autotracked counts were compared for each transducer (channel) because there are important differences in passage characteristics, ranges of interest, trace slopes and lengths, and noise conditions for each deployment.

Dam operations and fish passage

Powerhouse 1 operations data were entered into a data set and integrated with fish passage data. Fish passage was set to zero when passage routes were closed. Turbine discharge at Powerhouse 1 was estimated from megawatts (MW) and head (the difference between the forebay and tailwater elevations)

using multiple regression equations. Data files were obtained that listed MW, head, and other operations data by 5-minute intervals throughout the season. Another equation was used to estimate discharge through the PSC slot from PSC unit discharge and forebay elevation.

Missing data

All hydroacoustic systems were operated continuously (> 23 hours / day), except for a 15-45 minute period every morning when data were copied from the acquisition computers, or when equipment failed and data from the affected routes were not collected. Short equipment failures lasting up to 45 minutes were not a problem because fish counts and associated variances could still be estimated from the remaining within-hour samples. Computer lock ups usually were fixed within an hour because staff were on duty from 0800 to 1700 hours and contractors monitored systems from 1700 to 0800 hours. Missing hourly data that resulted from equipment outages > 45 minutes were estimated by temporal linear interpolation for periods < 6 hours and by spatial interpolation or linear regression for periods > 6 hours.

Detectability modeling and spatial expansions

The count of every fish was expanded based upon the ratio of the opening width to beam diameter at the range of detection:

$$EXP\_NUM = \frac{OW}{[MID\_R \times TAN(\frac{EBA}{2}) \times 2]} \qquad \text{(S1)}$$

where OW is opening width in meters, MID_R is the mid-point range of a trace in meters, TAN is the tangent, and EBA is effective beam angle in degrees.

EBA depends upon the detectability of fish of different sizes in the acoustic beam and is a function of nominal beam width, ping rate, trace criteria, and fish size, aspect, trajectory, velocity, and range. Detectability for every transducer deployment was modeled to determine EBA as a function of range from a transducer. Target-strength estimates were obtained from the average backscattering cross section of fish detected by split-beam transducers and flow-velocity data by 1-m depth strata from a physical or computational fluid design (CFD) model. These data and other hydroacoustic-acquisition data were entered into a stochastic detectability model. Model output consisted of effective beam angle as a function of range from a transducer. Polynomials fitted to those data were substituted for EBA in the equation above to correct for differences in detectability by range among transducers and locations.

Statistical estimators and comparisons

Detailed statistical methods are presented under **Materials and Methods** in the body of the report.

Results and Discussion

Hydroacoustic detectability

In spring, most deployments had EBAs > 4° for the ranges that were sampled. Exceptions included deployments where sampling had to begin at relatively short ranges < 4 m (e.g., near transducers at Unit 8). In summer, curves for EBA by range had similar shapes to those modeled in spring, although angles at all ranges tended to be narrower because the average backscattering cross section of summer-run juvenile fish was lower than that of spring-run fish.

The motivating force behind efforts to improve detectability modeling is the desire to provide hydroacoustic estimates that are quantitative as well as reliable relative indices to fish passage. Ratio estimators like the fish guidance efficiency of the PSC, ESBSs, and submerged traveling screens (STSs) only require that hydroacoustic beams sampling guided and unguided fish have equal detectability so that ratios of counts, not necessarily the counts themselves, are accurate. Similarly, combining counts from different locations such as powerhouses and a spillway also requires equalization of detectability so that counts from different locations are comparable, although the counts themselves may not be accurate. Nevertheless, accurate counts estimated by proper expansion of detected fish have the potential to provide estimates with inherent quantitative value as well as providing acceptable relative estimates.

Quality control on automated fish tracking

The autotracker count for each transducer channel proved to be a reasonably good predictor of the mean human count, with the autotracker count explaining about 81 percent of the variation in the mean human tracker count in 222 samples. It was found that individuals tend to have characteristic biases that manifest themselves in different counts of fish from the same hydroacoustic data sets and that the mean of human counts from several people is what the autotracker should approximate. Consequently, it is recommended that the data be distributed in such a way that the bias-induced differences are averaged over time.

Powerhouse 1 fish passage efficiency

Powerhouse 1 FPE declined by only about 6 percent from spring to summer, and the PSC was a major contributor to Powerhouse 1 FPE in summer, when the FGE of in-turbine screens at Units 7-10 declined significantly. If the entire powerhouse had been as efficient as the PSC, Powerhouse 1 FPE in summer

would have been about 22 percent higher than a hypothetical FPE provided by 10 turbines with screen efficiencies comparable to that of the ESBS in Unit 8. A full powerhouse PSC would have been about 42 percent more efficient than 10 turbines with STS efficiencies.

Adjustment of PSC efficiency in spring and summer to compensate for not sampling center sluiceways in PSC units would increase mean PSC guidance efficiency from 72 to 87 percent and raise the PSC's contribution to Powerhouse 1 FPE significantly in summer. According to radio telemetry results, about 50 percent of tagged fish in the PSC passed through sluice gates in the center intakes of PSC units (Scott Evans, USGS and Gary Johnson, BioAnalysts, Personal Communication) where they could not be sampled with hydroacoustics. If that 50 percent estimate held for run-of-the-river (untagged) fish, in-turbine sampling with hydroacoustics would have underestimated PSC efficiency by 15 percent.

Conservative estimates of PSC performance indicate that it was a highly used route in 2000. The PSC guided an estimated 18 percent of the total Bonneville Dam passage (guided, unguided, and spilled fish combined) in spring and 21 percent of passage in summer.

Horizontal distribution

Horizontal passage patterns at Powerhouse 1 were consistent between seasons, but the relative discharge through the primary passage routes was generally a poor indicator of the relative proportion of fish passage among those same routes. More fish passed through PSC units than through three of the four units north of the pier between Units 6 and 7 despite a relatively even distribution of flow.

Vertical distribution

The vertical distribution of fish in front of the PSC at Powerhouse 1 was conducive for successful surface collection with a deep slot configuration. Sample volumes 1-3 m upstream of the PSC detected 92 to 99 percent of fish in spring and from 85 to 96 percent in summer above the elevation of the PSC floor.

Temporal trends in fish passage

The temporal correspondence of major peaks in the daily proportion of fish passage as determined by physical capture methods and by hydroacoustics was reassuring. Correspondence was found between hydroacoustic estimates of the peak daily proportion of fish passing Powerhouse 1 and the daily proportion of smolt sampled in the Powerhouse 2 JBS. Passage of juvenile salmon through the Powerhouse 1 JBS could not be used for comparison because sampling there was qualitative to determine descaling rates. Daily netting and hydroacoustic estimates of passage at Unit 8 were correlated.

There are two reasons why Powerhouse 1 FPE did not decline precipitously in summer as did the FGE of turbines with screens (Units 7-10). First, the efficiency of the PSC did not decline in summer and contributed more to

Powerhouse 1 FPE in late spring and summer than it did most of spring. Second, the proportion of fish relative to the proportion of water passed was relatively constant in spring and summer at the PSC.

Perhaps the most significant finding of this study was the summer decline in FGE of turbines with screens while the efficiency of the PSC remained high and stable. Even the efficiency of the ESBS in Unit 8 was as poor as that of STSs in other turbines in summer. Two factors may contribute to the continued success of the PSC in summer. First, the interception location of the PSC was upstream of the powerhouse; second, the PSC was open to the sky and passed relatively more fish during the day than at night. In contrast, most fish passage through Powerhouse 1 turbines occurred at night. The success of the PSC also probably has a lot to do with depth (45 ft), entrance velocities, and upstream hydraulics. The diel pattern of smolt passage through Powerhouse 2 turbines was more corpuscular in spring and summer than nocturnal.

Higher fish passage through the PSC than through Units 7, 8, and 10 in spring and summer and higher nighttime densities upstream and downstream of PSC slots suggest that fish may be accumulating at PSC units when daylight conditions permit them to search for preferred passage routes. The loss of visual position cues likely is responsible for increased fish passage into turbines just after sunset because smolt passage at turbine units is not a function of increased flow there. During the daytime when fish could orient by visual cues, densities upstream of PSC slots and the proportion guided by the PSC were both significantly higher than they were at night. The depth distribution of fish and associated exposure to ambient light conditions apparently have a pronounced effect on the diel distribution of fish passage through the PSC, through turbines and on the number of fish detected upstream of PSC entrances. Whereas fish are aware of changes in their body acceleration via their otolith, for relatively continuous motions and gradual accelerations, visual orientation is important. Fish rely on the migration of sensory cells and masking chemicals in the retina, a process that takes much longer than mammalian adaptation.

Fish guidance efficiencies

In-turbine sampling shows that the PSC performed as well as the ESBS did in spring and much better than the ESBS or STSs in summer. At Powerhouse 1, the PSC and the ESBS performed equally well in spring with estimated FGEs of 72 percent. The two southernmost units of the PSC performed best with FGEs of over 80 percent. In summer, the average FGE of STSs were 36 percent at Powerhouse 1 and 35 percent at Powerhouse 2, and the FGE of the ESBS in Unit 8 had dropped to 50 percent.

A large proportion of spring migrants and an even larger proportion of summer migrants passed south of the wing wall that extends upstream between Units 6 and 7, and most of those fish were guided by the PSC. Therefore, it is important to consider the horizontal distribution of passage in addition to the horizontal distribution of FGE among units.

Comparing FGE sampling methods for the PSC and Unit 8

No significant correlations were found between fish counts in turbine intakes downstream of the PSC with fish counts upstream of 20-ft wide PSC slots, unlike a significant correlation observed for the 5-ft wide slot in 1999. It is believed that differences in the probability of detected fish passing into the PSC may explain why significant correlations were found in 1999 but not in 2000. In 1999, the 5-ft wide slot had a linear flow velocity of 5 ft per second, which was 39 percent higher than the linear velocity at the 20-ft wide slots in 2000 (3.5 fps). If fish were not entrained or committed to passing into the 20-ft wide slot, they could be detected moving toward an entrance and still swim away after passing through the hydroacoustic beam.

Although counts from split-beam sampling upstream from the PSC were not correlated with the in-turbine single-beam counts, those data can still be used to evaluate the availability of fish for collection. However, expanded counts showed that there were twice as many fish above the level of the floor at night and an even higher proportion above the floor during the daytime hours.

The correlation of hydroacoustic and netting estimates of FGE at Unit 8 (r^2=0.65) was better than those for guided and unguided components of FGE. The assumption of equal detectability of guided and unguided smolts must have been reasonable most of the time given correlations between hydroacoustic and netting estimates of FGE with a correlation slope approaching 1. A near 1:1 ratio was found for numbers of guided fish netted in the gatewell to hydroacoustic counts above the ESBS and of numbers of unguided, fyke-netted fish to hydroacoustic counts below the ESBS. Paired t-tests indicated that mean estimates of FGE by the two sampling methods did not differ significantly in spring, and although differences were significant for both seasons combined, means only differed by 3 percent and probably were biologically meaningless. In summer, the mean hydroacoustic estimate was 6 percent higher than the mean netting estimate.

PSC guidance efficiency by different methods

Average collection efficiency of the PSC was 83 percent in spring and 84 percent summer after it was adjusted by radio telemetry estimates of the proportion of smolts in the PSC that passed into the center-slot sluiceways, and the adjusted estimates agree favorably with estimates by other methods. Radio telemetry data indicated that approximately half of all radio-tagged fish in the PSC passed through the sluiceway. Therefore, in-turbine hydroacoustic estimates of total passage at the PSC were at least 15 percent low in 2000. Radio-telemetry and acoustic-telemetry estimates of PSC efficiency for all species combined in spring 2000 were 83 percent and 92 percent, respectively, and those estimates agree with an 83-84 percent hydroacoustic estimate corrected for sluiceway passage. In 1998, hydroacoustic estimates of PSC collection efficiency for 20-ft slot openings in Units 3 and 5 were 87.8 percent in spring and 92 percent in summer. A radio-telemetry estimate for 1998 was 97.5 percent for the 20-ft slot treatment. In 1999, hydroacoustic estimates for a 20-ft slot entrance at Unit 5 were 84.4 percent in spring and 75.2 percent in summer. Radio-

telemetry studies in 1999 estimated the 20-ft slot efficiency at 65 percent, the lowest estimate by any method.

The PSC was more efficient than a prototype ESBS based upon 1998 and 2000 studies using hydroacoustics and radio telemetry at the PSC, and hydroacoustics and netting at Unit 8. The PSC was clearly more efficient than existing STSs. In spring 1998, PSC collection efficiency for a 20-ft wide slot was estimated as 87.8 percent by hydroacoustics and as 97.5 percent by radio telemetry compared with estimates of about 72 percent FGE for the ESBS according to NMFS netting and 80 percent FGE according to hydroacoustics. In summer 1998, the hydroacoustic estimate of PSC FGE was 92 percent compared with 40 and 50 percent for the ESBS by NMFS netting and hydroacoustic sampling. In spring 2000, PSC collection efficiency was estimated to be 83 percent by radio telemetry, 92 percent by acoustic telemetry, and 83-84 percent by hydroacoustic sampling with a radio-telemetry adjustment for sluiceway passage compared with an estimate of 69.6 percent and 72.0 percent for the ESBS by NMFS netting and hydroacoustics, respectively. In summer 2000, NMFS netting provided an average ESBS efficiency of 47.6 percent (which was close to the hydroacoustic estimate of 50 percent) compared with a PSC efficiency of 72 percent based upon unadjusted hydroacoustic sampling. Whether the summer hydroacoustic estimate of FGE at the PSC in 2000 is adjusted or not, it was from 22 to 37 percent more efficient than the ESBS in Unit 8.

1 Introduction

Background

Giorgi and Stevenson (1995) indicated that available biological information was inadequate to design and locate successful surface collector prototypes at Bonneville Dam. They found that information on the vertical and lateral distributions of smolts in forebay areas of both powerhouses and spillway was very limited. No mobile hydroacoustic sampling had been collected before 1996, and the proportion of smolts approaching Powerhouse 1, the spillway, and Powerhouse 2 had not been estimated.

Since Giorgi and Stevenson's literature review (1995), the Portland District acquired mobile hydroacoustic data on fish distributions in both forebays in 1996 (Ploskey et al. 1998) and 1997 (BioSonics, Incorporated 1998). For Powerhouse 1, these data indicated that higher average densities occurred upstream of Units 4-6 in spring and upstream of Units 4-6, 8, and 9 in summer. For Powerhouse 2, average fish densities were highest upstream of Units 11-13 adjacent to the south eddy and sluice chute in spring and in summer. Fish densities also were high upstream of Unit 18 in 1996 but not in 1997. Vertical distribution data showed that most fish were in the upper 15 m of the water. The low fish guidance efficiency (FGE) of many submerged traveling screens (STSs) at Bonneville Dam would not be expected from examining the vertical distribution of fish these years. If fish did not alter their vertical distributions from what was observed in forebay areas, data from 1996 and 1997 would suggest that FGE usually would exceed 80 percent.

Diel patterns of smolt passage are not uniform for either sluiceways (Uremovich et al. 1980; Willis and Uremovich 1981) or the juvenile bypass system (JBS; Hawkes et al. 1991; Wood et al. 1994). Diel passage through the JBS often has a bimodal distribution with a major peak occurring just after dark and a minor peak after sunrise. In contrast, passage through the sluiceway usually is higher during the day than at night (Willis and Uremovich 1981). However, patterns apparently are influenced by the operation of sluice gates, flow, unit outages, and fish species (Willis and Uremovich 1981). Diel patterns of passage have important implications for statistical designs to estimate fish passage efficiency (FPE) for all three structures at Bonneville. Diel patterns of turbine passage above and below screens were estimated in spring and summer 1996 for intakes of Units 3 and 5 at Powerhouse 1 (Ploskey et al. 1998).

Available data from gatewell sampling indicate that the horizontal distribution of smolt passage among intakes at Powerhouse 1 is not uniform but apparently is influenced by the number and location of operating units and sluice gates as well as the species of juvenile salmon passing (Willis and Uremovich 1981). Interactions among factors may account for a lack of consistency in measures of horizontal patterns. Uremovich et al. (1980) found concentrations of fish at Units 6, 7, and 10, Willis and Uremovich (1981) found variable patterns depending on operations, and Krcma et al. (1982) observed most passage at Units 4-6.

A prototype surface collector (PSC) was installed at Powerhouse 1 and tested in 1998. The 40.5-46.5-ft deep slots in 3b and 5b were configured to have 5- or 20-ft wide openings that were changed according to a blocked experimental design for evaluating effects of slot width on Prototype Fish Passage Efficiency (PFPE). Two measures of efficiency used were within about 10 percent of one another. Data from fixed-aspect hydroacoustic sampling in turbine intakes downstream of the PSC indicated that the PSC had efficiencies of about 90 percent in spring and summer. Estimates based upon counts at the PSC entrance averaged about 95 percent for the 20-ft slot and 85 percent for the 5-ft slot, but estimates potentially were biased by multiple counts of circulating fish in the PSC. Nevertheless, preliminary data indicated that the PSC showed great promise for meeting FPE goals at Powerhouse 1.

In-turbine data collected in spring 1999 with up- and down-looking transducers suggested that our assumption of a uniform vertical distribution of passage through the PSC in 1998 likely was incorrect. In 1998 the estimates of PSC passage were increased by 1.33 to compensate for the inability of single beam down-looking transducers to sample the upper 2.5 m of the intake. The spring 1999 data indicated that a correction factor of 1.14 would have been more appropriate, as only 12.4 percent of the fish detected passing through the collector in spring 1999 were within the upper 2.5 m. This is different than typical vertical distributions, which usually are skewed toward the ceiling of the intake. Readjusting the 1998 data would yield a PFPE of 77 percent in spring and summer instead of 90 percent. These results show the benefits of multiple-year evaluations and the risk in conducting single-year studies. Nevertheless, the readjusted efficiency (77 percent) is an improvement relative to efficiencies of traveling screens.

Researchers in the Columbia and Snake River Basin first began estimating the FGE of STSs in the 1970s (Gessel et al. 1991) and of extended-length submersible bar screens (ESBSs) after 1991 (Bardy et al. 1991). Fish guidance screens are located inside turbine intakes. There are three screens per turbine intake, one in each of the three intake segments that make up a single turbine unit. The screens are designed to divert juvenile salmon in the upper portion of a turbine intake into a gatewell slot where they can pass through openings in the gatewell that lead to a bypass channel around the dam. The screens function by modifying hydraulic characteristics of the flow they intercept and have an appreciable effect on flow through the turbine intake (Nestler and Davidson 1995). The underlying premise is that bypassed fish have a higher probability for

survival during dam passage than do fish passing through turbines. Physical capture and enumeration of fish traditionally have been used to determine the FGE of guidance screens. Large dip-nets (Swan et al. 1979) are used to capture juvenile salmon from the gatewell slot above an intake to estimate numbers of guided fish. Fyke netting is used to physically capture fish in the intake downstream of the fish guidance screen. Fish captured by fyke netting are used to estimate the number and species composition of "unguided" fish, i.e., those not diverted into the gatewell slot by the screen (Gessel et al. 1991). Efficiency is estimated as the count of guided fish divided by the sum of counts of guided and unguided fish.

Fixed-aspect hydroacoustics also has a history of use to estimate guided and unguided fish and the FGE of guidance screens. Examples include studies at Rocky Reach (Steig et al. 1988), Little Goose (Johnson et al. 1987), McNary (Johnson and Schadt 1986), and Bonneville dams (Thorne and Kuehl 1989; Magne et al. 1989; Stansell et al. 1990). Evaluations of bar-screen efficiencies have been conducted at Rock Island (Raemhild et al. 1988), Rocky Reach (Steig and Ransom 1989; Steig 1993; Steig and Nealson 1994; Steig et al. 1995; and Ransom et al. 1996), Lower Granite (Thorne and Kuehl 1990; Johnson et al. 1998), and Wanapum dams (Ransom et al. 1996). Hydroacoustic fish passage and guidance estimates have been correlated with estimates based on net catches (Thorne and Kuehl 1989; Magne et al. 1989; Ransom et al. 1996).

The STSs are ineffective at Bonneville Dam Powerhouse 1. FGE is less than 40 percent for yearling and less than 15 percent for sub-yearling chinook. ESBSs have proven superior to STSs at The Dalles, McNary, Little Goose, and Lower Granite dams. An ESBS was tested in Unit 8 at Bonneville in 1998 and will be tested again in 2000. Both hydroacoustics and the traditional National Marine Fisheries Service (NMFS) fyke net and gatewell dipping will be used. These two studies will complement each other; fyke nets are limited in hours of sampling but provide FGE estimates by species, whereas hydroacoustics can sample nearly full time but cannot supply species-specific estimates.

Site Description

Quantification of any enhancement by a surface collector is difficult because the Bonneville Project is among the most complex on the Columbia River (Figure 1). From the Oregon shore north toward Washington, the Bonneville Dam Project is composed of a navigation lock, 10-unit Powerhouse 1, Bradford Island, an 18-gate spillway, Cascades Island, and 8-unit Powerhouse 2. In 2000, Units 1-6 at Powerhouse 1 were modified to create a PSC.

Principal passage routes through the project include the spillway and two powerhouses, but within each powerhouse, passage can be through ice/trash sluiceways, turbines, or the JBS. Smolts enter the JBS after they encounter traveling screens in the upper part of turbine intakes and are diverted to gatewell slots and orifices opening to a bypass channel. In 2000, the PSC was not designed to be a fish bypass structure. Fish entering the PSC passed through the structure and into the turbine intake. The sole purpose was to allow testing of the

efficiency and effectiveness of the PSC for collecting juvenile salmon before building a full-scale collector.

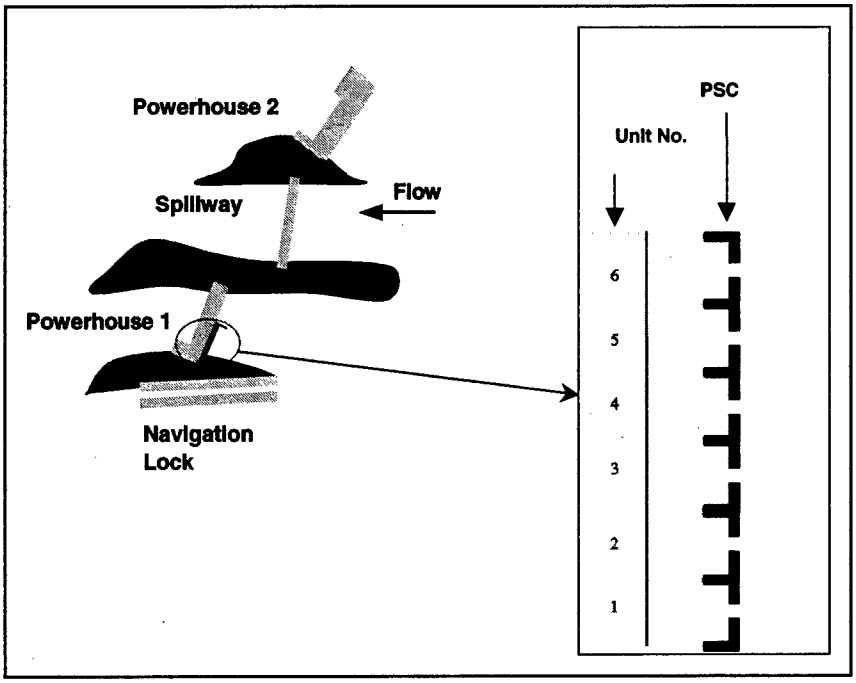

Figure 1. Plan-view of the Bonneville Project showing locations of Powerhouse 1 and the PSC at Units 1-6

2000 Research

This study was one of many investigations of the U.S. Army Engineer District, Portland (CENWP) to resolve critical uncertainties in the implementation of surface collector technologies at Bonneville Dam. The program is described in detail in a comprehensive Monitoring and Evaluation Plan developed by the District. Other research efforts in 2000 included a U.S. Geological Survey (USGS) radio-telemetry study of yearling chinook and steelhead passage. The Pacific Northwest National Laboratory (PNNL) evaluated approach behavior and fish distributions using multi-beam and split-beam sonar techniques in front of the PSC entrance at Unit 5. A joint effort by PNNL and USGS investigated behavior of tagged yearling chinook as they approached the project using three-dimensional sonic tag technologies.

Based upon results from 1998 and 1999, the PSC slot configuration for 2000 consisted of a constant 20-ft wide slot width for all six PSC units. The primary effects evaluated in 2000 were weekly changes throughout spring and summer in a variety of fish passage measures, including numbers passing into and under the PSC, efficiency, effectiveness, diel patterns, and horizontal and vertical patterns of distribution.

Goals

The primary goal of this study was to resolve critical uncertainties in the implementation of surface collection technologies at Powerhouse 1 of Bonneville Dam by testing the efficiency of a 6-unit version of the PSC. The secondary goal was to resolve critical uncertainties in the implementation of ESBSs at Powerhouse 1 at Bonneville Dam.

Objectives

a. Estimate the number of fish entering the PSC above the floor elevation at all six PSC slot entrances and the number passing through the PSC based upon in-turbine sampling at all 18 intakes of Units 1-6.

b. Estimate the number of juvenile salmon passing under the PSC and into the 18 intakes of Units 1-6.

c. Test for significant changes in the number of fish entering and passing under the PSC among weeks each season.

d. Estimate FPE for each of the PSC units and for the entire PSC by season and week, where efficiency is the number of fish passing into the PSC divided by the number entering and passing under the PSC.

e. Estimate FPE for each of the PSC units and for the entire PSC by season and week, where effectiveness is the ratio of the proportion of fish collected to the proportion of water collected.

f. Compare the number of fish collected by the PSC and prototype FPE with hydroacoustic estimates of fish passage and guidance efficiency in Units 7, 9, and 10 with STSs and Unit 8 with an ESBS.

g. Compare estimates of collected fish based upon in-turbine sampling with estimates based upon entrance sampling with split-beam transducers.

h. Describe diel patterns of fish passage, efficiency, and effectiveness for each season and the horizontal distribution of passage among the six PSC slots.

i. Continuously sample numbers of fish passing above and below an ESBS at Unit 8 with fixed-aspect hydroacoustics and estimate fish passage and FGE for spring and summer.

j. Compare hydroacoustic and netting estimates of fish passage and FGE in spring and summer.

k. Estimate the vertical distributions of salmon immediately downstream of trash racks and upstream of the ESBS in spring and summer.

l. Compare the vertical distributions and smolt numbers and trajectories immediately downstream of trash racks with vertical distributions sampled upstream of trash racks and FGE estimated by netting.

m. Integrate all findings in an attempt to explain decreasing FGE in late spring and summer.

2 Materials and Methods

Equipment

PSC Units 1-6 and Turbines 7-10 were sampled with nine hydroacoustic systems. Each system consisted of an echosounder, cables, transducers, an oscilloscope, and a computer system. Each echosounder and computer was plugged into an uninterruptible power supply. An echosounder generates electric signals of specific amplitude and at the required pulse repetition rates, and cables conduct those transmit signals from the echosounder to transducers and return data signals from transducers. Transducers convert voltages into sound on transmission and sound into voltages after echoes return to the transducer. The oscilloscopes were used to display echo voltages and calibration tones as a function of time, and the computer system controlled echosounder activity and recorded data to a hard disk. The 420 kHz, circular, single- or split-beam Precision Acoustic Systems (PAS) transducers were controlled by PAS 103 echosounders and Hydroacoustic Assessments' HARP software running on Pentium-class computers.

Calibrations

Before deployment, all hydroacoustic equipment was transported to Seattle, WA, where PAS electronically checked the echosounders and transducers and calibrated the transducers using a standard transducer from the U.S. Navy. After calibration, we calculated receiver gains to equalize the output voltages among transducers for on-axis targets ranging in hydroacoustic size from -56 to -36 dB ‖ $4\pi m^2$ (Tables 1 and 2). Lengths of fish corresponding to that acoustic size range would be about 1.3 and 15 inches, respectively, for fish insonified within 21° of dorsal aspect (Love 1977). Inputs for receiver-gain calculations included calibration data [i.e., echosounder source levels and 40 log (range) receiver sensitivities for specific transducers and cable lengths] and acquisition equipment data and settings (installed cable lengths, maximum output voltage, and on-axis target strengths of the smallest and largest fish of interest). In most instances, calibrated and installed cable lengths were identical. When those cable lengths proved to be different because insufficient cable was available for a deployment, an empirically derived correction factor was used to compensate for cable length effects on source levels, receiver sensitivity, and receiver gain settings.

Table 1

Calibration Data, Acquisition Settings, and Calculated Receiver Gains for Split-beam Transducers to Provide Equal Detectability for On-axis Targets Ranging From –36 to –56 dB in Acoustic Size at Powerhouse 1. Results for each transducer are presented for the x phase, y phase, and mean of x and y phases

Echo-sounder Number	Trans-ducer Number and Phase (if split beams)	Calibrated Cable Length (ft)	Source Level (dB)	Maximum Output Voltage (dB)	40 logR Receiver Sensitivity (dB)	Target Strength of largest on-axis target of interest (db)	Calculated Receiver gain (dB)	Installed Cable Length (ft)	Difference in Cable Length Between Calibrated Cable and Installed Cable (ft)	Receiver Gain Adjusted for Difference in Cable Length (dB)	Source Level Adjusted for Difference in Cable Length (dB)	Receiver Sensitivity Adjusted for Difference in Cable Length (dB)	Target Strength of Smallest On-axis Target (dB)	Voltage of Smallest On-axis Target (dB)	Voltage of Smallest On-axis Target at 20 dB per Volt (V)
3	8	650	214.82	70	-112.25	-36	3.43	650	0	3.43	214.82	-112.25	-56	50	2.5
3	7	650	215.25	70	-111.91	-36	2.66	650	0	2.66	215.25	-111.91	-56	50	2.5
3	6	650	214.61	70	-112.81	-36	4.20	674	-24	4.41	214.52	-112.93	-56	50	2.5
3	5	650	215.25	70	-111.83	-36	2.58	625	25	2.36	215.35	-111.70	-56	50	2.5
3	4	650	214.82	70	-112.35	-36	3.53	677	-27	3.77	214.72	-112.49	-56	50	2.5
3	3	650	214.21	70	-113.05	-36	4.84	650	0	4.84	214.21	-113.05	-56	50	2.5
3	2	650	214.88	70	-112.27	-36	3.39	646	4	3.35	214.90	-112.25	-56	50	2.5
3	1	650	214.97	70	-112.05	-36	3.08	647	3	3.05	214.98	-112.03	-56	50	2.5
3	66	650	213.95	70	-113.37	-36	5.42	650	0	5.42	213.95	-113.37	-56	50	2.5
3	67	650	215.40	70	-111.79	-36	2.39	650	0	2.39	215.40	-111.79	-56	50	2.5
4	19	650	215.55	70	-111.87	-36	2.32	650	0	2.32	215.55	-111.87	-56	50	2.5
4	18	650	215.43	70	-111.75	-36	2.32	650	0	2.32	215.43	-111.75	-56	50	2.5
4	17	650	215.49	70	-111.87	-36	2.38	625	25	2.16	215.59	-111.74	-56	50	2.5
4	13	650	214.74	70	-112.75	-36	4.01	648	2	3.99	214.75	-112.74	-56	50	2.5
4	12	650	214.76	70	-112.79	-36	4.03	617	33	3.73	214.89	-112.62	-56	50	2.5
4	11	650	214.97	70	-112.45	-36	3.48	621	29	3.22	215.08	-112.30	-56	50	2.5
4	10	650	215.01	70	-112.17	-36	3.16	681	-31	3.44	214.89	-112.33	-56	50	2.5
4	9	650	214.86	70	-112.33	-36	3.47	651	-1	3.48	214.86	-112.33	-56	50	2.5
4	65	650	214.68	70	-112.99	-36	4.31	650	0	4.31	214.68	-112.99	-56	50	2.5
5	29	650	215.53	70	-111.71	-36	2.18	650	0	2.18	215.53	-111.71	-56	50	2.5
5	28	650	214.76	70	-112.61	-36	3.85	650	0	3.85	214.76	-112.61	-56	50	2.5
5	27	650	215.34	70	-112.05	-36	2.71	649	1	2.70	215.34	-112.04	-56	50	2.5
5	26	650	215.54	70	-111.71	-36	2.17	650	0	2.17	215.54	-111.71	-56	50	2.5
5	23	650	215.49	70	-111.65	-36	2.16	648	2	2.14	215.50	-111.64	-56	50	2.5
5	22	650	215.38	70	-111.91	-36	2.53	648	2	2.51	215.39	-111.90	-56	50	2.5
5	21	650	215.34	70	-111.83	-36	2.49	653	-3	2.52	215.33	-111.84	-56	50	2.5
5	20	650	215.29	70	-111.95	-36	2.66	650	0	2.66	215.29	-111.95	-56	50	2.5
6	24	650	216.09	70	-111.09	-36	1.00	650	0	1.00	216.09	-111.09	-56	50	2.5
6	25	650	215.81	70	-111.39	-36	1.58	650	0	1.58	215.81	-111.39	-56	50	2.5
6	33	650	215.45	70	-112.13	-36	2.68	650	0	2.68	215.45	-112.13	-56	50	2.5
6	32	650	215.44	70	-112.25	-36	2.81	650	0	2.81	215.44	-112.25	-56	50	2.5
6	31	650	215.30	70	-112.37	-36	3.07	650	0	3.07	215.30	-112.37	-56	50	2.5
6	30	650	215.53	70	-111.69	-36	2.16	651	-1	2.17	215.53	-111.69	-56	50	2.5

Table 2

Calibration Data, Acquisition Settings, and Calculated Receiver Gains for Split-beam Transducers to Provide Equal Detectability for On-axis Targets Ranging From –36 to –56 dB in Acoustic Ssize at Powerhouse 1. Results for each transducer are presented for the x phase, y phase, and mean of x and y phases

Echo-sounder Number	Trans-ducer Number and Phase (if split beams)	Calibrated Cable Length (ft)	Source Level (dB)	Maximum Output Voltage (dB)	40 logR Receiver Sensitivity (dB)	Target Strength of largest on-axis target of interest (db)	Calculated Receiver gain (dB)	Installed Cable Length (ft)	Difference in Cable Length Between Calibrated Cable and Installed Cable (ft)	Receiver Gain Adjusted for Difference in Cable Length (dB)	Source Level Adjusted for Difference in Cable Length (dB)	Receiver Sensitivity Adjusted for Difference in Cable Length (dB)	Target Strengthof Smallest On-axis Target (dB)	Voltage of Smallest On-axis Target (dB)	Voltage of Smallest On-axis Target at 20 dB per Volt (V)
1	105 (x)	387	214.53	80	-106.01	-36	7.48	430	-43	7.86	214.36	-106.23	-56	60	3.0
1	105 (y)	387	214.52	80	-106.13	-36	7.61	430	-43	7.99	214.35	-106.35	-56	60	3.0
1-mean	105	387	214.53	80	-106.07	-36	7.54	430	-43	7.93	214.36	-106.29	-56	60	3.0
1	53 (x)	387	214.60	80	-105.91	-36	7.31	387	0	7.31	214.60	-105.91	-56	60	3.0
1	53 (y)	387	214.62	80	-105.93	-36	7.31	387	0	7.31	214.62	-105.93	-56	60	3.0
1-mean	53	387	214.61	80	-105.92	-36	7.31	387	0	7.31	214.61	-105.92	-56	60	3.0
21	400 (x)	627	214.89	80	-108.13	-36	9.24	627	0	9.24	214.89	-108.13	-56	60	3.0
21	400 (y)	627	214.90	80	-108.11	-36	9.21	627	0	9.21	214.90	-108.11	-56	60	3.0
21-mean	400	627	214.90	80	-108.12	-36	9.23	627	0	9.23	214.90	-108.12	-56	60	3.0
21	401 (x)	627	214.83	80	-108.11	-36	9.28	627	0	9.28	214.83	-108.11	-56	60	3.0
21	401 (y)	627	214.83	80	-108.17	-36	9.34	627	0	9.34	214.83	-108.17	-56	60	3.0
21-mean	401	627	214.83	80	-108.14	-36	9.31	627	0	9.31	214.83	-108.14	-56	60	3.0
21	402 (x)	627	214.91	80	-108.19	-36	9.28	627	0	9.28	214.91	-108.19	-56	60	3.0
21	402 (y)	627	214.93	80	-108.19	-36	9.26	627	0	9.26	214.93	-108.19	-56	60	3.0
21-mean	402	627	214.92	80	-108.19	-36	9.27	627	0	9.27	214.92	-108.19	-56	60	3.0
21	403 (x)	627	214.91	80	-108.07	-36	9.16	627	0	9.16	214.91	-108.07	-56	60	3.0
21	403 (y)	627	214.89	80	-108.11	-36	9.22	627	0	9.22	214.89	-108.11	-56	60	3.0
21-mean	403	627	214.90	80	-108.09	-36	9.19	627	0	9.19	214.90	-108.09	-56	60	3.0
22	404 (x)	627	214.83	80	-107.27	-36	8.44	627	0	8.44	214.83	-107.27	-56	60	3.0
22	404 (y)	627	214.82	80	-107.31	-36	8.49	627	0	8.49	214.82	-107.31	-56	60	3.0
22-mean	404	627	214.83	80	-107.29	-36	8.47	627	0	8.47	214.83	-107.29	-56	60	3.0
22	405 (x)	627	214.82	80	-107.47	-36	8.65	627	0	8.65	214.82	-107.47	-56	60	3.0
22	405 (y)	627	214.82	80	-107.47	-36	8.65	627	0	8.65	214.82	-107.47	-56	60	3.0
22-mean	405	627	214.82	80	-107.47	-36	8.65	627	0	8.65	214.82	-107.47	-56	60	3.0
23	408 (x)	627	214.68	80	-107.51	-36	8.83	627	0	8.83	214.68	-107.51	-56	60	3.0
23	408 (y)	627	214.70	80	-107.51	-36	8.81	627	0	8.81	214.70	-107.51	-56	60	3.0
23-mean	408	627	214.69	80	-107.51	-36	8.82	627	0	8.82	214.69	-107.51	-56	60	3.0
23	409 (x)	627	214.76	80	-107.57	-36	8.81	627	0	8.81	214.76	-107.57	-56	60	3.0
23	409 (y)	627	214.75	80	-107.57	-36	8.82	627	0	8.82	214.75	-107.57	-56	60	3.0
23-mean	409	627	214.76	80	-107.57	-36	8.82	627	0	8.82	214.76	-107.57	-56	60	3.0
23	407 (x)	627	214.79	80	-107.51	-36	8.72	627	0	8.72	214.79	-107.51	-56	60	3.0
23	407 (y)	627	214.75	80	-107.53	-36	8.78	627	0	8.78	214.75	-107.53	-56	60	3.0
23-mean	407	627	214.77	80	-107.52	-36	8.75	627	0	8.75	214.77	-107.52	-56	60	3.0
23	411 (x)	627	214.64	80	-107.69	-36	9.05	627	0	9.05	214.64	-107.69	-56	60	3.0
23	411 (y)	627	214.65	80	-107.69	-36	9.04	627	0	9.04	214.65	-107.69	-56	60	3.0
23-mean	411	627	214.65	80	-107.69	-36	9.05	627	0	9.05	214.65	-107.69	-56	60	3.0
24	413 (x)	387	215.02	80	-103.71	-36	4.69	387	0	4.69	215.02	-103.71	-56	60	3.0
24	413 (y)	387	215.01	80	-103.75	-36	4.74	387	0	4.74	215.01	-103.75	-56	60	3.0
24-mean	413	387	215.02	80	-103.73	-36	4.72	387	0	4.72	215.02	-103.73	-56	60	3.0
24	412 (x)	387	215.05	80	-103.85	-36	4.80	387	0	4.80	215.05	-103.85	-56	60	3.0
24	412 (y)	387	215.01	80	-103.85	-36	4.84	387	0	4.84	215.01	-103.85	-56	60	3.0
24-mean	412	387	215.03	80	-103.85	-36	4.82	387	0	4.82	215.03	-103.85	-56	60	3.0

Transducer Deployments and Sampling

This section describes hydroacoustic deployments and sampling schemes. Table 3 provides details of transducer locations and aiming angles for sampling to estimate guided and unguided numbers of fish passing the PSC, Units 7, 9, and 10 with STSs, and Unit 8 with an ESBS.

Table 3
Transducer Locations at Bonneville Powerhouse 1

System	Transducer	Unit	Intake	Lateral Position	Structure	Description of Location on Structure	E-coord[2]	N-coord	Elevation (ft)	Aim	Aiming Angle[1] (Deg.)
3	1	1	A	North	Rack 1[3]	4.4 ft below top; 8.8 ft S of N Side	1630251.1	722505.1	63.7	Down	0 (D)
3	2	1	B	Center	Rack 1	4.4 ft below top; 11 ft S of N Side	1630260.5	722527.6	63.7	Down	0 (D)
3	3	1	C	Center	Rack 1	4.4 ft below top; 11 ft S of N Side	1630271.0	722551.7	63.7	Down	0 (D)
3	4	2	A	South	Rack 1	4.4 ft below top; 13.2 ft S of N Side	1630281.7	722576.6	63.7	Down	0 (D)
3	5	2	B	North	Rack 1	4.4 ft below top; 8.8 ft S of N Side	1630293.9	722604.8	63.7	Down	0 (D)
3	6	2	C	South	Rack 1	4.4 ft below top; 13.2 ft S of N Side	1630302.6	722625.0	63.7	Down	0 (D)
4	9	3	A	North	Rack 1	4.4 ft below top; 8.8 ft S of N Side	1630316.0	722655.9	63.7	Down	0 (D)
4	10	3	B	Center	Rack 1	4.4 ft below top; 11 ft S of N Side	1630325.6	722678.1	63.7	Down	0 (D)
4	11	3	C	North	Rack 1	4.4 ft below top; 8.8 ft S of N Side	1630336.9	722704.4	63.7	Down	0 (D)
4	12	4	A	South	Rack 1	4.4 ft below top; 13.2 ft S of N Side	1630346.8	722727.1	63.7	Down	0 (D)
4	13	4	B	South	Rack 1	4.4 ft below top; 13.2 ft S of N Side	1630357.2	722751.4	63.7	Down	0 (D)
4	17	4	C	Center	Rack 1	4.4 ft below top; 11 ft S of N Side	1630368.6	722777.6	63.7	Down	0 (D)
5	20	5	A	Center	Rack 1	4.4 ft below top; 11 ft S of N Side	1630380.1	722804.3	63.7	Down	0 (D)
5	21	5	B	North	Rack 1	4.4 ft below top; 8.8 ft S of N Side	1630391.5	722830.6	63.7	Down	0 (D)
5	22	5	C	Center	Rack 1	4.4 ft below top; 11 ft S of N Side	1630401.1	722852.9	63.7	Down	0 (D)
5	23	6	A	North	Rack 1	4.4 ft below top; 8.8 ft S of N Side	1630413.6	755881.7	63.7	Down	0 (D)
5	26	6	B	South	Rack 1	4.4 ft below top; 13.2 ft S of N Side	1630422.3	722901.9	63.7	Down	0 (D)
5	27	6	C	South	Rack 1	4.4 ft below top; 13.2 ft S of N Side	1630432.7	722926.1	63.7	Down	0 (D)
6	31	7	A	Center	Rack 5	4.4 ft below top; 8.8 ft S of N Side	1630454.0	722951.1	11.0	Up	29 (D)
6	32	7	A	Center	Rack 1	4.4 ft below top; 11 ft S of N Side	1630446.2	722957.0	63.7	Down	20 (D)
24	413	8	B	Center	Rack 5	4.4 ft below top; 11 ft S of N Side	1630497.1	723050.6	14.0	Up	28 (D)
24	412	8	B	Center	ESBS[4]	2 ft below pivot; 13 ft S of N Side	1630482.6	723057.7	39.18	Down	15 (U)
6	30	9	C	South	Rack 1	4.4 ft below top; 13.2 ft S of N Side	1630530.2	723151.9	63.7	Down	9 (D)
6	33	9	C	North	Rack 5	4.4 ft below top; 8.8 ft S of N Side	1630540.9	723152.0	11.0	Up	29 (D)
1	53	10	B	North	Rack 1	4.4 ft below top; 8.8 ft S of N Side	1630554.0	723207.1	63.7	Down	9 (D)
1	105	10	B	North	Rack 5	4.4 ft below top; 8.8 ft S of N Side	1630563.0	723203.2	11.0	Up	29 (D)
21	400	1	B	North	Frame[5]	3.5 ft S of N side of slot at EL 25'	1630301.5	722517.8	25.0	Up	5 (D)
21	401	1	B	North	Frame	3.5 ft S of N side of slot at EL 70'	1630293.1	722521.4	70.0	Down	17 (U)
21	402	2	B	Center	Frame	10 ft S of N side of slot at EL 25'	1630331.4	722587.1	25.0	Up	5 (D)
21	403	2	B	Center	Frame	10 ft S of N side of slot at EL 70'	1630323.1	722590.8	70.0	Down	17 (U)
22	405	4	B	Center	Frame	10 ft S of N side of slot at EL 25'	1630396.5	722737.7	25.0	Up	5 (D)
22	404	4	B	Center	Frame	10 ft S of N side of slot at EL 70'	1630388.1	722741.3	70.0	Down	17 (U)
23	408	5	B	North	Frame	3.5 ft S of N side of slot at EL 25'	1630431.6	722818.9	25.0	Up	5 (D)
23	409	5	B	North	Frame	3.5 ft S of N side of slot at EL 70'	1630423.2	722822.6	70.0	Down	17 (U)
23	411	6	B	South	Frame	3.5 ft S of N side of slot at EL 25'	1630464.1	722894.2	25.0	Up	5 (D)
23	410	6	B	South	Frame	3.5 ft S of N side of slot at EL 70'	1630455.7	722897.8	70.0	Down	17 (U)

[1] Measured in degees off of a vertical plane separating upstream and downstream directions
[2] Geographical Coordinates were provided by Marshall Richmond's team at PNNL
[3] Rack refers to a trash rack, six of which are stacked in an intake slot. Racks are number from top to bottom.
[4] ESBS refers to an extended length submerged bar screen
[5] All transducers on frames at PSC slot entrances were located 3.5 ft upstream of the slot entrance

Sampling the prototype surface collector

Two different approaches were used to sample smolt passage at the PSC units (1-6). The first was based upon in-turbine deployments and sampling with single-beam transducers and the second relied on split-beam deployments and sampling in the forebay immediately upstream of the PSC slot entrances.

In each of 18 intakes downstream of the PSC, one 7° single-beam transducer was mounted at the top of Trash Rack 1 and aimed straight down 11° off the plane of the trash racks (Figure 2). Fish passing through the beam above an elevation 0.5 m below the top of the PSC floor were classified as collected by the PSC. This elevation was selected based upon flow trajectories from the PSC floor to the center of the hydroacoustic beam. The down-looking beams had a blanking distance of 1 m and limited detectability in the first 3 m, and they also could not sample the shallow sluice opening (mean depth = 2 ft) inside the center slot of every PSC unit. The loss of the uppermost 1 m may not have been significant as it accounted for only 1.4 percent of the fish passage sampled with six up-looking beams in 1999. The in-turbine transducer in the B slot of every PSC unit also could not count fish passing into the sluice opening at those locations. Sluice gates at A and C intakes were always closed. Fish passing through a down-looking beam > 0.5 m below the PSC floor were classified as passing under the PSC.

The upper portion of a down-looking beam covered 10 percent of the cross sectional area in the upper one-half of the intake, and the lower portion covered 30.5 percent of the bottom half of the intake. Therefore, the down-looking in-turbine transducers provided excellent spatial coverage for estimating numbers of fish passing under the PSC and adequate coverage for fish passing through the PSC. All in-turbine transducers had a pulse-repetition rate of 14 pings per second and sampled 20 1-minute periods per hour.

Slot entrances at center intakes of PSC Units 1, 2, 4, 5, and 6 were sampled with 6° split-beam transducers (Figure 2). A team of PNNL researchers sampled the slot entrance at Unit 3. Opposing split-beam transducers were mounted at the top and bottom of a 45-ft tall frame (Figure 3). The lateral position of the transducer pair on the frame was chosen at random so that the pair would sample the north, center, or south third of the 20-ft slot entrance. The frames were deployed by crane and rested on horizontal crossbeams that tied the front of the A and C modules of the PSC together at several elevations. At each slot entrance, the deep transducer was aimed upward 6° upstream of the plane of the slot entrance to count fish near the upper half of the slot. The shallow transducer was aimed downward 6° upstream of the plane of the entrance to count fish entering the bottom half of the slot. Fish passage estimates through every slot were based on counts of fish traces with trajectories into the PSC and average displacements ≥ 1 cm/ping.

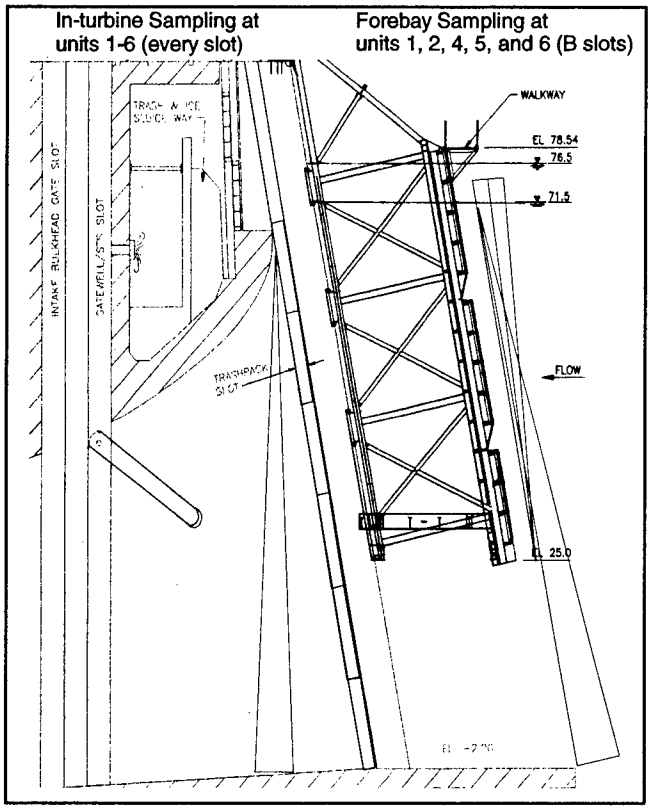

Figure 2. Cross sectional view through the center slot of a Powerhouse 1 turbine unit with the PSC attached to the upstream side. Numbers of guided fish were estimated from counts in the upper portion of the in-turbine hydroacoustic beams or the beams upstream of the PSC slot. The deep portion of the in-turbine beam was used to estimate unguided fish numbers

Fish passage estimates through every slot were based on counts of traces with trajectories into the PSC, each with an average displacement ≥ 1 cm/ping. Counts from the PSC slots were considered as guided fish as an alternative to the guided counts derived from the upper portion of the single-beam transducers within each turbine slot. Thus, there were two competing estimators of collection efficiency depending on the source of the estimate of guided numbers. Unguided numbers were always obtained from counts of fish passing through the deep portion of the in-turbine beams. Vertical distribution estimates in the forebay were obtained by counting fish within 1-m strata in the upper portion of the up-looking split-beam > 6.5 m from that transducer and in 1-m strata in the down-looking split-beam from 6.5 to 25 m from the down-looking transducer. All split-beam transducers had a pulse repetition rate of 10 pings per second and sampled 20 1-minute intervals per hour.

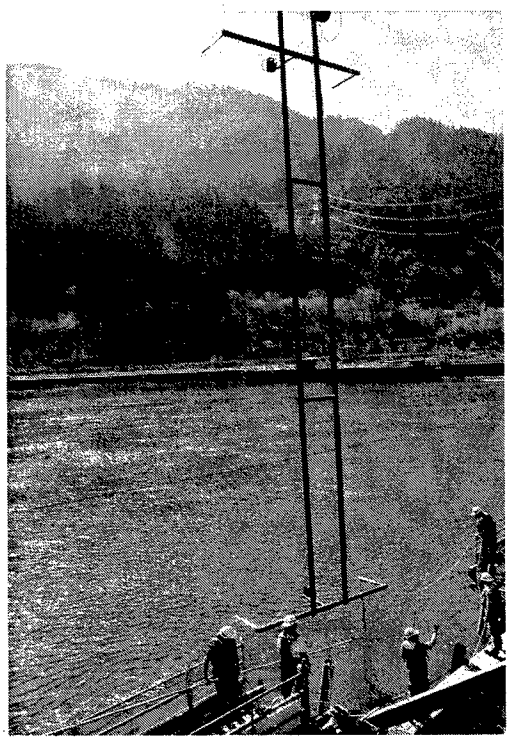

Figure 3. Installation of a 45-ft tall frame with split-beam transducers at the top and bottom center

Sampling Units 7, 9, and 10

At turbine Units 7, 9, and 10, hydroacoustic sampling was performed within one of three randomly selected intake slots per turbine. In Units 7 and 9, 7° single-beam transducers, one upward- and one downward-angled, were placed in the selected slots to monitor guided and unguided passage, respectively (Figure 4). An identical deployment was made in Unit 10, except that the transducers were 6° split-beams. Sampling was for 20 1-minute intervals per hour per transducer location, and the pulse repetition rate was 14 pings per second for each transducer.

Sampling Unit 8

At Unit 8, the center slot with an ESBS was sampled with an upward- and a downward-angled 6° split-beam transducer to estimate guided and unguided numbers, respectively (Figure 5). Sampling was continuous, 60 minutes per hour, and the pulse repetition rate was 16.7 pings per second for each transducer.

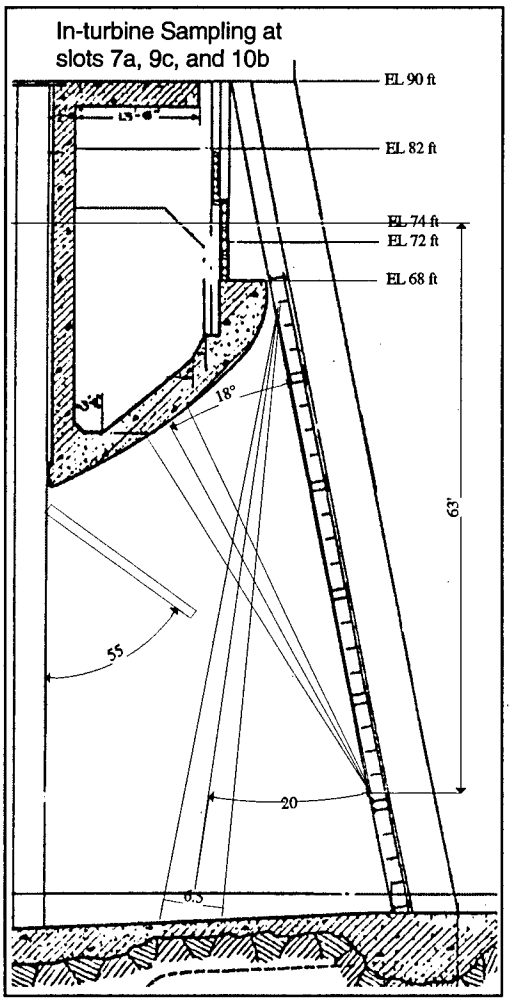

Figure 4. Cross sectional view through an intake like those sampled at Units 7, 9, and 10 showing up- and down-looking hydroacoustic beams

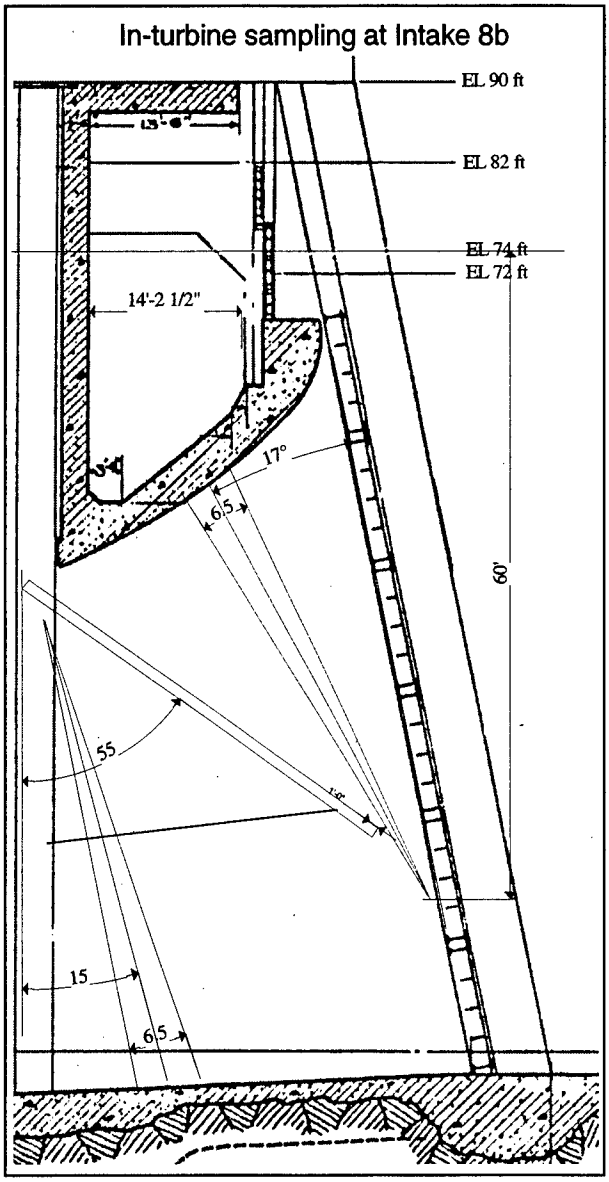

Figure 5. Cross sectional view through Intake 8b where up- and down-looking split-beam transducers were used to sample guided and unguided fish, respectively

Fish Tracking and Filtering Criteria

The criteria used to accept or reject echo patterns as fish and to filter tracked fish observations are presented in Table 4. The greatest differences in criteria were between sampling in forebay areas and inside turbine units because fish were not entrained through beams in the forebay, except at the spillway. Criteria for sampling turbine units were consistent, or if different (e.g., range), were corrected for in spatial expansions by results of detectability modeling, which is described below.

Table 4
List of Fish-tracking Criteria for Deployments at Three Major Passage Routes

Tracking Criterion Or Filters	PSC Units 16	PSC Slot Entrances	Unit 8	Units 7, 9, and 10
Minimum number of echoes with core of at least 4 echoes in 5 pings	4	4	4	4
Maximum ping gap for track segments	6	6	6	6
Maximum number of echoes	30	60	30	30
Structural filters = drop traces where the first ping and last ping are within a designated range bin	Yes	Yes	Yes	Yes
Trace slope	-9 to 9 cm / ping	-9 to 9 cm / ping	-9 to 9 cm / ping	-9 to 9 cm / ping and not between -0.05 and 0.05 cm / ping on down-looking beams
Fit to line or parabola (Route Mean Square Error in cm) was used to accept only very linear or parabolic traces in noisy areas on some beams	Line < 3 cm Parabola < 2 cm	Line < 3 cm Parabola < 2 cm	Line < 3 cm Parabola < 2 cm	Line < 3 cm Parabola < 2 cm
Range	3.0-10.5 m = guided 10.5-max = unguided	Upper slot = 6.75 m to the surface Lower slot = 6.75 to 13.5 m Under slot = 13.5 m to bottom	Up-looking = 3 m to ceiling Down-looking = 3 m to bottom	Up-looking = 9.0 m to ceiling Down-looking = 8.5 m to bottom
Direction of movement	None	Yes[1]	None	None
Target or echo strength				
-Spring and summer until 15 June -Summer from 15 June to 30 June -Summer after 30 June	-56 to -37 dB -56 to -45 dB -56 to -47 dB	-56 to -37 dB -56 to -45 dB -56 to -47 dB	-56 to -37 dB -56 to -45 dB -56 to -47 dB	-56 to -37 dB -56 to -45 dB -56 to -47 dB

[1] Azimuth angle from first to last echo had to indicate movement between the edges of the 20-ft PSC slot entrances.

Since the hydroacoustic sampling effort on Bonneville Dam was so extensive and generated such a large volume of data (156 Gigabytes) in 2000, it was impossible to manually track enough data to make reliable FPEs with available staff. Therefore, autotracking software developed over the last 3 years by the Fisheries Field Unit and the ERDC/EL was relied on to process raw data into tracked fish observations. The autotracker software tells the computer to:

a. Identify and remove echoes at constant range from structure.

b. Find seed echoes for candidate tracks.

(1) Go to every echo.

(2) Define a 10 ping by 1-m window centered on that echo.

(3) Place all echoes in the window into 5° angle bins.

(4) If any bin count >3, flag the center echo as a candidate seed.

c. Re-examine candidate seed echoes.

(1) Go to every seed-echo window.

(2) Count echoes in all possible line features (Hough transform).

(3) If no echoes in the window are part of a strong line feature, then drop the seed echo (to distinguish between dense noise and dense fish tracks).

d. Initiate alpha-beta tracking.

(1) Track forward starting at each seed echo.

(2) Track backward from the same seed echo after forward tracking has ended.

(3) Check the track segment against criteria (core criterion; minimum and maximum gap).

(4) Link track segments that are collinear into single tracks (i.e., project track segments forward and backward and link them if the ping gap < 6 pings and forward and backward projections of two track segments line up).

e. Write out track statistics (echo statistics optional).

For several months in spring, samples of the autotracker's performance for every deployment were reviewed on a fish-by-fish basis to evaluate and fine-tune the autotracker. Researchers released the autotracker to process data for a given

deployment only after they determined that it was tracking the same echo patterns that the researchers would track most of the time.

Although the autotracker was a very efficient analysis tool, its performance had to be continually verified with respect to trained human trackers. Five human trackers were employed who received extensive training on raw hydroacoustic data from years before the 2000 tracking season began. The autotracker was evaluated by comparing its counts to those of several human trackers who all processed the same sample data sets. This approach was used because fish counts, even for the same files, can vary widely among human trackers. The hope was that the autotracker would perform like an average human tracker rather than like trackers at either extreme.

To evaluate inter-tracker differences, all of the human trackers tracked the same daily samples of all systems from five different days. These calibration days were scattered throughout the passage seasons, three in spring and two in summer. For each calibration day, a single file was selected for each of the hydroacoustic systems from every hour between downloads on consecutive days. The calibration days were: Early spring, Julian Day 111-112; Middle spring, Julian Day 152-153; Late spring, Julian Day 157-158; Early summer, Julian Day 176-177, and Late summer, Julian Day 196-197. This arrangement was devised to evaluate inter-tracker differences under seasonally changing conditions of fish passage and fish size. The autotracker also processed the same samples from all five days.

Human and autotracked counts were compared for each transducer (channel) because there are important differences in passage characteristics, ranges of interest, trace slopes and lengths, and noise conditions for each deployment site and aiming angle. Although tracker performance has previously been compared by system (including several transducer channels), it was decided that comparing transducer channels gives the best measure of human and autotracker differences because it removes site and aiming differences within comparisons and evaluates performance across the greatest possible range of different tracking conditions among comparisons. For each of the 5 days, the fish count output files from each human or automatic tracker were post-processed identically. Post-processing included deployment-specific "filtering" for trace length, trace slope, echo or target strength, structure and other regular noise, and other characteristics described in Table 4. The resulting filtered fish counts for each tracker (human or automatic) on each day were then summed separately for each transducer channel.

Counts were compared from five human trackers on all of the calibration days by examining scatter plots and correlation statistics and by plotting the cumulative count of the human trackers and the autotracker over time to examine cumulative temporal deviations.

Dam Operations and Fish Passage

Project operations data, including discharge by spill bay and turbine unit were entered into a data set and integrated with fish passage data. Fish passage was set

to zero when passage routes were closed. Turbine discharge at Powerhouse 1 was estimated from megawatts (MW) and head (the difference between the forebay and tailwater elevations) using multiple regression equations.

Standard units with STSs (Units 1-3, 5, and 7-10):

$$CFS = 9396.49 + 257.43(MW) - 173.27(HEAD) \quad (1)$$

Minimum gap runner with STSs (Units 4 and 6):

$$CFS = 9396.49 + 257.43(MW) - 173.27(HEAD) \quad (2)$$

The data used to derive these equations were obtained from the Hydroelectric Design Center (HDC), Portland District, through Karen Kuhn, a District Hydraulic Engineer. The first equation had an r^2 of 0.96 (N = 3,269) and the second had an r^2 of 0.94 (N = 2,502). Data files listing MW, head, and other operations data by 5-minute intervals were obtained throughout the season from Rod Hurst at HDC. Daryl Hunt, Chief of Operations at Bonneville Dam, and his staff of operators supplied data that were missing from the electronic files. Another equation was used to estimate discharge through the PSC slot from PSC unit discharge and forebay elevation, as follows:

$$CFS = -4405.429 + 45.667(EL) + 0.445(Q) \quad (3)$$

where CFS is discharge through the PSC slot in feet per second, EL is forebay elevation in feet, and Q is the discharge in feet per second through the same turbine. This equation has an r^2 of 0.75; N=12.

Missing Data

A special effort was made to make certain that missing samples were accounted for in the spring and summer data sets. First, a data set was created consisting of all possible sample locations and times each season and an expanded fish variable was set to missing in every observation. Second, the missing data set was merged with the acquired data set and counts of expanded fish, if present in the acquired data, overwrote missing counts. When a sample had not been collected, there was nothing in the acquired data set to overwrite the missing value for expanded fish; therefore, that observation was appropriately designated as missing and could be addressed as follows before data analysis:

All hydroacoustic systems were operated continuously (> 23 hours/day), except for a 15-45 minute period every morning when data were copied from the acquisition computer onto removable Jaz disks, or when equipment failed and data from the affected routes were not collected. Short equipment failures lasting up to 45 minutes were not a problem because fish counts and associated variances could still be estimated from the remaining within-hour samples. Computer lock ups usually were fixed within an hour because staff were on duty from 0800 to 1700 hours and contractors monitored systems from 1700 to 0800 hours.

Transducer cables that failed once at Unit 6, twice at Unit 8, and once at Unit 10 were repaired within a few days as soon as project support or divers became available.

Missing hourly data that resulted from equipment outages > 45 minutes were estimated by temporal linear interpolation for periods < 6 hours and by spatial interpolation or linear regression for periods > 6 hours. When an up-looking beam for counting fish guided by an STS failed, the upper portion of the paired down-looking beam was sometimes used to estimate those numbers. Occasionally the ratio of guided to unguided numbers at adjacent turbines with similar screens was useful for interpolating estimates of guided or unguided numbers. Regression equations relating hourly variances with hourly sums were sometimes used to estimate missing variance estimates.

Detectability Modeling and Spatial Expansions

The count of every fish was expanded based upon the ratio of the opening width to beam diameter at the range of detection:

$$EXP\_NUM = \frac{OW}{\left[MID\_R \times TAN\left(\frac{EBA}{2}\right) \times 2\right]} \quad (4)$$

where OW is opening width in meters, MID_R is the mid-point range of a trace in meters, TAN is the tangent, and EBA is effective beam angle in degrees.

EBA depends upon the detectability of fish of different sizes in the acoustic beam and is a function of nominal beam width, ping rate, trace criteria, and fish size, aspect, trajectory, velocity, and range. Detectability was modeled for every transducer deployment to determine EBA as a function of range from a transducer. Target-strength estimates were obtained from the average backscattering cross section of fish detected by split-beam transducers and flow-velocity data by 1-m depth strata from a physical or computational fluid design (CFD) model. These data and other hydroacoustic-acquisition data (e.g., beam tilt, ping rate, target-strength threshold, number of echoes, and maximum ping gaps) were entered into a stochastic detectability model. Model inputs are described in Tables 5 and 6. Model output consisted of effective beam angle as a function of range from a transducer. Polynomials fitted to those data were substituted for EBA in Equation 4 to correct for differences in detectability by range among transducers and locations.

Statistical Estimators and Comparisons

The sections following Tables 5 and 6 describe how the estimate of smolt passage was calculated at the various locations at Powerhouse 1.

Table 5
Values of Variable Inputs to the Detectability Model for Every Type of Deployment Used In 2000

Deployment	-3dB Beam Angle	Transducer		Pings / Second	Mean TB	Standard Deviation	TS Threshold	Min Echoes	Ping Gap	Maximum Range
		Tilt from Vertical	Blanking Range							
Spring										
Units 1-6; forebay; down-looking	6	0	1	13	-45.0	4.2	-56	4	4	17
Units 1-6; forebay; up-looking	6	4	1	13	-45.0	4.2	-56	4	4	17
Units 1-6; in-turbine; down-looking	6	0	1	14	-45.0	4.2	-56	4	4	21
Units 7 and 9; in-turbine; down-looking	6	20	1	14	-45.0	4.2	-56	4	4	22
Units 7 and 9; in-turbine; up-looking	6	29	1	14	-45.7	4.0	-56	4	4	15
Unit 10; in-turbine; down-looking	6	20	1	14	-45.0	4.2	-56	4	4	22
Unit 10; in-turbine; up-looking	6	29	1	14	-45.7	4.0	-56	4	4	15
Unit 8; in-turbine; down-looking	6	-15	1	17	-45.0	4.0	-56	4	4	15
Unit 8; in-turbine; up-looking	6	28	1	17	-44.9	4.3	-56	4	4	15
Summer										
Units 1-6; forebay; down-looking	6	0	1	13	-49.3	1.9	-56	4	4	17
Units 1-6; forebay; up-looking	6	4	1	13	-49.3	1.9	-56	4	4	17
Units 1-6; in-turbine; down-looking	6	0	1	14	-49.3	1.9	-56	4	4	21
Units 7 and 9; in-turbine; down-looking	6	20	1	14	-49.3	1.9	-56	4	4	22
Units 7 and 9; in-turbine; up-looking	6	29	1	14	-50.1	2.3	-56	4	4	15
Unit 10; in-turbine; down-looking	6	20	1	14	-49.3	1.9	-56	4	4	22
Unit 10; in-turbine; up-looking	6	29	1	14	-50.1	2.3	-56	4	4	15
Unit 8; in-turbine; down-looking	6	-15	1	17	-47.8	1.9	-56	4	4	15
Unit 8; in-turbine; up-looking	6	28	1	17	-49.0	2.2	-56	4	4	15

Note: Target strength is abbreviated TS and Min refers to the minimum.

Table 6
Polynomials Used to Describe Transducer beam Shapes and Flow Trajectory and Speed as a Function of Range from Transducers

Deployment	Input Variable	Polynomial or Constants
Units 1-6; forebay; down-looking	Beam Shape	$B = .011170692053X^4 - .158786483125X^3 + .231914384635X^2 - .5101118323179999X + .056466461582$
	Trajectory	plunge = 11
	Speed	mps = 1.07
Units 1-6; forebay; up-looking	Beam Shape	$B = .011170692053X^4 - .158786483125X^3 + .231914384635X^2 - .5101118323179999X + .056466461582$
	Trajectory	plunge = 11
	Speed	mps = 1.07
Units 1-6; in-turbine; down-looking	Beam Shape	$B = -.003330226586X^4 + .017471453954X^3 - .310142606627X^2 + .035753868397X - .004849601465$
	Trajectory	$plunge = -.001281603844X^4 + .049052933499X^3 - .515811823786X^2 + 1.518635260846X - 16.59383269705$
	Speed	$mps = -.000106500555X^4 + .00478133785X^3 - .077676690819X^2 + .559559789228X - .17997330301$
Units 7 and 9; in-turbine; down-looking	Beam Shape	$B = -.003330226586X^4 + .017471453954X^3 - .310142505527X^2 + .035753868397X - .004849602465$
	Trajectory	$plunge = .002373764589X^4 - .112735778158X^3 + 1.56076075983X^2 - 6.603395811676X + 36.885504201695$
	Speed	$mps = .000018623951X^4 - .001270343248X^3 + .025384265243X^2 - .103042996658X + .677731764708$
Units 7 and 9; in-turbine; up-looking	Beam Shape	$B = -.003330226586X^4 + .017471453954X^3 - .310142505527X^2 + .035753868397X - .004849602465$
	Trajectory	$plunge = -.000308771027X^4 + .001553540498X^3 + .275668020657X^2 - 5.22697691328X - 4.1964285714$
	Speed	$mps = .000000000001X^4 + .000291396396X^3 - .003501776837X^2 - .051568234978X + 1.362891428571$
Unit 10; in-turbine; down-looking	Beam Shape	$B = -.00738221648X^4 + .040217634582X^3 - .404438802016X^2 + .036170817387X - .00152995463$
	Trajectory	$plunge = .002373764589X^4 - .112735778158X^3 + 1.56076075983X^2 - 6.603395811676X + 36.885504201695$
	Speed	$mps = .000018623951X^4 - .001270343248X^3 + .025384265243X^2 - .103042996658X + .677731764708$
Unit 10; in-turbine; up-looking	Beam Shape	$B = -.00738221648X^4 + .040217634582X^3 - .404438802016X^2 + .036170817387X - .00152995463$
	Trajectory	$plunge = -.000308771027X^4 + .001553540498X^3 + .275668020657X^2 - 5.22697691328X - 4.1964285714$
	Speed	$mps = .000000000001X^4 + .000291396396X^3 - .003501776837X^2 - .051568234978X + 1.362891428571$
Unit 8; in-turbine; down-looking	Beam Shape	$B = .011170692053X^4 - .158786483125X^3 + .231914384635X^2 - .5101118323179999X + .056466461582$
	Trajectory	$plunge = -.000086076347X^4 + .016096619208X^3 - .667377525502X^2 + 10.273234879192X - 56.813249624336$
	Speed	$mps = -.000607X^3 + .0388228X^2 - .201837X + .8758629$
Unit 8; in-turbine; up-looking	Beam Shape	$B = .011170692053X^4 - .158786483125X^3 + .231914384635X^2 - .5101118323179999X + .056466461582$
	Trajectory	plunge = -26
	Speed	$mps = .000018340049X^4 - .001702427407X^3 + .04529765004X^2 - .435040205779X + 2.2606$
	Speed	$mps = -.000499129625X^4 + .010107508945y^3 - .072403499059X^2 + .194463002585X + 1.254298181816$

Note: The variable X in polynomials is half-beam angle (degrees) for beam shape and mid-range for trajectory and speed. B is the beam-pattern factor; plunge is degrees below horizontal and mps is m/second.

Estimating in-turbine PSC unguided passage

The estimate of unguided numbers at the PSC was calculated according to the formula:

$$\hat{PU} = \sum_{i=1}^{d} \sum_{j=1}^{23} \sum_{k=1}^{18} \frac{N_{ijk}}{n_{ijk}} \sum_{l=1}^{n_{ijk}} u_{ijkl} \tag{5}$$

where u_{ijkl} = expanded unguided fish count in the lth sampling unit $\left(l = 1, \ldots n_{ijk}\right)$ of the kth intake slot $(k = 1, \ldots, 18)$ of the jth hour $(j = 1, \ldots, 23)$ of the ith day $(i = 1, \ldots, d)$.

Based on simple random sampling (SRS) of minutes within the hour, the variance of $\hat{PU}$ can be estimated by

$$\hat{Var}\left(\hat{PU}\right) = \sum_{i=1}^{d} \sum_{j=1}^{23} \sum_{k=1}^{18} \left[N_{ijk}^2 \left(1 - \frac{n_{ijk}}{N_{ijk}}\right) \frac{s_{u_{ijk}}^2}{n_{ijk}} \right] \tag{6}$$

where $s_{u_{ijk}}^2 = \dfrac{\sum_{l=1}^{n_{ijk}} \left(u_{ijkl} - \overline{u_{ijk}}\right)^2}{\left(n_{ijk} - 1\right)}$,

$$\overline{u_{ijk}} = \frac{\sum_{l=1}^{n_{ijk}} u_{ijkl}}{n_{ijk}},$$

and where N_{ijk} = possible number of sample units within an hour (i.e., nominally $N_{ijk} = 60$),

n_{ijk} = actual number of samples drawn within the jth hour $(j = 1, \ldots, 23)$ of the kth intake $(k = 1, \ldots, 8)$ of the ith day $(i = 1, \ldots, d)$ (i.e., nominally $n_{ijk} = 20$).

Estimating in-turbine PSC guided passage

The estimates of guided passage within the single-beam transducer beams are analogous to the estimates of unguided passage within the single-beam transducer beam. The estimate of guided numbers was calculated according to the formula

$$\hat{PG}_1 = \sum_{i=1}^{d}\sum_{j=1}^{23}\sum_{k=1}^{18}\frac{N_{ijk}}{n_{ijk}}\sum_{l=1}^{n_{ijk}} v_{ijkl} \tag{7}$$

where v_{ijkl} = expanded number of guided fish count in the lth sampling unit ($l = 1, \ldots, n_{ijk}$) of the kth intake slot ($k = 1, \ldots, 18$) of the jth hour ($j = 1, \ldots, 23$) of the ith day ($i = 1, \ldots, d$).

Again, based on a simple random sample (SRS) of minutes within the hour, the variance of $\hat{PG}_1$ can be estimated by

$$\hat{Var}\left(\hat{PG}_1\right) = \sum_{i=1}^{d}\sum_{j=1}^{23}\sum_{k=1}^{18}\left[N_{ijk}^2\left(1-\frac{n_{ijk}}{N_{ijk}}\right)\frac{s_{v_{ijk}}^2}{n_{ijk}}\right] \tag{8}$$

where $s_{v_{ijk}}^2 = \dfrac{\sum_{l=1}^{n_{ijk}}\left(v_{ijkl} - \overline{v_{ijk}}\right)^2}{\left(n_{ijk}-1\right)}$,

and where $\overline{v_{ijk}} = \dfrac{\sum_{l=1}^{n_{ijk}} v_{ijkl}}{n_{ijk}}$.

Estimating PSC-guided passage from forebay sampling

Sampling within the PSC slots can be envisioned as stratified sampling of two distinct strata composed of top and bottom positions of each of the five surface collector slots sampled. In this case, PSC-guided passage can also be estimated as

$$\hat{PG}_2 = \sum_{h=1}^{d}\sum_{i=1}^{23}\sum_{j=1}^{6}\sum_{k=1}^{2}\frac{M_{hijk}}{m_{hijkl}}\sum_{l=1}^{m_{hijk}} y_{hijkl} \tag{9}$$

where y_{hijkl} = expanded number of guided fish in the lth sampling unit $\left(l = 1, \ldots, m_{hijk}\right)$ of the kth vertical stratum $(k = 1,2)$ of the jth PSC slot $(j = 1, \ldots, 6)$ in the ith hour $(i = 1, \ldots, 23)$ of the hth day $(h = 1, \ldots, d)$;

M_{hijk} = possible number of sampling units within an hour (i.e., nominally $M_{hijk} = 60$);

m_{hijk} = actual number of samples drawn within the ith hour $(i = 1,\ldots,23)$ at the jth intake slot $(j = 1,\ldots,6)$ and kth vertical stratum $(k = 1,2)$ of the hth day $(h = 1,\ldots,d)$ (i.e., nominally $m_{ijkl} = 20$).

The variance of $\hat{P}G_2$ can be estimated by the formula

$$\hat{Var}\left(\hat{P}G_2\right) = \sum_{h=1}^{d}\sum_{i=1}^{23}\sum_{j=1}^{6}\sum_{k=1}^{2} M_{hijk}^2 \left(1 - \frac{m_{hijk}}{M_{hijk}}\right)\frac{s_{y_{hijk}}^2}{m_{hijk}} \qquad (10)$$

where $s_{y_{hijk}}^2 = \dfrac{\sum_{l=1}^{m_{hijk}} \left(y_{hijkl} - \overline{y_{hijk}}\right)^2}{\left(m_{hijk} - 1\right)}$

and where $\overline{y_{hijk}} = \dfrac{\sum_{l=1}^{m_{hijk}} y_{hijkl}}{m_{hijk}}$.

Estimating Unit 8 fish guidance efficiency

Background. At turbine intake slot 8b at Powerhouse 1, an ESBS was deployed. The goal of the statistical analysis was to estimate FGE at Intake 8B using hydroacoustic data and to compare those estimates with FGE estimates collected using netting. The following describes estimators for FGE and associated variance estimates and statistical tests of FGE comparison.

Estimating unguided numbers. Using the single continuously sampled split-beam transducer, total unguided smolts numbers $\left(\hat{N}\right)$ were estimated using the formula

$$\hat{U} = \sum_{i=1}^{d}\sum_{j=1}^{23}\sum_{k=1}^{60} \hat{w}_{ijk}$$

where $\hat{w}_{ijk}$ = expanded number of unguided smolts entering the turbine intake slot during the kth minute $(k = 1,\ldots,60)$ of the jth hour $(j = 1,\ldots,23)$ of the ith day $(i = 1,\ldots,d)$.

The value of $\hat{w}_{ijk}$ is the expanded number of smolt detections across the intake slot during a 1-minute interval. The above estimate was compared directly to fyke-net estimates by the NMFS but was expanded by a factor of three to estimate unguided passage for all intakes at Unit 8 in comparisons with PSC estimates.

Unlike many previous hydroacoustic investigations, sampling was continuous over time, precluding the use of finite sampling methods to estimate the variance of $\hat{U}$. Nevertheless, there was measurement error associated with the interpretation of acoustic signals and the spatial expansion of the counts to the entire intake. For convenience and to extract estimates of hydroacoustic sampling error empirically, estimates of error variance were calculated on an hourly basis during the duration of estimation. Hence, the variance of $\hat{U}$ was expressed as

$$\hat{Var}\left(\hat{U}\right) = \sum_{i=1}^{d}\sum_{j=1}^{23}\hat{Var}\left(\hat{w}_{ij}\right)$$

where $\hat{w}_{ij} = \sum_{k=1}^{60}\hat{w}_{ijk}$.

Methods for estimating the hourly measurement error associated with $\hat{w}_{ij}$ will be discussed below. The variance estimate was expanded by a factor of nine to estimate the variance of all three intakes at Unit 8 for comparison with PSC estimates.

Estimating guided numbers. Using the single continuously sampled split-beam transducer, an estimate of total guided smolts $\left(\hat{G}\right)$ can be estimated according to the formula

$$\hat{G} = \sum_{i=1}^{d}\sum_{j=1}^{23}\sum_{k=1}^{60}\hat{x}_{ijk}$$

where $\hat{x}_{ijk}$ = expanded number of guided smolts bypassed during the kth minute $(k = 1,\ldots,60)$ of the jth hour $(j = 1,\ldots,23)$ of the ith day $(i = 1,\ldots,d)$.

The value of $\hat{x}_{ijk}$ was the expanded number of smolts detected across the intake slot during a 1-minute interval. The above estimate was compared directly to gatewell dipping estimates but was expanded by a factor of three to estimate guided passage for all intakes at Unit 8 in comparisons with the PSC estimates.

The variance of $\hat{G}$ was expressed on an hourly basis as

$$\hat{Var}\left(\hat{G}\right) = \sum_{i=1}^{d}\sum_{j=1}^{23}\hat{Var}\left(\hat{x}_{ij}\right)$$

where $\hat{x}_{ij} = \sum_{k=1}^{60}\hat{x}_{ijk}$.

Methods for estimating the hourly measurement error associated with $\hat{x}_{ij}$ will be discussed in a subsequent section. This variance estimate was expanded by a factor of nine to estimate the variance of all three intakes at Unit 8 for comparison with PSC estimates.

Fish guidance efficiency estimate. Using the independent estimates of guided $\left(\hat{G}\right)$ and unguided $\left(\hat{U}\right)$ fish numbers for a time interval of interest, FGE was estimated according to the formula

$$\hat{FGE} = \frac{\hat{G}}{\hat{G}+\hat{U}}$$

with associated variance estimator

$$\hat{Var}\left(\hat{FGE}\right) = \hat{FGE}^2\left(1-\hat{FGE}\right)^2\left[\frac{\hat{Var}\left(\hat{G}\right)}{\hat{G}^2}+\frac{\hat{Var}\left(\hat{U}\right)}{\hat{U}^2}\right].$$

Asymptotic $(1-\alpha)$ 100 percent confidence intervals for FGE were calculated as

$$\hat{FGE} \pm Z_{1-\frac{\alpha}{2}}\sqrt{\hat{Var}\left(\hat{FGE}\right)}.$$

Comparing methods. The NMFS sampled the center slot of Unit 8 to calculate FGE using netting and gatewell data concurrent with this study. Paired hydroacoustic and fyke-net estimates of FGE were calculated for each NMFS trial and compared using a paired t-test. The paired t-test tested the null hypothesis of equal mean FGE estimates for the two estimation techniques at a significance level of $\alpha = 0.05$ two-tailed. When numbers of fish detected by hydroacoustics during concurrent sampling with netting were low, hydroacoustic FGEs were calculated from estimates of guided and unguided fish for a 4-hour sampling period instead of the concurrent sampling period. The extended hydroacoustic sampling period was used to collect additional smolt counts and to dampen the binomial sampling variance associated with the hydroacoustic FGE estimates.

Estimating hydroacoustic measurement error. Because of the continuous within-hour sampling, sampling error was eliminated from the estimates of guided and unguided numbers. Nevertheless, measurement error persisted and needed to be estimated. The approach to estimating measurement error was an extension of a compound-Poisson process Skalski and Robson (1992) used to model abundance in continuous intervals.

The estimate of measurement error was based on the assumptions:

a. Per-minute measurement error $\left(\sigma^2_{ME}\right)$ was constant within an hour.

b. Within an hour, smolt passage has a constant mean and variance.

c. Within a minute, smolt counts were Poisson-distributed with mean and variance λ_k $(k = 1, \ldots, 60)$.

d. Within an hour, the Poisson parameters λ_k were distributed with mean μ and variance σ^2.

e. The λ_k were auto-correlated with a function of distance between the 1-minute intervals.

Based on the above assumptions, the variance for the estimated smolt count in a 1-minute interval $(\hat{x}_k)$ can be calculated to be

$$Var(\hat{x}_k) = Var_3\left[E_2\left[E_1(\hat{x}_k|2,3)\right]\right] + E_3\left[Var_2\left[E_1(\hat{x}_k|2,3)\right]\right] + E_3\left[E_2\left[Var_1(\hat{x}_k|2,3)\right]\right]$$

where 1 = stage 1 of hydroacoustic measurement error of $\hat{x}_k$ about x_k with variance σ^2_{ME},

2 = stage 2 of x_k Poisson-distributed with mean λ_k,

3 = stage 3 of λ_k distributed with mean μ and variance σ^2 within the hour.

Then

$$\begin{aligned} Var(\hat{x}_k) &= Var_3\left[E_2\left[x_k|3\right]\right] + E_3\left[Var_2\left[x_k|3\right]\right] + E_3\left[E_2\left[\sigma^2_{ME}|3\right]\right] \\ &= Var_3\left[\lambda_k\right] + E_3\left[\lambda_k\right] + E_3\left[\sigma^2_{ME}\right] \\ Var(\hat{x}_k) &= \sigma^2 + \mu + \sigma^2_{ME}\,. \end{aligned} \tag{11}$$

If an additional assumption was that the variance σ^2 is insignificantly small between consecutive 1-minute intervals (i.e., $\sigma^2 = 0$), then Equation 1 reduces to

$$Var(\hat{x}_k) = \mu + \sigma^2_{ME}\,. \tag{12}$$

Equation 2 suggested the method of moment estimator

$$\sigma^2_{ME} = \hat{Var}(\hat{x}_k) - \hat{\mu}_k \tag{13}$$

where

$$\hat{Var}(\hat{x}_k) = \frac{(\hat{x}_k - \hat{x}_{k+1})^2}{2},$$

$$\hat{\mu}_k = \frac{(x_k + x_{k+1})}{2}.$$

If σ^2 is not zero, then $\hat{\sigma}^2_{ME}$ overestimates the size of σ^2_{ME}.

The within-hour measurement error associated with $\hat{x}_{ij}$ was expressed as

$$\hat{Var}(\hat{x}_{ij}) = \frac{60}{59}\sum_{k=1}^{59}\left[\frac{(\hat{x}_{ijk} - \hat{x}_{ijk+1})^2}{2} - \frac{(\hat{x}_{ijk} + \hat{x}_{ijk+1})}{2}\right]. \quad (14)$$

If $\hat{Var}(\hat{x}_{ij}) < 0$, it was set equal to zero for the *ij*th hour. The variance of $\hat{G}$ was then a sum of the within-hour measurement errors where

$$\hat{Var}(\hat{G}) = \sum_{i=1}^{d}\sum_{j=1}^{23}\hat{Var}(\hat{x}_{ij}). \quad (15)$$

An analogous procedure for estimating the variance of $\hat{U}$ was used. Variance estimator (Equation 14) was used whenever the complete hour was acoustically monitored. It was applied when unintentional losses of data occurred such as an equipment outage or data downloading. In these events, the variance was calculated according to the formula

$$\hat{Var}(\hat{x}_{ij}) = \frac{60}{a}\sum_{k=1}^{a}\left[\frac{(\hat{x}_{ijk} - \hat{x}_{ijk+1})^2}{2} - \frac{(\hat{x}_{ijk} + \hat{x}_{ijk+1})}{2}\right] \quad (16)$$

where a is the number of intervals with two successive 1-minute samples intact.

It should be noted that if σ^2 in Equation 11 was zero, then Equation 14 could be alternatively estimated by the formula

$$60 \cdot s^2_{x_{ijk}}$$

where

$$s^2_{x_{ijk}} = \frac{\sum_{k=1}^{60}(\hat{x}_{ijk} - \hat{x}_{ij})^2}{(60-1)},$$

because, in this case,

$$E\left(60\, s^2_{x_{ijk}}\right) = 60\,\sigma^2_{ME},$$

the same expected value as that of Equation 14. Any difference in magnitude between Equation 14 and Equation 16 is an estimate of the within-hour value of σ^2. Equations 14 and 16 provide similar results for a situation with little temporal variability in smolt counts.

Estimating unguided passage at Units 7, 9, and 10

The unguided passage into Units 7, 9, and 10 can be estimated by the formula

$$\hat{TU} = 3\sum_{i=1}^{d}\sum_{j=1}^{23}\sum_{k=1}^{3}\frac{H_{ijk}}{h_{ijk}}\sum_{l=1}^{h_{ijk}} z_{ijkl} \qquad (17)$$

where z_{ijkl} = expanded unguided fish counts in the lth sampling unit $\left(l = 1,\ldots,h_{ijk}\right)$ at the kth turbine intake $(k = 1,2,3)$ in the jth hour $(j = 1,\ldots,23)$ of the ith day $(i = 1,\ldots,d)$;

H_{ijk} = possible number of sampling units within an hour (i.e., nominally $H_{ijk} = 60$);

h_{ijk} = actual number of samples drawn within the jth hour $(j = 1,\ldots,23)$ at the kth turbine unit $(k = 1,2,3)$ on the ith day $(i = 1,\ldots,d)$ (i.e., nominally $h_{ijk} = 20$).

Here, the z_{ijkl} are counts in only the single intake slots that were actually monitored. The estimator (Equation 17) expands these counts by a factor of three to estimate total unguided passage through Units 7, 9, and 10.

To account for the slot-to-slot variance within turbine units, the sampling scheme for Units 7, 9, and 10 was viewed as sampling of three of nine intakes with STSs. The second stage of sampling was the sampling of time intervals within the slot-hour. So, instead of using a variance estimator based upon simple random sampling, the following formula was used:

$$\hat{Var}\left(\hat{HU}\right) = \sum_{g=1}^{5}\frac{L_g^2\left(1-\frac{l_g}{L_g}\right)s^2_{\hat{U}_g}}{l_g} + \sum_{g=1}^{5}\left[\frac{L_g\sum_{k=1}^{l_g}\hat{Var}\left(\hat{U}_{gk}\right)}{l_g}\right] \qquad (18)$$

where

L_g = number of turbine intake slots in the gth stratum $(g = 1)$ (here, $l_g = 9$);

l_g = number of turbine intake slots sampled in the gth stratum $(g = 1)$ (here, $l_g = 3$);

$$s^2_{\hat{U}_g} = \frac{\sum_{k=1}^{l_g}\left(\hat{U}_{gk} - \hat{\bar{U}}_g\right)^2}{\left(l_g - 1\right)};$$

$$\hat{\bar{U}}_g = \frac{\sum_{k=1}^{l_g}\hat{U}_{gk}}{l_g};$$

$$\hat{U}_{gk} = \sum_{i=1}^{d}\sum_{j=1}^{23}\frac{R_{ijgk}}{r_{ijgk}}\sum_{l=1}^{r_{ijgk}} b_{ijkl};$$

$$\hat{Var}\left(\hat{U}_{gk}\right) = \sum_{i=1}^{d}\sum_{j=1}^{23}\left[\frac{R^2_{ijgk}\left(1 - \frac{r_{ijgk}}{R_{ijgk}}\right)s^2_{b_{ijgk}}}{r_{ijgk}}\right]$$

and where

r_{ijgk} = actual number of time intervals sampled in the *j*th hour $\left(j = 1,\ldots,23\right)$ of the *i*th day $\left(i = 1,\ldots,d\right)$ at the *k*th intake slot $\left(k = 1,\ldots,l_g\right)$ in the *g*th stratum $\left(g = 1\right)$ (i.e., nominally 15 1-minute samples);

R_{ijgk} = number of possible time intervals that could be sampled in the *j*th hour $\left(j = 1,\ldots,23\right)$ of the *i*th day $\left(i = 1,\ldots,d\right)$ at the *k*th intake slot $\left(k = 1,\ldots,l_g\right)$ in the *g*th stratum $\left(g = 1\right)$ (i.e., nominally 60 1-minute samples);

b_{ijgkl} = estimated unguided fish passage in the *l*th sample $\left(l = 1,\ldots,r_{ijgk}\right)$ in *j*th hour $\left(j = 1,\ldots,23\right)$ of the *i*th day $\left(i = 1,\ldots,d\right)$ at the *k*th intake slot $\left(k = 1,\ldots,l_g\right)$ in the *g*th stratum $\left(g = 1\right)$;

$$s^2_{b_{ijgk}} = \frac{\sum_{l=1}^{r_{ijgk}}\left(b_{ijgkl} - \overline{b_{ijgk}}\right)^2}{\left(r_{ijgk} - 1\right)};$$

$$\overline{b_{ijgk}} = \frac{\sum_{l=1}^{r_{jgk}} b_{ijgkl}}{r_{ijgk}}.$$

Estimating guided passage at Units 7, 9, and 10

The estimation scheme for the guided passage at sampled intake slots at Units 7, 9, and 10 is analogous to the estimation of unguided numbers at Units 7, 9, and 10. An estimate of guided numbers at these turbine units is then

$$\hat{TG} = 3\sum_{i=1}^{d}\sum_{j=1}^{23}\sum_{k=1}^{3}\frac{H_{ijk}}{h_{ijk}}\sum_{l=1}^{h_{ijk}}a_{ijkl} \tag{19}$$

where a_{ijkl} = expanded guided fish counts in the lth sampling unit $(l = 1, \ldots, h_{ijk})$ at the kth turbine intake $(k = 1,2,3)$ in the jth hour $(j = 1, \ldots, 23)$ of the ith day $(i = 1, \ldots, d)$.

The same two-stage sampling scheme that was used for estimating unguided passage also was used in analyzing the guided fish passage in order to calculate a conservative variance estimator, as follows:

$$\hat{Var}\left(\hat{TG}\right) = \sum_{g=1}^{5}\frac{L_g^2\left(1-\frac{l_g}{L_g}\right)s^2_{\hat{G}_g}}{l_g} + \sum_{g=1}^{5}\left[\frac{L_g\sum_{k=1}^{l_g}\hat{Var}\left(\hat{G}_{gk}\right)}{l_g}\right] \tag{20}$$

$$s^2_{\hat{G}_g} = \frac{\sum_{k=1}^{l_g}\left(\hat{G}_{gk}-\hat{\bar{G}}_g\right)^2}{\left(l_g-1\right)};$$

$$\hat{\bar{G}}_g = \frac{\sum_{k=1}^{l_g}\hat{G}_{gk}}{l_g};$$

$$\hat{G}_{gk} = \sum_{i=1}^{d}\sum_{j=1}^{23}\frac{R_{ijgk}}{r_{ijgk}}\sum_{l=1}^{r_{ijgk}}c_{ijgkl};$$

$$\hat{Var}\left(\hat{G}_{gk}\right) = \sum_{i=1}^{d}\sum_{j=1}^{23}\left[\frac{R^2_{ijgk}\left(1-\frac{R_{ijgk}}{r_{ijgk}}\right)s^2_{c_{ijgk}}}{r_{ijgk}}\right];$$

$$s^2_{c_{ijgk}} = \frac{\sum_{l=1}^{r_{ijgk}} \left(c_{ijgkl} - \overline{c_{jgk}}\right)^2}{r_{ijgk}};$$

where

$$\overline{c_{jgk}} = \frac{\sum_{l=1}^{r_{ijgk}} c_{ijgkl}}{r_{ijgk}};$$

and where

c_{ijgkl} = estimated guided fish passage in the lth sample $\left(l = 1,\ldots,r_{ijgk}\right)$ in the jth hour $\left(j = 1,\ldots,23\right)$ of the ith day $\left(i = 1,\ldots,d\right)$ at the kth intake slot $\left(k = 1,\ldots,l_g\right)$ in the gth stratum $\left(g = 1,\ldots,5\right)$.

Estimating PSC performance

The PSC performance was evaluated on a unit-by-unit basis and for the entire structure using two performance measures. The PSC efficiency was estimated by

$$\hat{PSCE} = \frac{\hat{PG}_2}{\hat{PG}_2 + \hat{PU}} \tag{21}$$

with associated variance estimator

$$\hat{Var}\left(\hat{PSCE}\right) = \hat{PSCE}^2\left(1 - \hat{PSCE}\right)^2\left[\frac{\hat{Var}\left(\hat{PG}_2\right)}{\hat{PG}_2^2} + \frac{\hat{Var}\left(\hat{PU}\right)}{\hat{PU}^2}\right] \tag{22}$$

using the variances of $\hat{PU}$ and $\hat{PG}_2$ calculated using Equations 6 and 9, respectively.

The PSC performance can also be estimated by the formula

$$\hat{PSCE} = \frac{\hat{PG}_1}{\hat{PG}_1 + \hat{PU}}. \tag{23}$$

In this case, $\hat{PG}_1$ and $\hat{PU}$ are correlated because the sampling data was coming from the same single-beam downward-angled transducers (Figure 2). The variance of $\hat{PSCE}$ was estimated by

$$\hat{Var}\left(\hat{PSCE}\right) = \left(PSCE\right)^2 \left(1 - PSCE\right)^2 \left[\frac{\hat{Var}\left(\hat{PG}_1\right)}{\hat{PG}_1^2} + \frac{\hat{Var}\left(\hat{PU}\right)}{\hat{PU}^2} - 2\frac{\hat{Cov}\left(\hat{PG}_1, \hat{PU}\right)}{\hat{PG}_1 \cdot \hat{PU}} \right] \tag{24}$$

and where

$$\hat{Cov}\left(\hat{PG}_1, \hat{PU}\right) = \sum_{i=1}^{d} \sum_{j=1}^{23} \sum_{k=1}^{18} N_{ijk}^2 \left(1 - \frac{n_{ijk}}{N_{ijk}}\right) \frac{\hat{Cov}\left(v_{ijk}, u_{ijk}\right)}{n_{ijk}},$$

$$\hat{Cov}\left(v_{ijk}, u_{ijk}\right) = \frac{\sum_{l=1}^{n_{ijk}} \left(u_{ijkl} - \overline{u_{ijk}}\right)\left(v_{ijkl} - \overline{v_{ijk}}\right)}{\left(n_{ijk} - 1\right)}.$$

The PSC effectiveness was estimated by the quantity

$$\hat{PSCF} = \frac{\left(\frac{\hat{PG}}{V_{SPC}}\right)}{\left(\frac{\hat{PG} + \hat{PU}}{V_T}\right)} = \hat{PSCE} \cdot \frac{V_T}{V_{SPC}} \tag{25}$$

where V_{SPC} = water volume entering SPC slots,

V_T = total water volume entering the PSC and Turbine Slots 1 – 6

and associated variance estimator

$$\hat{Var}\left(\hat{PSCF}\right) = \left(\frac{V_T}{V_{SPC}}\right)^2 \cdot \hat{Var}\left(\hat{SPCE}\right). \tag{26}$$

The general forms of Equations 17 and 19 allow PSC efficiency and effectiveness to be calculated over any temporal and spatial scale of interest. It should also be noted that PSC effectiveness could be estimated using either guided numbers $\hat{PG}_1$ (Equation 7) or $\hat{PG}_2$ (Equation 9).

Asymptotic $(1-\alpha)$ 100 percent confidence intervals were calculated according to the general formula

$$\hat{\theta} \pm Z_{1-\frac{\alpha}{2}} \sqrt{\hat{Var}\left(\hat{\theta}\right)}$$

for any parameter estimate $\hat{\theta}$.

Estimating FGE for Units 7-10

The FGE for Units 7-10 was estimated according to the formula

$$\hat{FGE} = \frac{\hat{TG}}{\hat{TG} + \hat{TU}} \tag{27}$$

with associated variance estimator

$$\hat{Var}\left(\hat{FGE}\right) = \hat{FGE}^2 \left(1 - \hat{FGE}\right)^2 \left[\frac{\hat{Var}\left(\hat{TG}\right)}{\hat{TG}^2} + \frac{\hat{Var}\left(\hat{TU}\right)}{\hat{TU}^2}\right]. \tag{28}$$

Asymptotic $(1-\alpha)$ 100 percent confidence intervals were calculated according to the general formula

$$\hat{\theta} \pm Z_{1-\frac{\alpha}{2}} \sqrt{\hat{Var}\left(\hat{\theta}\right)}$$

for FGE. It should be noted that variance formula (Equation 28) underestimates the variance of the FGE estimates when making inferences to all of Unit 8. However, the variance formula (Equation 28) is appropriate when making inferences to the specific intake slots sampled (e.g., Slot 8b with the ESBS). The FGE variance estimate for Units 7, 9, and 10 should be conservative because of the conservative variance estimator for those units.

Comparing fish passage performance at Powerhouse 1

Comparison of FPE at the PSC, turbine Units 7, 9, and 10 or turbine Unit 8 was based on inspection of the $(1-\alpha)$ 100 percent confidence intervals. Overlapping intervals suggested no significant difference; non-overlapping intervals suggested a statistically significant difference at α.

Comparing guided fish passage at the PSC

The two estimates of guided fish passage at the PSC were compared by regressing the single-beam counts on split-beam counts. It was anticipated that the data would fit a regression line with a zero intercept and a slope of one if the sampling approaches were equivalent. This regression analysis was based on daily estimates of guided fish numbers by each method. The two estimates were compared by examining for overlap between $(1-\alpha)$ 100 percent confidence

interval estimates of $\hat{P}G_1$ and $\hat{P}G_2$ and by calculating a $(1-\alpha)$ 100 percent confidence interval for the difference:

$$\left(\hat{P}G_1 - \hat{P}G_2\right) \pm Z_{1-\frac{\alpha}{2}} \sqrt{\hat{Var}\left(\hat{P}G_1\right) + \hat{Var}\left(\hat{P}G_2\right)}.$$

The above comparisons can be performed on any time intervals of interest such as daily, weekly, or seasonally.

3 Results

Hydroacoustic Detectability

Comparison of counts of guided and unguided fish by netting and hydroacoustic methods at Unit 8 provided valuable feedback for modeling detectability. After the final round of detectability modeling, the average ratio of net counts to hydroacoustic counts was close to unity for guided fish (0.85) and unguided fish (0.93). Preliminary estimates based upon models using average target strength instead of target strength converted from the average backscattering cross section produced ratios as low as 0.2-0.3 netted fish for every acoustically detected fish.

In spring, most deployments had effective beam angles > 4° for the ranges that were sampled (Figure 6). Examples include all transducers in and upstream of PSC units, and transducers in Units 7, 9, and 10. Exceptions included deployments where sampling had to begin at relatively short ranges < 4 m (e.g., near transducers at Unit 8).

In summer, curves for EBA by range had similar shapes to those modeled in spring, although angles at all ranges tended to be narrower because the average backscattering cross section of summer-run juvenile fish was lower than that of spring-run fish (compare Figure 6 with Figure 7).

Polynomial regressions were used to describe the relationships between effective beam angle and range from a transducer for every type of deployment (Table 7). Those equations and passage width data were used to expand the count of each detected fish and to equalize detectability among sample ranges and deployments. The coding solved a deployment-specific polynomial equation for effective beam angle based upon the range of detection of each individual fish, calculated the corresponding beam diameter at the same range, and multiplied the fish's count (i.e., one) by the ratio of the passage width to the beam diameter. The coefficients in Table 7 and the general form of the polynomial described in the table titles can be used to generate detectability curves. Sampling ranges that were used to solve for effective beam angle truncated the polynomial curves to what can be seen in Figures 6 and 7.

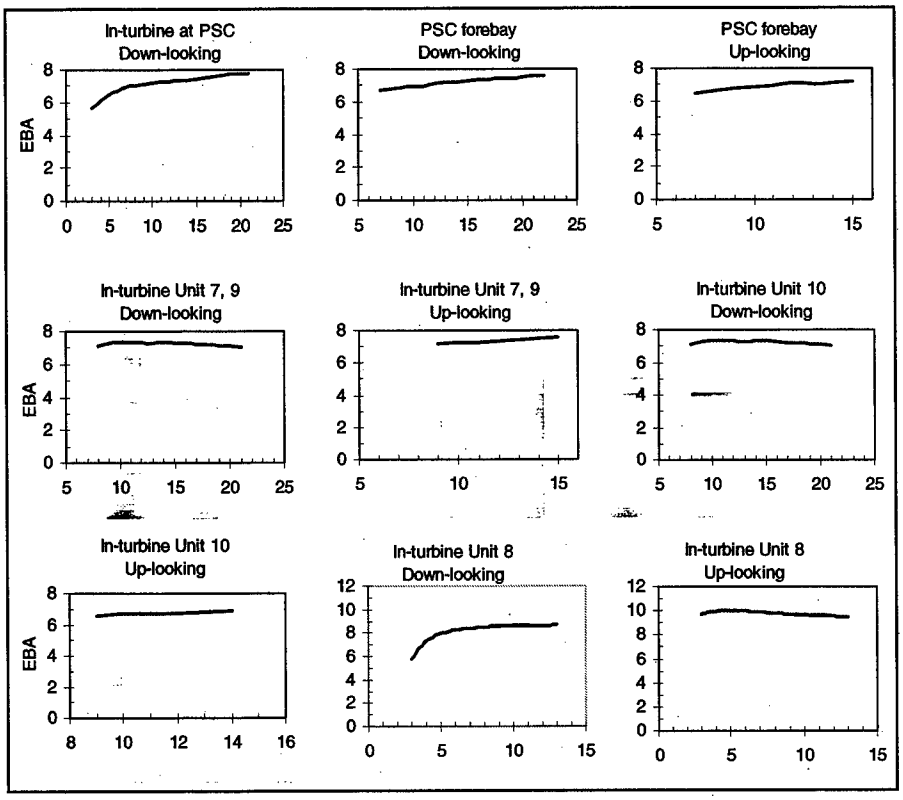

Figure 6. EBA as a function of range from transducers for every type of deployment in spring 2000

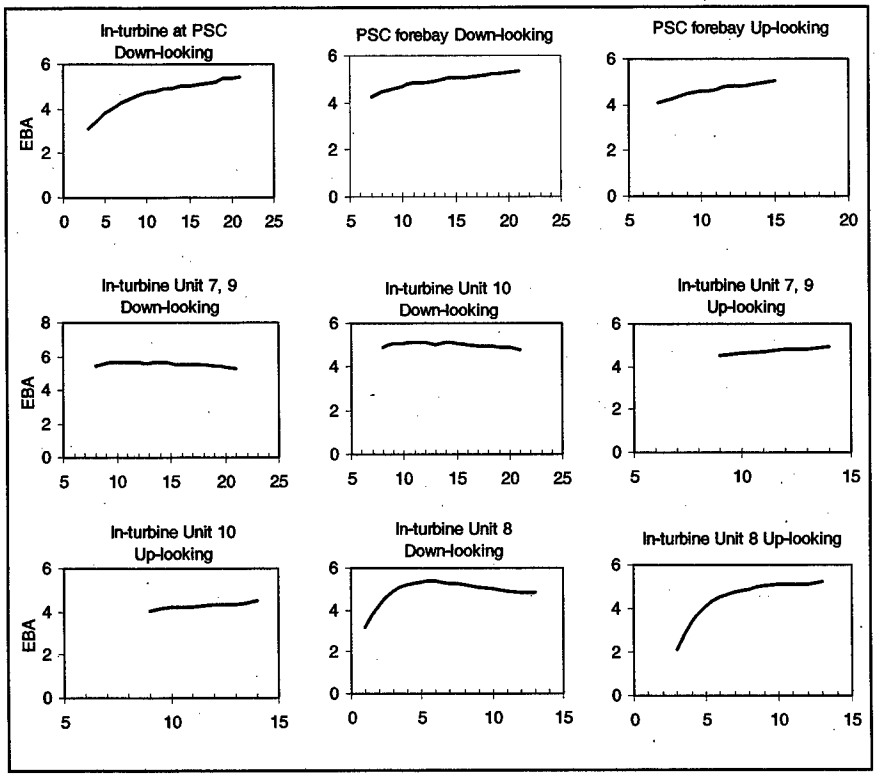

Figure 7. EBA as a function of range from transducers for every type of deployment in summer 2000

Table 7
Coefficients of Polynomials Used to Calculate EBA as a Function of Range From Transducers in Spring

Deployments	C1	C2	C3	C4	C5	C6	Intercept
			SPRING				
Units 1-6; in-turbine; down-looking			-0.00010460	0.00596750	-0.12321500	1.14541490	1.54384480
Units 1-6; forebay; down-looking	-0.00000140	0.00012693	-0.00463897	0.08693833	-0.88115638	4.66015682	-5.01897700
Units 1-6; forebay; up-looking			-0.00058530	0.02686940	-0.44858890	3.29629800	-3.90062780
Units 7 and 9; in-turbine; down-looking			-0.00004197	0.00248778	-0.05594245	0.54575503	4.42326031
Units 7 and 9; in-turbine; up-looking			-0.00075000	0.03215250	-0.51095680	3.65846030	-4.55698550
Unit 10; in-turbine; down-looking			-0.00003746	0.00224213	-0.05136822	0.51389289	3.83770666
Unit 10; in-turbine; up-looking			-0.00056840	0.02536730	-0.42282100	3.19867650	-4.38378370
Unit 8; in-turbine; down-looking		0.00047591	-0.02087290	0.35843872	-3.02830542	12.75503641	14.95659091
Unit 8; in-turbine; up-looking			-0.00086156	0.03043435	-0.38695604	2.01558838	4.76559538
			SUMMER				
Units 1-6; in-turbine; down-looking			-0.00002311	0.00179565	-0.05022499	0.66291092	0.92344757
Units 1-6; forebay; down-looking	-0.00000084	0.00007684	-0.00282981	0.05400850	-0.56855929	3.25169059	-4.13600354
Units 1-6; forebay; up-looking			-0.00033340	0.01580460	-0.27854960	2.25608170	-3.21430150
Units 7 and 9; in-turbine; down-looking			-0.00004422	0.00275196	-0.06467490	0.65369026	2.65521484
Units 7 and 9; in-turbine; up-looking			-0.00026630	0.01265690	-0.23135520	2.01057300	-2.95716280
Unit 10; in-turbine; down-looking			-0.00004427	0.00270207	-0.06250497	0.62710147	2.21344475
Unit 10; in-turbine; up-looking			-0.00011850	0.00698900	-0.15391560	1.56429790	-2.50202300
Unit 8; in-turbine; down-looking			-0.00038380	0.01714900	-0.26743080	1.65380260	1.26735260
Unit 8; in-turbine; up-looking			-0.00059890	0.02668100	-0.44457590	3.32571660	-5.00953050

Note: Polynomials had the general form: $C1 \times MID\_R^6 + C2 \times MID\_R^5 + C3 \times MID\_R^4 + C4 \times MID\_R^3 + C5 \times MID\_R^2 + C6 \times MID\_R +$ Intercept, where MID_R is the midrange in meters and C1-C6 are coefficients tabled below.

Validation of Autotracking Hydroacoustic Data

For the five "tracker calibration days" (early, middle, and late spring; early and late summer), there was good agreement between autotracker mean counts and autotracker counts and for most transducer channels the variation among human trackers, as indicated by the 80 percent confidence intervals, was a small fraction of the mean count (Figure 8). The exception was transducer channels with very low counts so that very small differences (one to a few fish) among individual counts produced relatively large confidence intervals.

Figures 9 and 10 show the differences in cumulative fish counts among individual humans, the human means, and the autotracker counts for each of the 5 days. These are the same data as in Figure 8, with the addition of the individual counts rather than just their means, but all are expressed as cumulative sums.

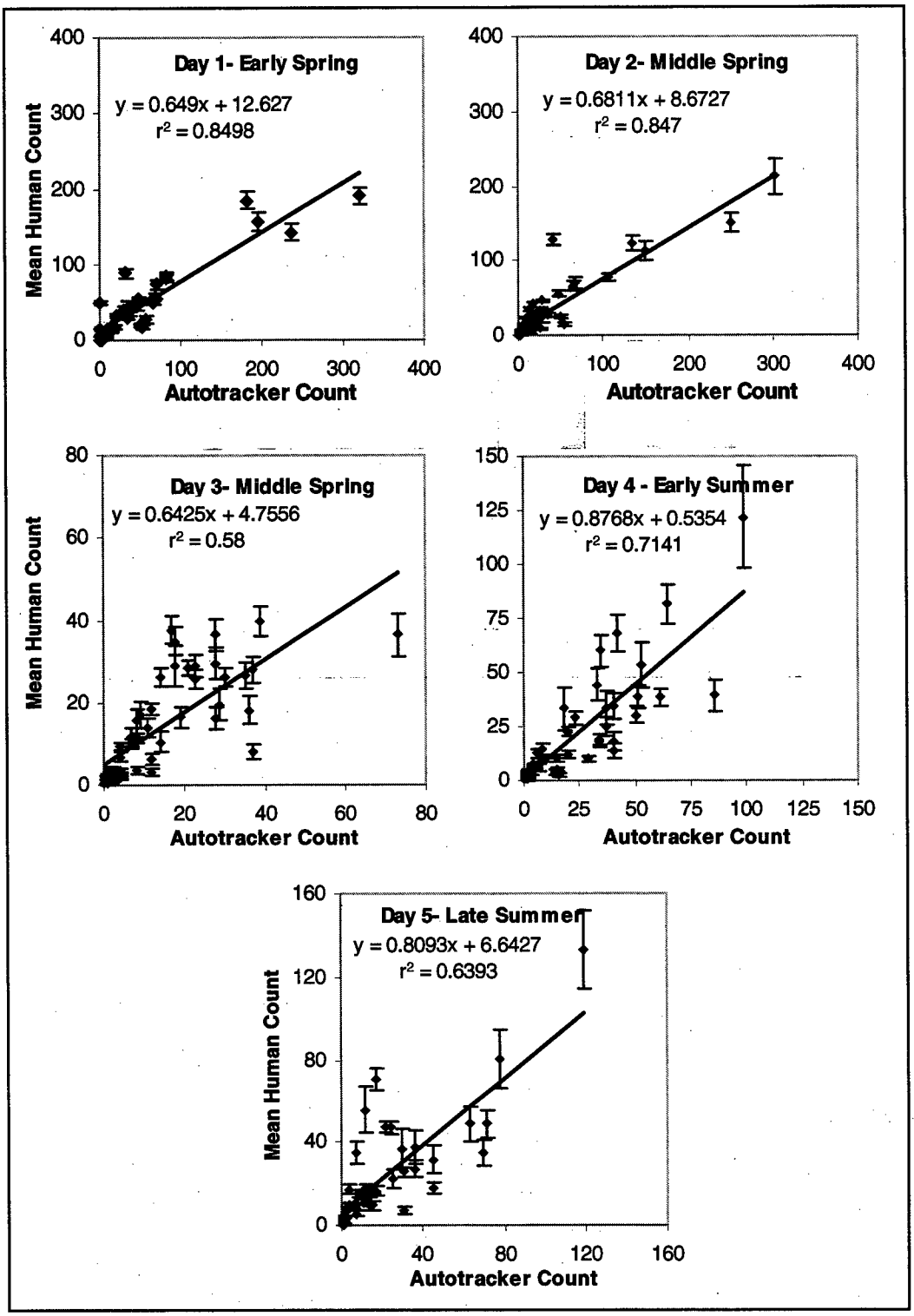

Figure 8. Means of fish counts made by different trained technicians plotted against autotracker counts on the same hydroacoustic data sets taken from five different days in early, middle, and late spring and early and late summer. Vertical error bars indicate 80 percent confidence limits on the human count means

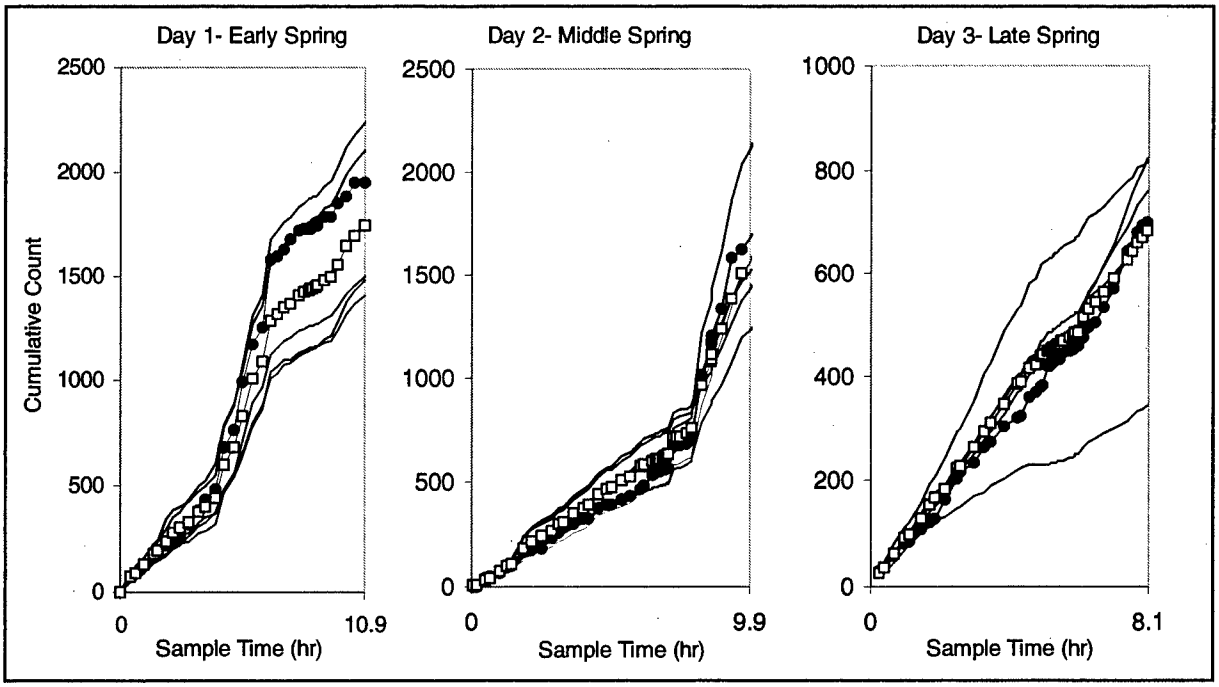

Figure 9. Cumulative counts by human trackers (lines are individuals; open squares are the mean) and by the autotracker (dots) for spring calibration days

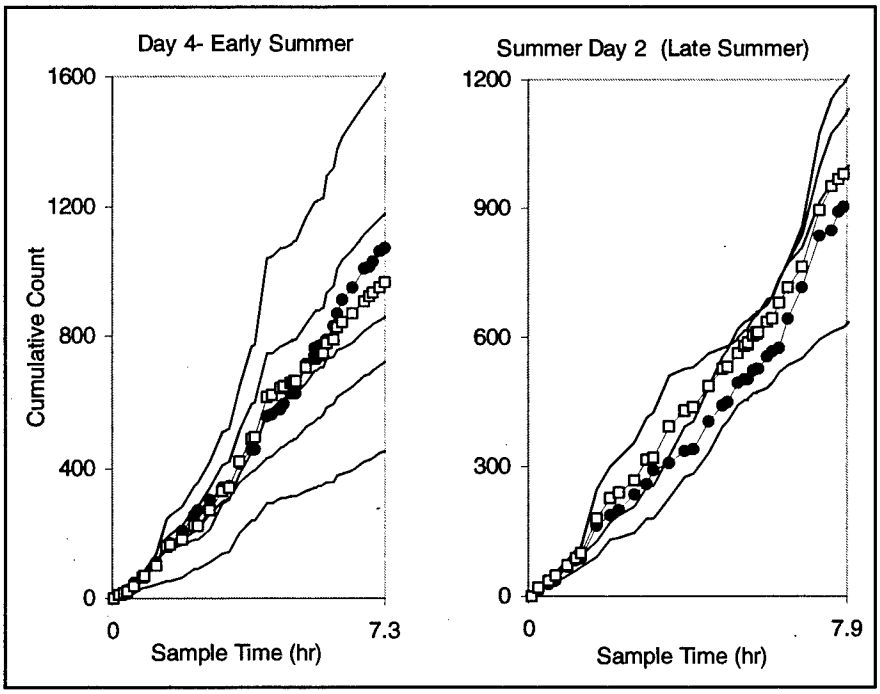

Figure 10. Cumulative counts by human trackers (lines are individuals; open squares are the mean) and by the autotracker (dots) for summer calibration days

It can be seen that the human error increases from left to right as new transducer channels are added to the sums. It is also clear that the differences among humans are cumulative over the different samples but that the autotracker fairly closely approximates the human mean. The time sampled for each day ranged from just over 7 hours (Day 4) to nearly 11 hours (Day 1; Table 8).

Table 8
Total Time Sampled (the summed time of all transducer channel samples) Contributing to the 5 Calibration Days, the Cumulative Difference and Percent Difference Between the Extreme Human (high or low, whichever was greater) and the Mean Human Tracker, and the Cumulative Difference and Percent Difference Between the Autotracker and the Mean Human Tracker

Calibration Day	Season	Total Hours Represented	Difference between extreme human and mean human tracker	Difference between autotracker and mean human tracker
Day 1	Early Spring	10.87	478.4 (28%)	205.4 (12%)
Day 2	Middle Spring	9.98	547.8 (34%)	108.8 (7%)
Day 3	Late Spring	8.07	388.8 (66%)	17.2 (2%)
Day 4	Early Summer	7.32	645.2 (67%)	107.2 (11%)
Day 5	Late Summer	7.95	331.7 (33%)	85.75 (7%)

Figure 11 presents a regression graph of the same data in Figure 8 except that all 5 days are included in one plot, and the 80 percent confidence bounds on the human means are omitted. The autotracker count for each transducer channel proved to be a reasonably good predictor of the mean human count for that transducer channel sample, the autotracker count explaining about 81 percent of the variation in the mean human tracker count for the 222 transducer channel samples over the 5 days.

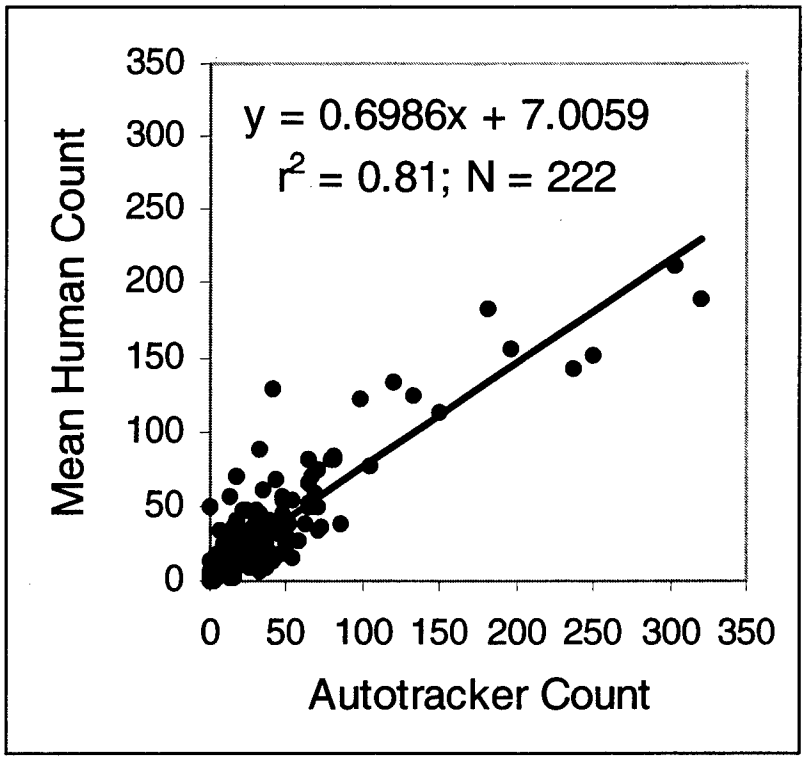

Figure 11. Correlation of mean human tracker counts with autotracker counts based upon five data sets

Major Passage Metrics — Spatial Aspects

Horizontal distributions of fish passage, flow, and fish density

Horizontal distribution of fish passage. The horizontal distribution of fish passage was examined at each of the main passage routes. Figure 12 and Figure 13 show the total estimated fish passage across Powerhouse 1 in spring and summer, respectively.

In spring just over 70 percent of the total 16.9 M fish that passed at Powerhouse 1 passed south of the wing wall through the PSC Units 1-6 (Figure 12). Of the remaining 4.75 M fish passing Units 7-10, over half (2.68 M) passed Unit 9, the turbine unit with the highest estimated total fish passage in spring.

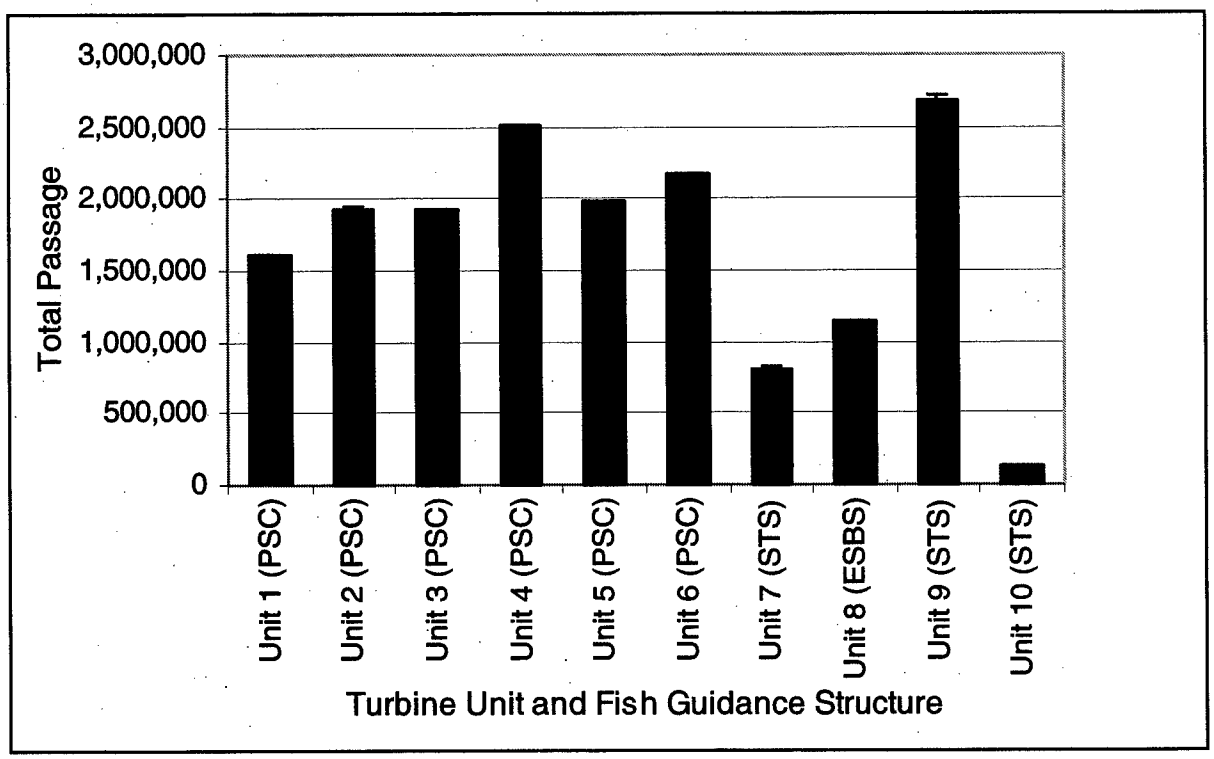

Figure 12. Horizontal distribution of total fish passage at Powerhouse 1 turbines in spring

The total passage at Powerhouse 1 was estimated to be about 13.8 M fish in summer. The horizontal distribution of passage at Powerhouse 1 was very similar to that in spring, with about 68 percent (9.4 M fish) passing through PSC Units 1-6 (Figure 13). Of the remaining 32 percent (4.4 M fish) that passed to the north of the wing wall, passage was divided almost equally between Unit 9 and the other three units combined (Units 7, 8, and 10). Unit 9 passed about 2.2 M fish and the other three units shared about the same number roughly equally. As in spring, Unit 9 passed more fish than did any other turbine unit at the project in summer.

Horizontal distribution of flow in spring. On the scale of specific turbine units, there was no clear relationship between the horizontal distribution of flow and that of fish passage in spring. Except for Unit 10, which ran only about half as much as the others, flow through all of the Powerhouse 1 turbine units was approximately equal (Figure 14). However, fish passage (Figure 12) was highest at Unit 9, and it also was high at Unit 6 and the rest of the units south of the wing wall (the PSC units) and was notably low at Units 7, 8, and 10.

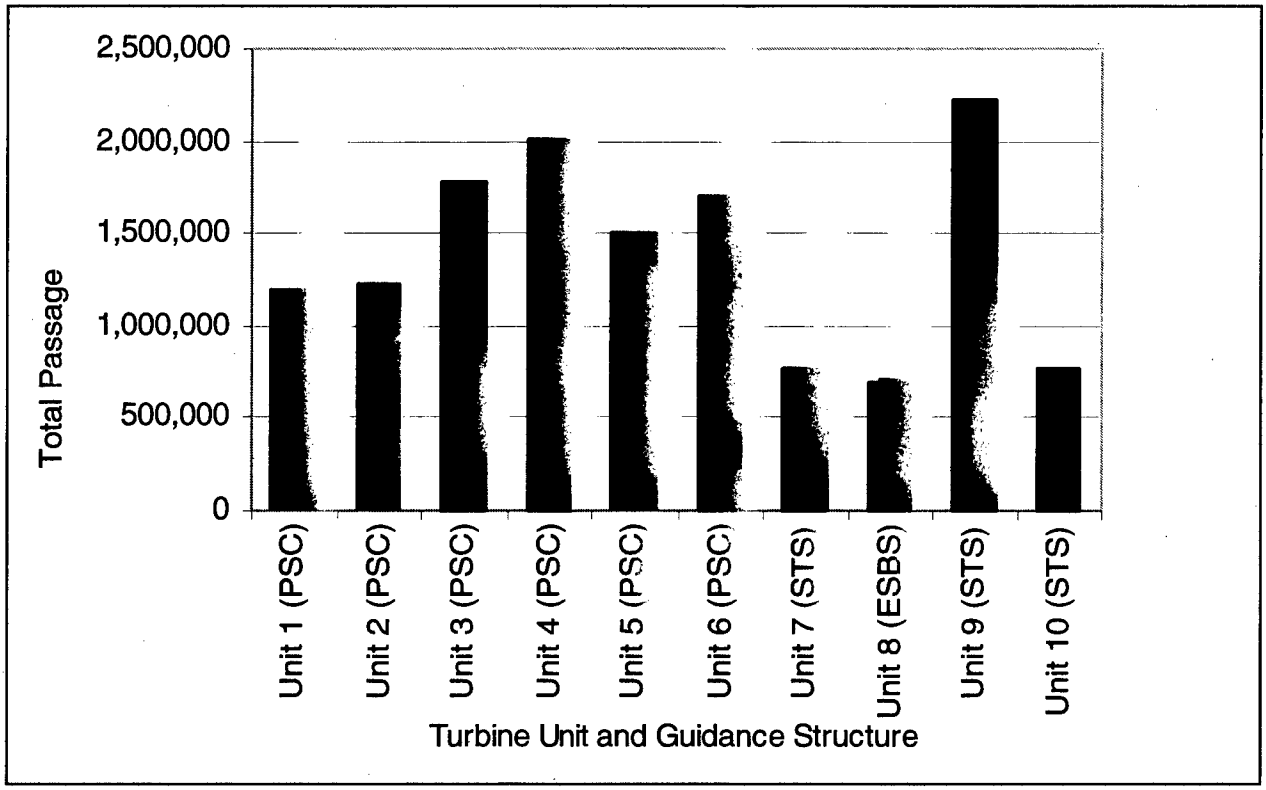

Figure 13. Horizontal distribution of fish passage at Powerhouse 1 turbines in summer

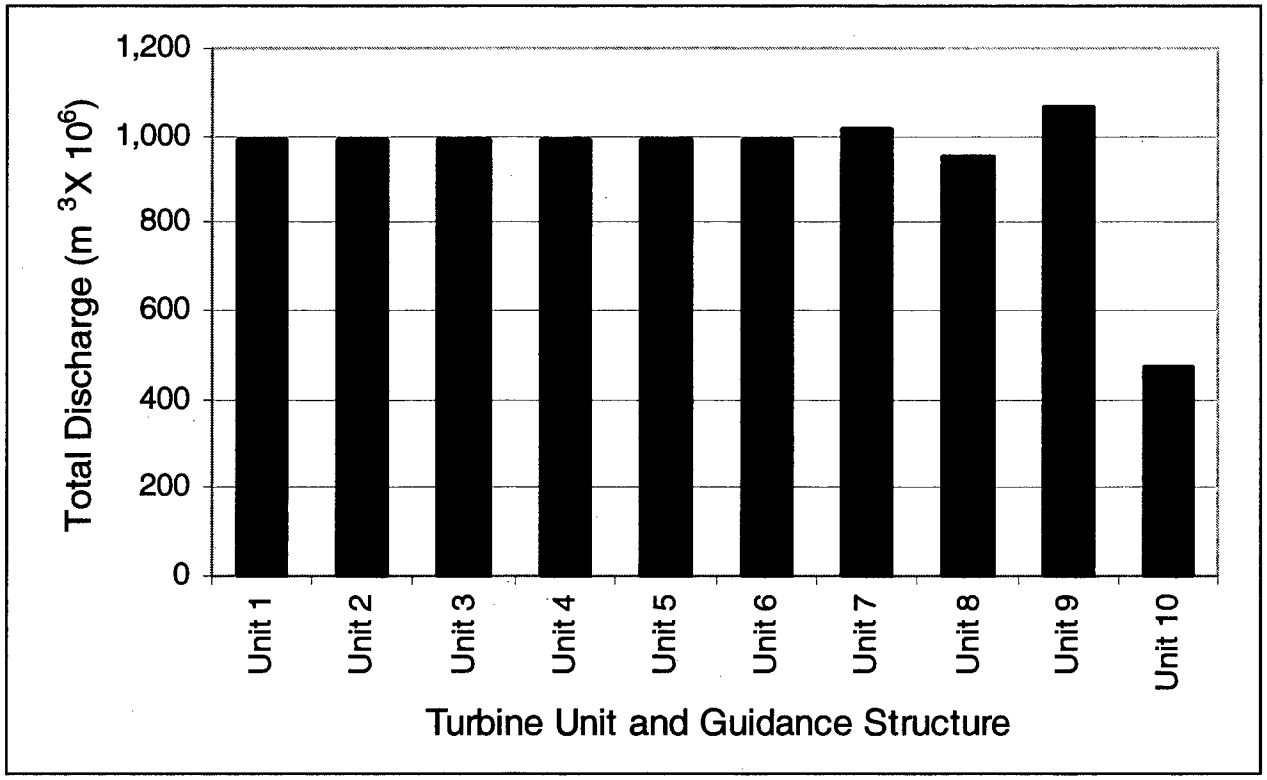

Figure 14. Horizontal distribution of discharge through turbines at Powerhouse 1 in spring

Summer discharge across Powerhouse 1 was ranged from 463 million m^3 through Unit 7 to 650 million m^3 through Unit 10 (Figure 15), and flow again did not closely mirror fish passage (compare Figures 13 and 15). Unit 9 again passed more fish than any other unit and Units 7, 8, and 10 passed fewer fish than their proportion of flow would predict.

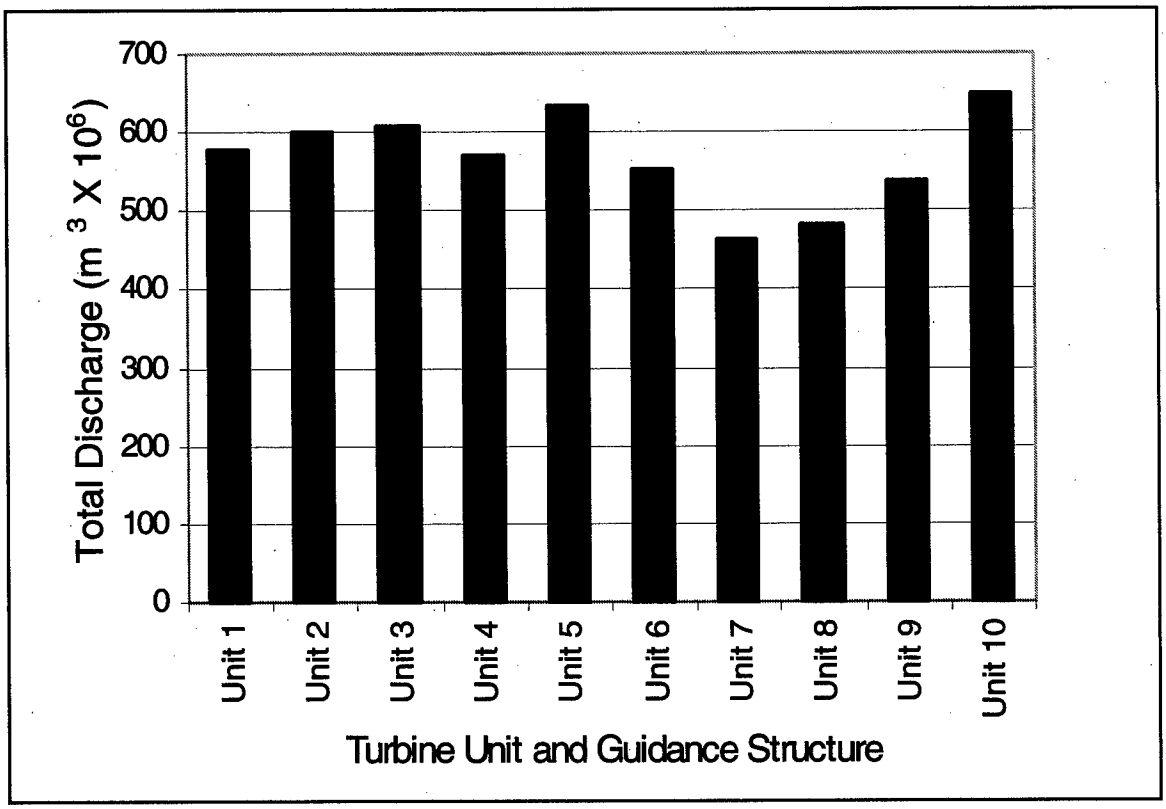

Figure 15. Horizontal distribution of discharge through turbines at Powerhouse 1 in summer

Horizontal distribution of fish passage density. To avoid the complexity inherent in different turbine units having different operating schedules, fish passage densities (the ratio of total fish passage to total discharge at each turbine unit or spill bay section) were calculated for both spring and summer (Figures 16 and 17).

Overall spring fish passage density was 1,643 fish per million m^3 of water passed. The highest fish passage densities were through Unit 4 south of the pier between Units 6 and 7 and through Unit 9 north of the pier. The lowest densities were through Units 7, 8, and 10. Note that the values from the turbine units represent both guided and unguided fish. Units 1-6 and 9 at Powerhouse 1 passed more fish per unit volume than Units 7, 8, and 10 in spring.

In summer, fish passage density was higher than it was in spring (Figure 17). Except that Unit 9 had a higher fish passage density than did Unit 4, the general horizontal distribution of fish passage density is very similar between the two seasons.

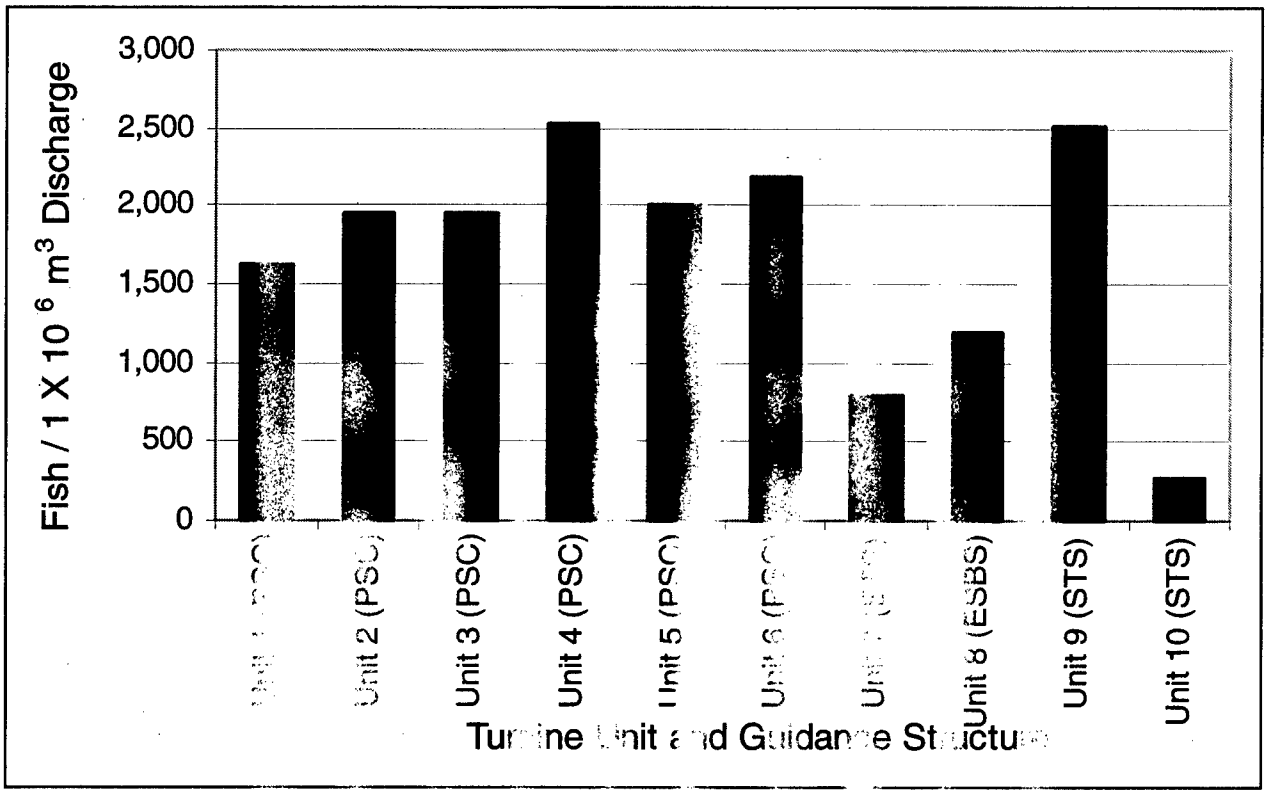

Figure 16. Horizontal distribution of fish density through turbines at Powerhouse 1 in spring

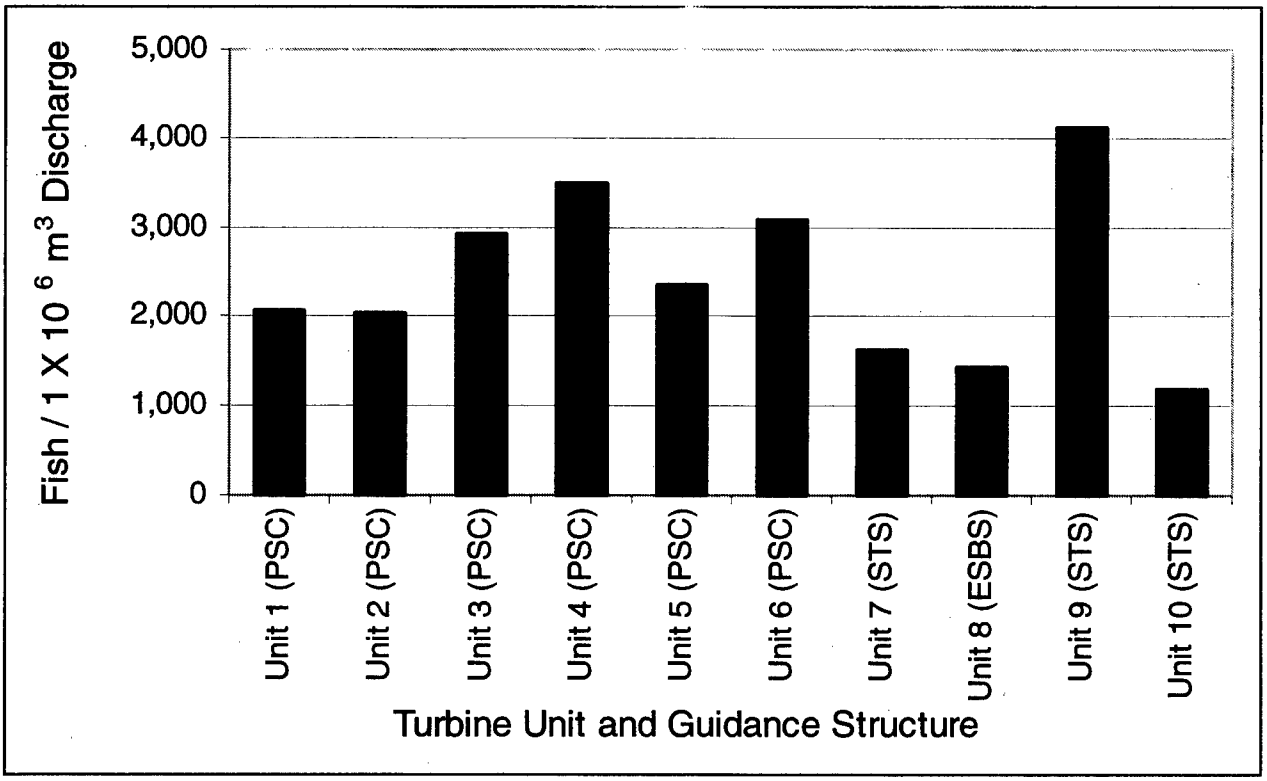

Figure 17. Horizontal distribution of fish density through turbines at Powerhouse 1 in summer

Vertical distribution of fish passage

At the first powerhouse most fish were detected high in the water column. Upstream of the PSC, from 92 to 99 percent of all fish detected at each unit during the spring were above the elevation of the floor of the PSC. Fish were highest in the water column at Unit 6, and were lowest at Units 2 and 5. For all five PSC slots that were sampled, 95 percent of all detected fish were above the elevation of the floor of the PSC (Figure 18).

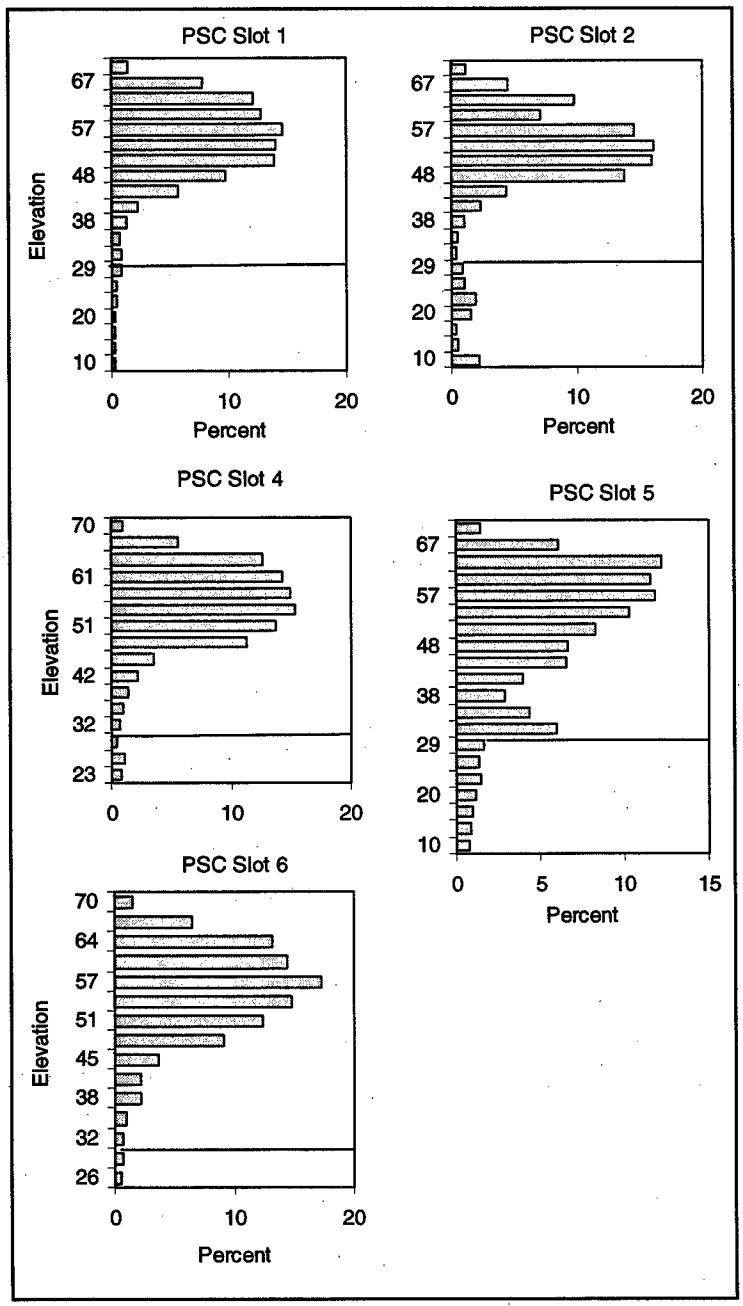

Figure 18. Vertical distribution of fish upstream of PSC slots sampled in this study in spring 2000. Horizontal lines denote the elevation of the top of the intake

At the first powerhouse, most fish detected during summer also were high in the water column (Figure 19), and the overall vertical distribution of fish was only slightly lower than it was during the spring. Upstream of the PSC, from 85 to 96 percent of all fish detected at each unit during the summer were above the elevation of the floor of the PSC. For all five sampled PSC slots combined, 93 percent of all detected fish were above the elevation of the floor of the PSC.

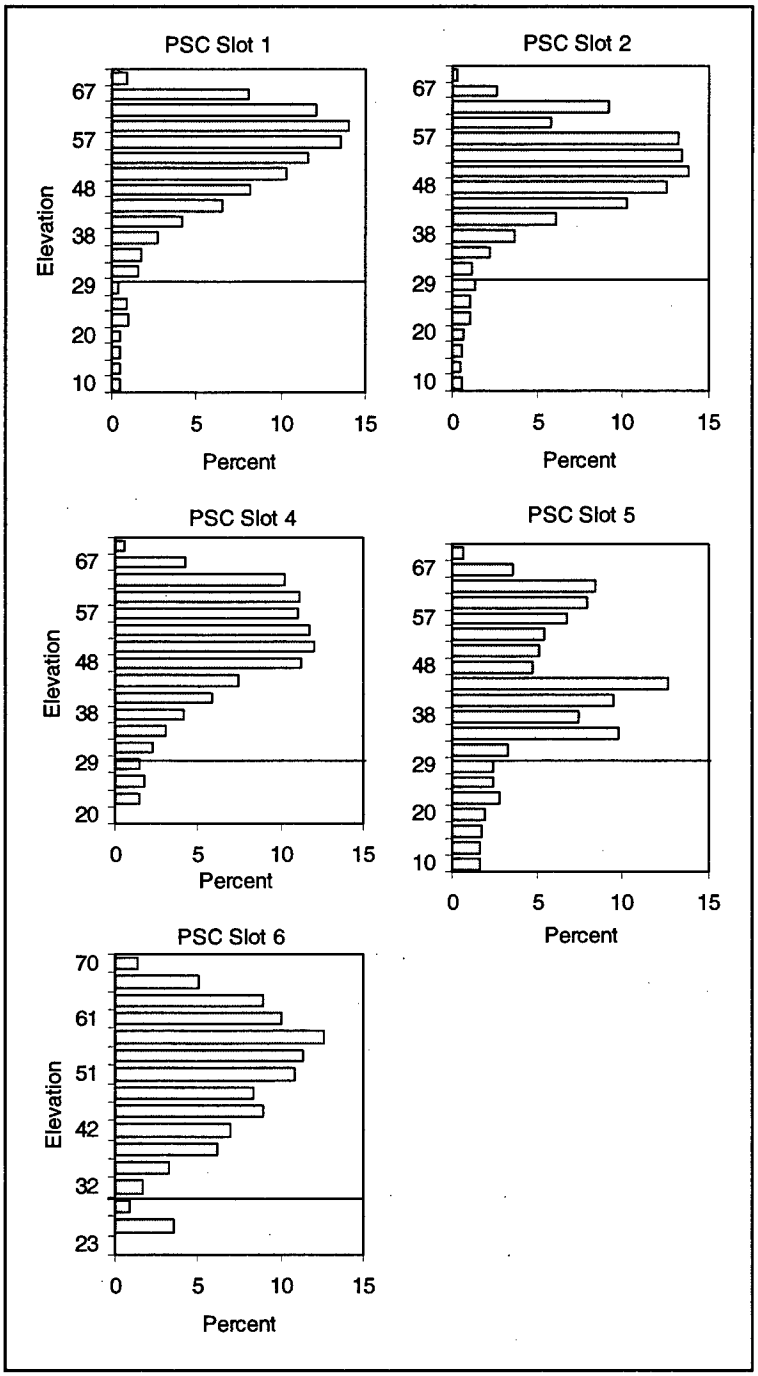

Figure 19. Vertical distribution of fish upstream of PSC slots sampled in this study in summer 2000. Horizontal lines denote the elevation of the top of the intake

A higher proportion of fish were detected deeper in the water column at night than during the day during both seasons (Figure 20; Table 9). From 93 to 99 percent of fish detected during the day and from 77 to 98 percent of fish at night were detected above the elevation of the floor of the PSC in spring. Overall, 97 percent of daytime fish and 88 percent of night time fish were detected above the elevation of the floor of the PSC in spring.

In summer and upstream of the sampled PSC slots, a higher proportion of fish were detected deeper in the water column at night than during the day (Figure 20; Table 9). From 86 to 96 percent of fish detected during the day and from 80 to 93 percent of fish at night were above the elevation of the floor of the PSC. Overall, 95 percent of daytime fish and 90 percent of night time fish were detected above the elevation of the floor of the PSC in summer.

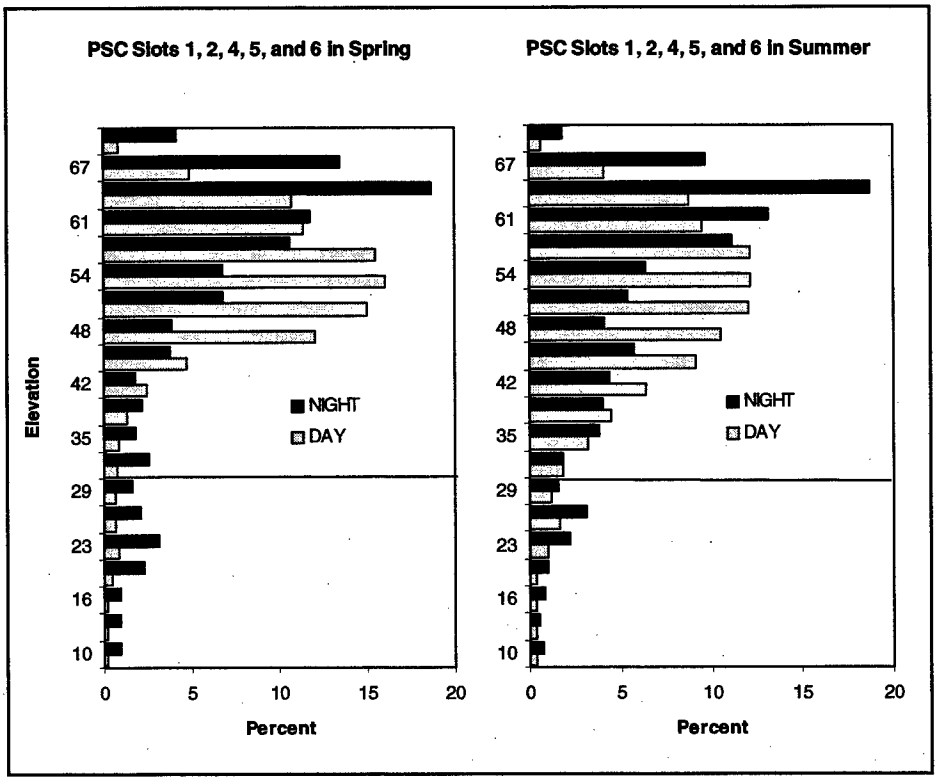

Figure 20. Day and night vertical distributions of fish upstream of sampled PSC slots in spring and summer. The horizontal line indicates the PSC floor elevation

Table 9
Percentage of Fish Detected Above the Floor of the Sampled PSC Slots. The floor was located at 30.5 ft mean sea level

	Spring			Summer		
Location	Day	Night	Overall	Day	Night	Overall
ALL	97	88	95	95	90	93
Slot 1	97	93	97	96	93	96
Slot 2	93	77	92	95	85	94
Slot 4	98	97	98	95	93	95
Slot 5	94	82	92	86	80	85
Slot 6	99	98	99	96	92	95

Major Passage Metrics — Temporal Trends

Seasonal trends

Spring hydroacoustic sampling at the Bonneville Powerhouse 1 and JBS sampling at Powerhouse 2 by the NMFS both indicated that peaks in the spring run occurred near 22 April and sometime during late May (Figure 21). Comparisons were not made in summer because passage through Powerhouse 2 JBS in summer was low and variable because only 2-3 units were operated. Sampling within the JBS at Powerhouse 1 by the NMFS was only designed to estimate rates of smolt descaling and thus was not quantitative enough to make a run timing estimate suitable for comparison to run timing by hydroacoustic sampling.

A comparison of run timing by netting and hydroacoustic estimates of fish passage at Unit 8 revealed similar patterns in spring and early summer, although the patterns diverged more in summer than in spring (Figure 22). The peak in late May (between Julian Days 140 and 145) was in the same time frame as that observed by hydroacoustic sampling at Powerhouse 1 and by NMFS sampling in the Powerhouse 2 JBS in spring (compare Figures 21 and 22). Sampling at Unit 8 with hydroacoustics and netting (Figure 22) began after the early spring peak detected between Julian Days 110 and 115 by general hydroacoustic sampling at Powerhouse 1 and JBS sampling at Powerhouse 2 (Figure 21).

Powerhouse 1 fish passage efficiency

The efficiency of fish passage at Powerhouse 1 declined significantly from early spring through mid-summer, although the means only differed by about 6 percent (Figure 23). Fish guidance structures at Powerhouse 1 included the PSC at Units 1-6, an ESBS at Unit 8 and STSs at Units 7, 9, and 10. The mean FPE estimate for Powerhouse 1 declined from 0.67 (CI = 0.004) in spring to 0.61 (CI = 0.002) in summer, and summer estimates were less variable than spring estimates (Figure 23).

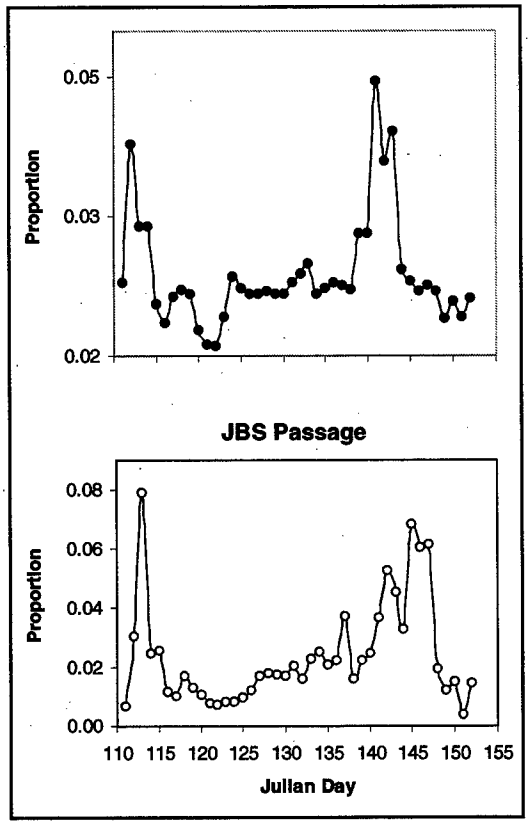

Figure 21. General pattern of spring run timing at Powerhouse 1 estimated by hydroacoustics compared with estimates by sampling smolts with a trap in the Powerhouse 2 JBS

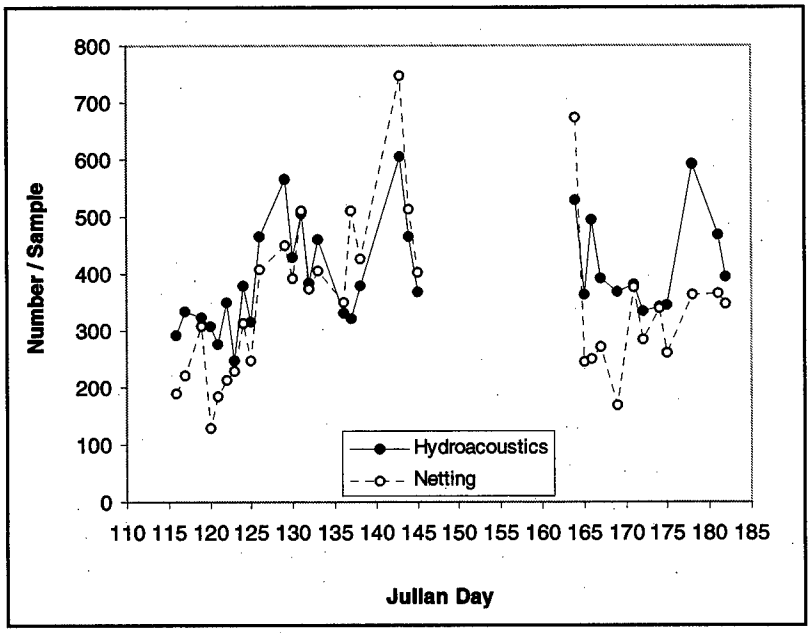

Figure 22. Run timing as determined by hydroacoustic sampling and by NMFS netting of Unit 8 at Powerhouse 1

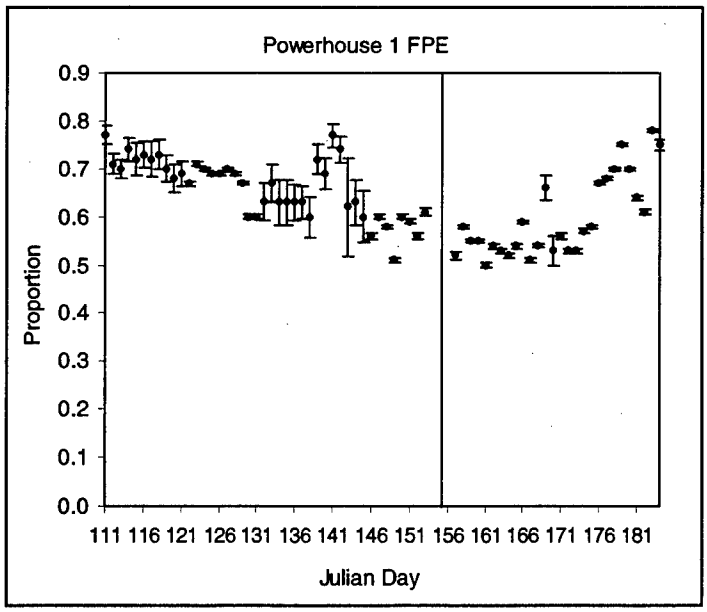

Figure 23. Plot of the average FPE of Powerhouse 1 from spring through summer

Unlike the efficiency of the ESBS and STSs, which declined significantly from spring through summer, the efficiency of the PSC remained high in both seasons (Figure 24).

The average effectiveness of the PSC at Powerhouse 1 ranged from about 1.8 to 2.4. It was just as high in summer as it was in spring (Figure 25).

Diel patterns of fish passage

At Powerhouse 1, the fish passage through turbines tended to be lowest during the day from about 1000 to 1800 hours in spring, whereas it was crepuscular in summer with a peak just after dark and another about sunrise (Figure 26). In contrast to fish passage through turbines, passage through the PSC was highest during the day from about 0900 to 2100 hours in spring and between 1000 and 1700 hours in summer (Figure 26).

The hourly proportion of fish passing under the PSC varied little among hours of the day in spring, whereas unguided passage under the PSC in summer and under in-turbine screens in spring and summer peaked around the time of sunset (Figure 27).

The diel pattern of fish detections in the upper and the bottom half of the PSC slots was strongly skewed toward daytime hours; most fish were detected in the upper water column, and there was no diel pattern in numbers detected below the PSC floor (Figures 28 and 29). Interestingly, the diel pattern for fish detected in the lower 22.5 ft of the PSC slot was more compressed around midday than the pattern for fish in the upper 22.5 ft of the slot.

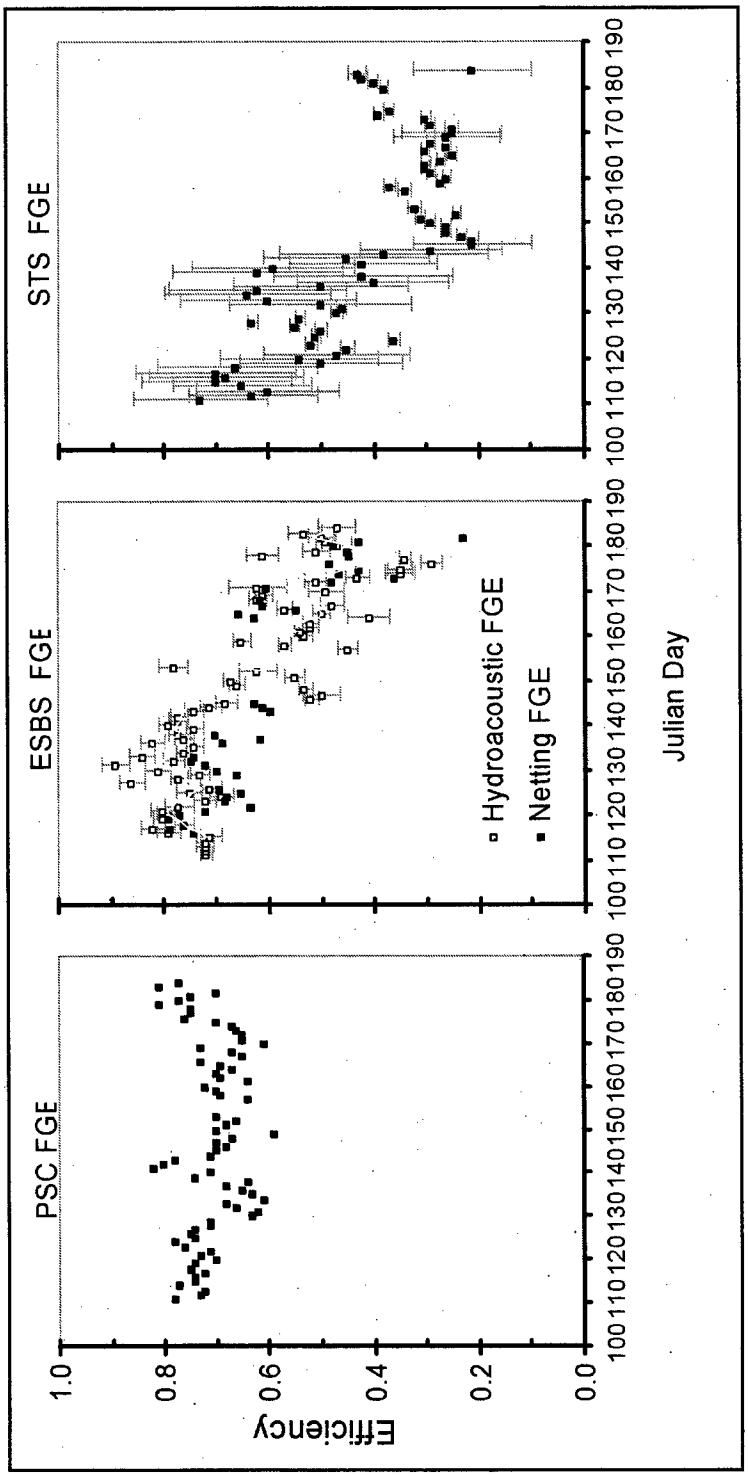

Figure 24. Plot of the FPE of the PSC, the ESBS at Unit 8, and the STS at Units 7, 9, and 10 by Julian Day in spring and summer

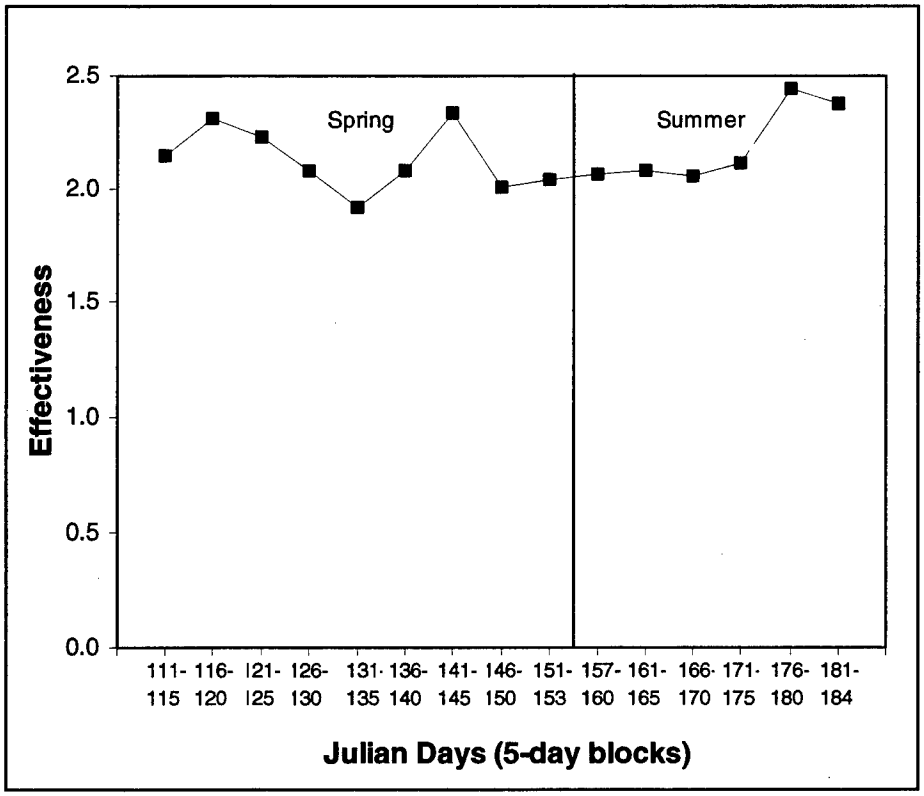

Figure 25. Plot of average PSC effectiveness by Julian Day in spring and summer

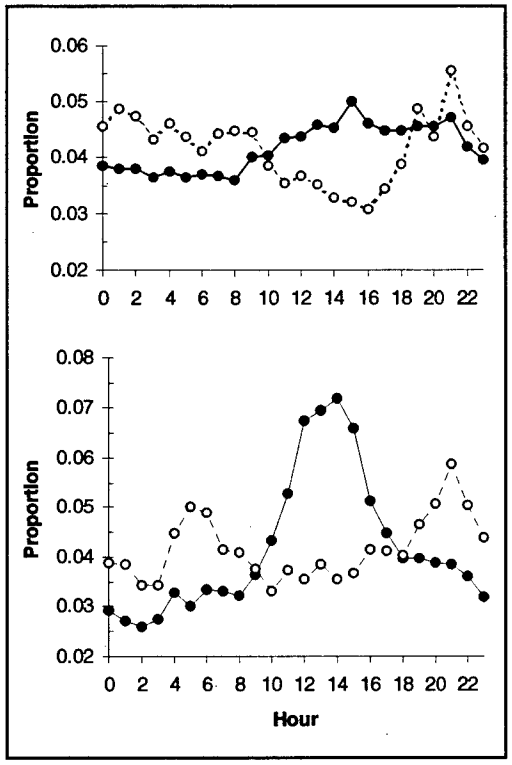

Figure 26. Diel patterns of fish passage through the PSC and turbines at Powerhouse 1 in spring (top) and summer (bottom)

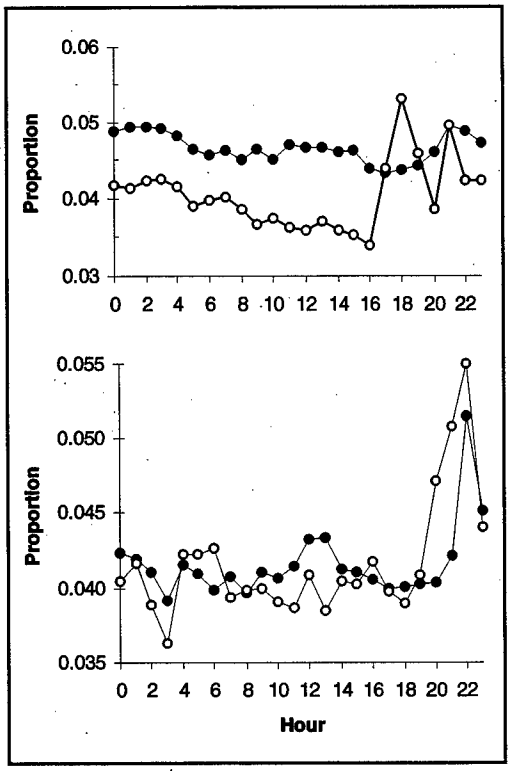

Figure 27. Diel trends in fish passage under the PSC and screens located in Turbines 7-10 at Powerhouse 1 in spring (top) and summer (bottom)

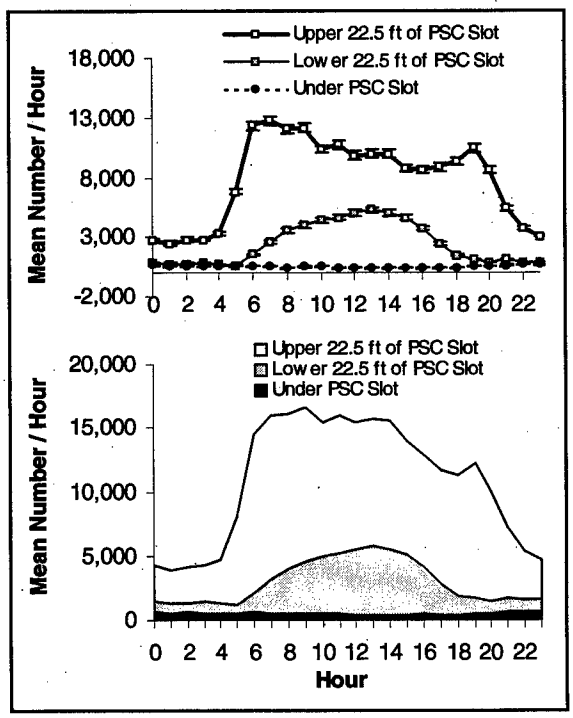

Figure 28. Diel pattern in the number of fish detected in three depth strata immediately upstream of PSC slot entrances in spring (top) and the cumulative number per hour (bottom)

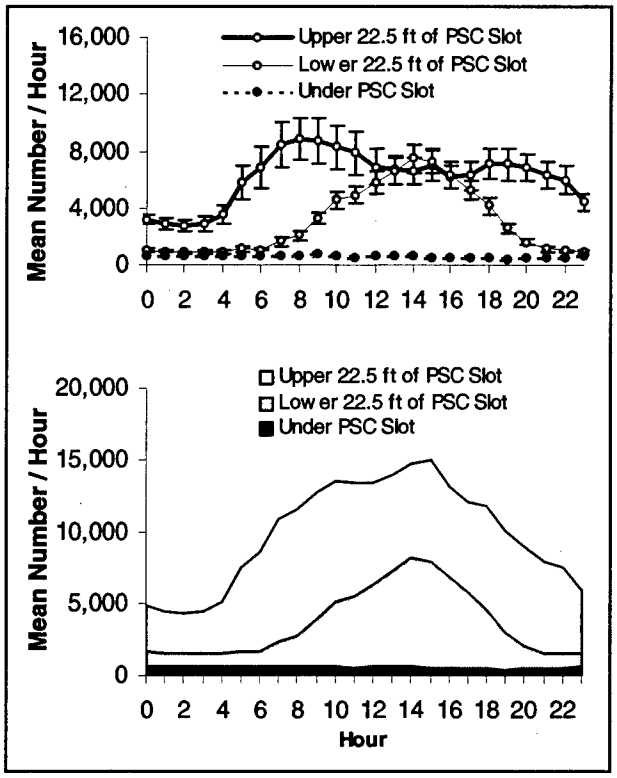

Figure 29. Diel pattern in the number of fish detected in three depth strata immediately upstream of PSC slot entrances in summer (top) and the cumulative number per hour (bottom)

Fish Guidance Efficiencies

Background

FGE is the ratio of the estimated number of fish passing a turbine by a non-turbine route (guided fish) to the estimated number of all of the fish passing that turbine (guided + unguided fish). FPE is the same calculation done on the scale of the PSC, a powerhouse, or the entire project.

Comparing performance of fish guidance structures

No significant correlations were found between hourly counts of fish detected in turbine intakes downstream of the PSC with hourly counts of fish detected immediately upstream of corresponding 20-ft wide PSC slot entrances. Similarly, the sum of hourly counts of fish detected in Turbines 1, 2, 4, 5, and 6 was not significantly correlated with the sum of hourly counts of fish upstream of slot entrances (Figure 30). The number of fish detected upstream of PSC slots almost always was significantly higher than the number detected in turbines downstream of the PSC. Interestingly, the diel patterns of fish detections upstream of PSC slots were generally similar to those of fish detected inside turbines downstream

of the PSC, i.e., both were skewed toward the daytime (compare Figure 26 with Figures 28 and 29).

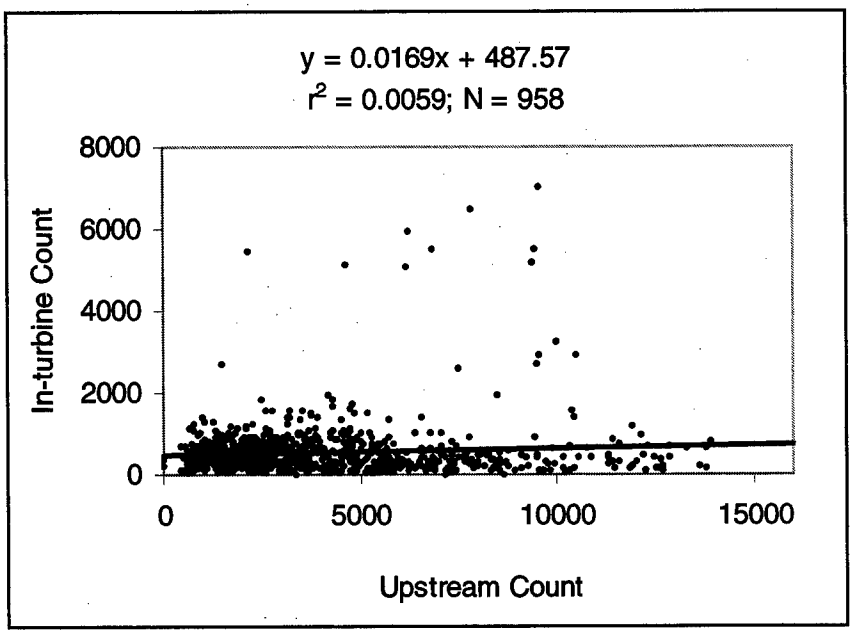

Figure 30. Scatter plot of hourly in-turbine counts of fish downstream of the PSC at Units 1, 2, 4, 5, and 6 as a function of counts upstream of the same 20-ft wide PSC slot entrances

The expected marked decline in FGE was observed at all of the turbine units that are only equipped with screens (11 STSs or the one ESBS) for fish guidance, but FGE of the PSC was found to remain as high in summer as it was in spring (0.72, see Figure 24). The Powerhouse 1 turbine units with STSs (Units 7, 9, and 10) had an estimated average FGE of 0.48 in spring and 0.36 in summer. FGE at the ESBS at Unit 8 was 0.72, as good as the average PSC FGE, in spring but it was only 0.50 in summer.

In both seasons, PSC Units 5 and 6 south of the pier between Units 6 and 7 had the highest FGEs among Powerhouse 1 units and the only estimated values over 80 percent (Figures 31 and 32; Table 10). In spring, PSC Units 2 and 8 (ESBS) shared the next highest echelon of estimated FGE values, between 0.70 and 0.80. Three PSC units (Units 1, 3, and 4) had FGEs between 0.60 and 0.70. Four STS units (Units 9 and 10 on Powerhouse 1 had FGEs of 0.50-0.60. Unit 7 (STS on Powerhouse 1) had the lowest spring FGE of 0.21. Unit 10 was off line for part of the spring and ran only about half as much as did the other turbine units.

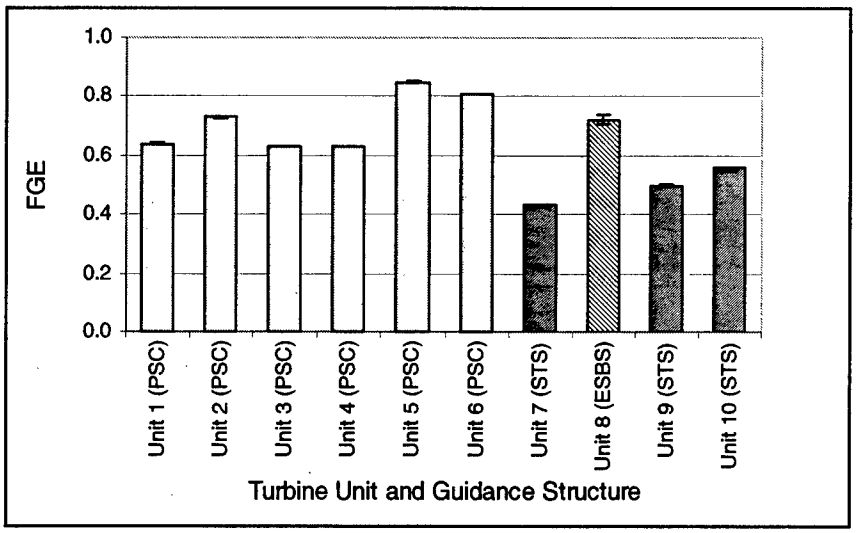

Figure 31. Estimated FGE by turbine unit in spring. Error bars are 95 percent confidence limits. Shading denotes units with different fish protection devices

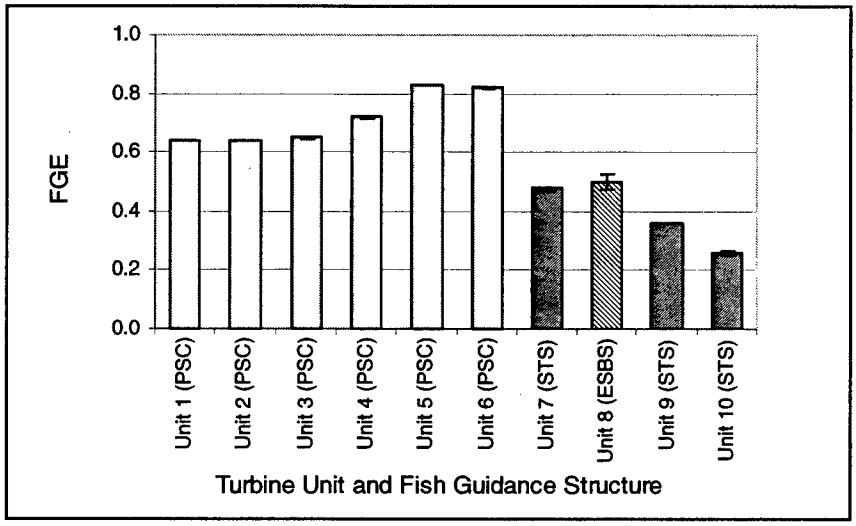

Figure 32. Estimated FGE by turbine unit in summer. Error bars are 95 percent confidence limits. Shading denotes units with different fish protection devices

In summer the turbine units with the highest FGEs were again Units 5 and 6, but the overall profile of FGE across the dam was considerably different from that in spring (compare Figures 31 and 32). The average FGE at the PSC was the same (0.72) for summer although the FGEs of the individual PSC turbine units were less variable than during spring. FGE estimates at Units 1-3 were similar and the lowest in the PSC (0.63-0.64), Unit 4 was slightly higher (0.72), and Units 5 and 6 had estimated summer FGEs of 0.83 and 0.82, respectively.

Whereas the FGEs at the PSC held up well in summer, those from the screened turbine units north of the wing wall had lower values (Figure 32). The most extreme decline from spring to summer was at Unit 10 (with STSs) where the estimated FGE dropped 30 percent from 0.56 in spring to 0.26 in summer.

Unlike in spring, Unit 10 was on line about as much as were the other turbine units at Powerhouse 1 in summer. The next most severe loss in FGE was at Unit 8 (with ESBS) where the estimate went from 0.72 in spring to 0.50 in summer, a decrease of 22 percent. Unit 9 dropped from 0.50 in spring to 0.36 in summer, but Unit 7 showed an increase of about 5 percent, from 0.43 to 0.48.

Table 10
Fish Guidance Efficiencies at Powerhouse 1 in Spring and Summer

FGE Range	Spring	Summer
> 80%	Units 5 & 6 (PH-1; PSC)	Units 5 & 6 (PH-1; PSC)
70-80%	Unit 2 (PH-1; PSC) Unit 8 (PH-1; ESBS)	Unit 4 (PH-1; PSC)
60-70%	Units 1, 3, & 4 (PH-1; PSC)	Units 1, 2, & 3 (PH-1; PSC)
50-60%	Unit 9 & 10 (PH-1; STS)	Unit 8 (PH-1; ESBS)
40-50%	Unit 7 (PH-1; STS)	Unit 7 (PH-1; STS)
30-40%		Unit 9 (PH-1; STS)
< 30%		Unit 10 (PH-1; STS)

Note: Turbine units are grouped in 10% bins according to their FGE estimates. Note that, in summer, the FGE estimate for the ESBS on Unit 8 is just 50%, and so it is on the line between the 40-50% and the 50-60% bins.

Simultaneous examination of guided and unguided fish passage trends by turbine (Figures 33 and 34) helps put the FGE estimates (Figures 31 and 32) into perspective. In Figures 33 and 34, the vertical axis at zero represents the dividing elevation of the fish guidance structure (e.g., the floor elevation of PSC Units 1-6, the tip of the ESBS on Unit 8, or the tips of the STSs at Units 7, 9, and 10. The negative numbers indicate unguided fish below the fish guidance structures and the positive numbers indicate guided fish above that elevation.

In spring Unit 8's ESBS had as high an FGE estimate as the mean for the PSC units (72 percent), but it is clear from Figure 33 that fewer fish passed at Unit 8 than passed at any of the PSC units. More fish encountered Unit 9 than any other turbine unit, but Unit 9 guided only about 50 percent of them.

In summer the PSC had a substantially higher FGE than Units 7-10 with screens and passed more fish (Figure 34). A surprisingly high number of fish encountered Unit 9 in summer, as compared to the other turbine units, but only about 36 percent were guided by the STSs there.

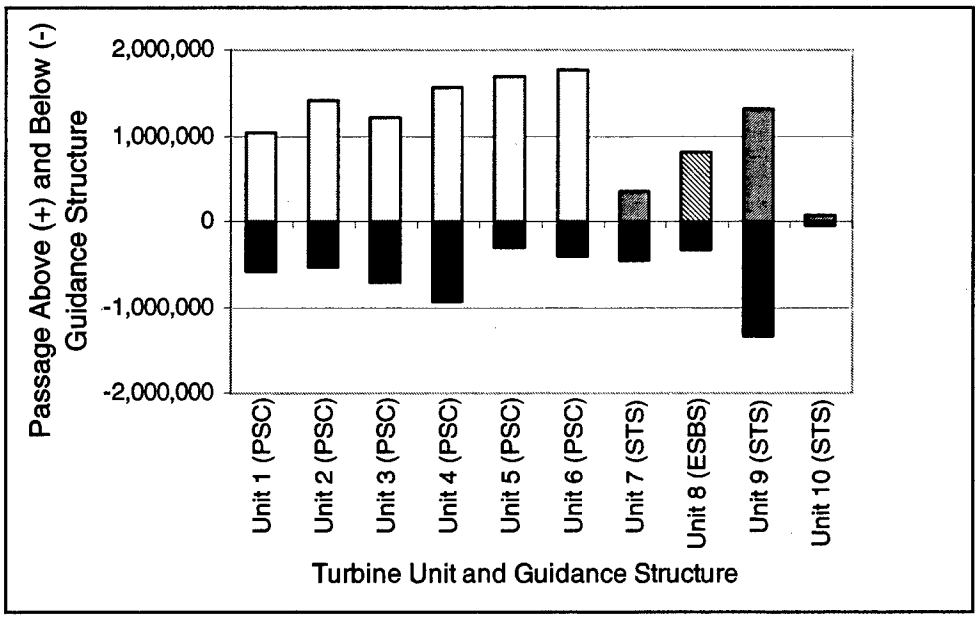

Figure 33. Estimated total fish passage above and below fish guidance structures (floor of PSC or screens) in spring. The vertical axis at zero represents the division between guided and unguided passage (PSC floor, ESBS tip, or STS tip). Shading denotes units with different fish protection devices

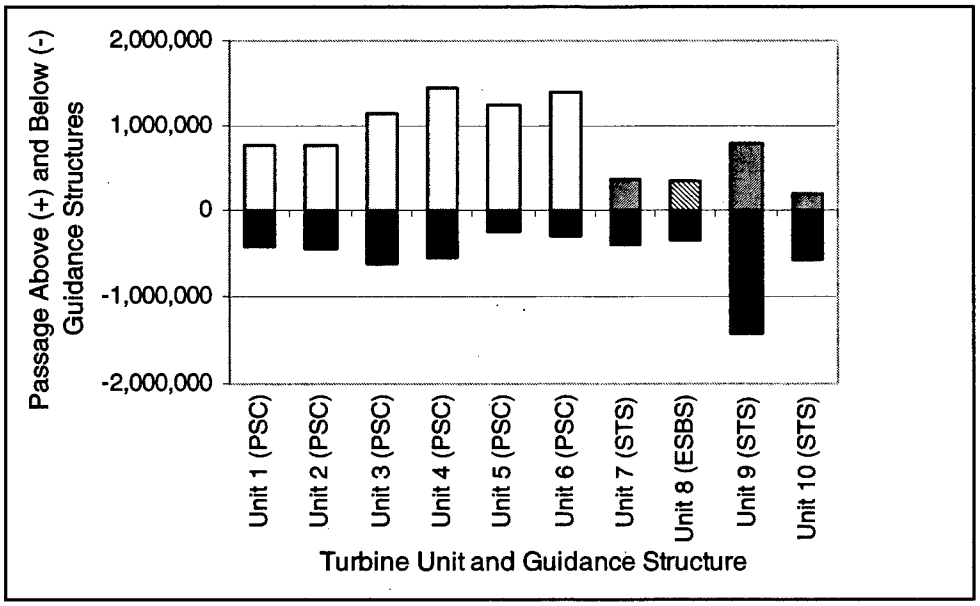

Figure 34. Estimated total fish passage above and below fish guidance structures (floor of PSC or screens) in summer. The vertical axis at zero represents the division between guided and unguided passage (PSC floor, ESBS tip, or STS tip). Shading denotes units with different fish protection devices

The effectiveness of the PSC was higher at Unit 5 and 6 (about 2.5) than it was at Units 1-4 (mean = 1.9-2.2) in spring and summer (Figures 35 and 36), where effectiveness is the efficiency for guiding fish relative to the efficiency for guiding water.

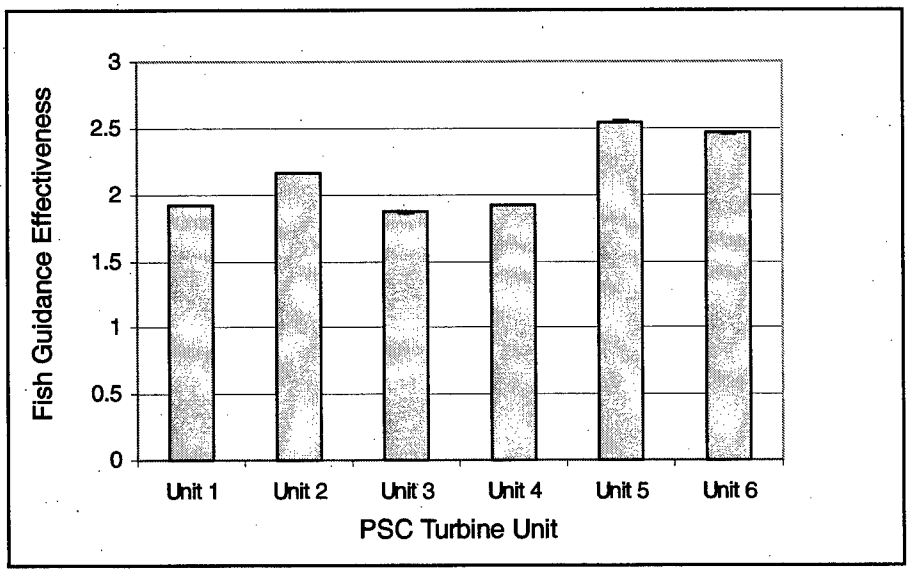

Figure 35. Relative effectiveness of PSC units for passing fish in spring, where effectiveness is the ratio of FGE to water guidance efficiency

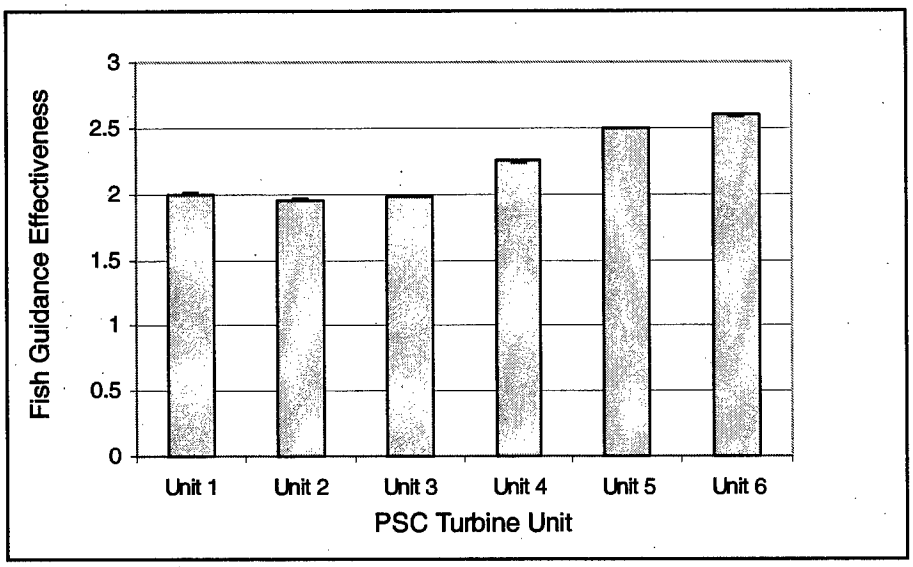

Figure 36. Relative effectiveness of PSC units for passing fish in summer, where effectiveness is the ratio of FGE to water guidance efficiency

Comparing FGE sampling methods at Unit 8

The fish passage estimates from the up-looking and down-looking beams at Unit 8 are compared with NMFS estimates based upon gatewell dipping of guided fish and fyke netting of unguided fish. The NMFS samples were collected on

40 evenings in both spring and summer for about 2 hours each (starting at 2000 hr and ending from 2205 hr to 2250 hr, the mean duration being 2 hr 31 min). Hydroacoustic samples were able to be paired up with netting samples from only 33 of the 40 days sampling in spring and summer because of equipment problems in spring (see Materials and Methods).

Hydroacoustic estimates of the number of fish guided by the ESBS were significantly correlated with the number of guided fish dipped from the gatewell (Figure 37), as were hydroacoustic estimates of unguided fish with numbers of unguided fish collected in fyke nets (Figure 38). The slopes of the correlation lines for guided and unguided fish were 0.85 and 0.93, when the intercepts were forced through zero. Only about 53 percent of the variation in netting estimates was explained by the hydroacoustic estimates.

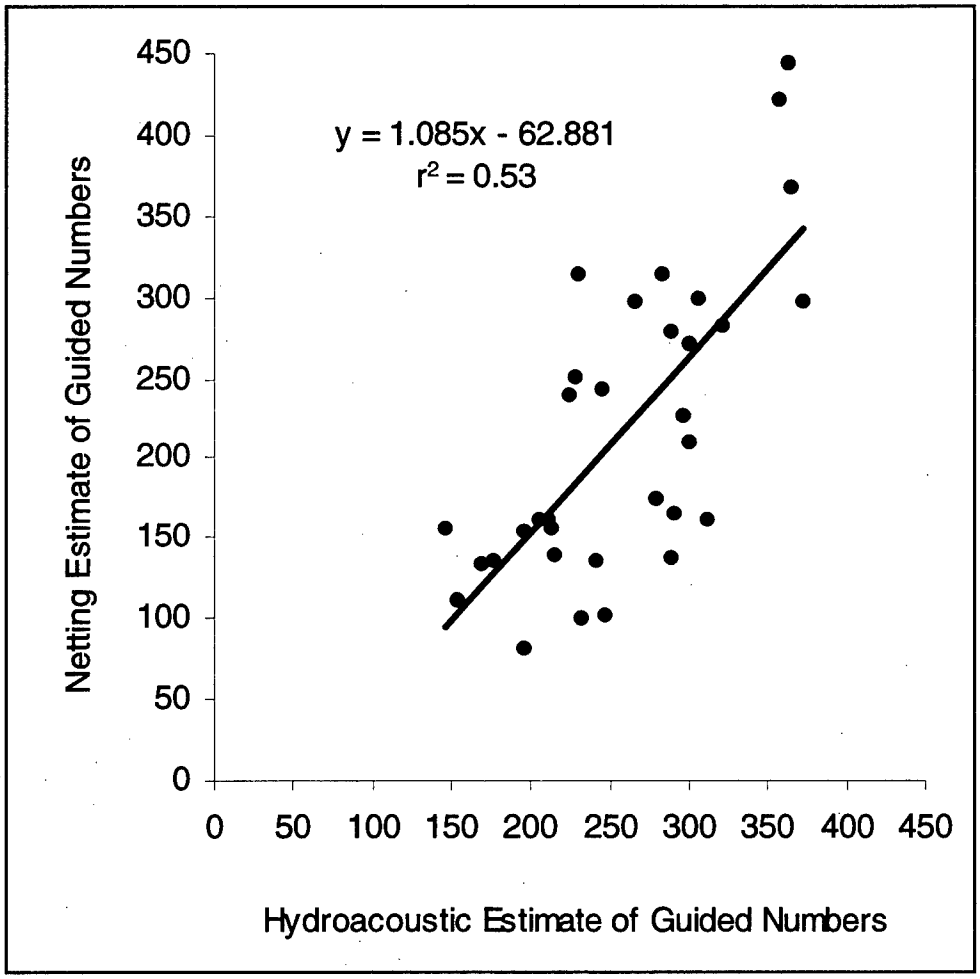

Figure 37. Correlation of gatewell-dipping estimates of the number of fish guided by the ESBS at Unit 8 with hydroacoustic estimates

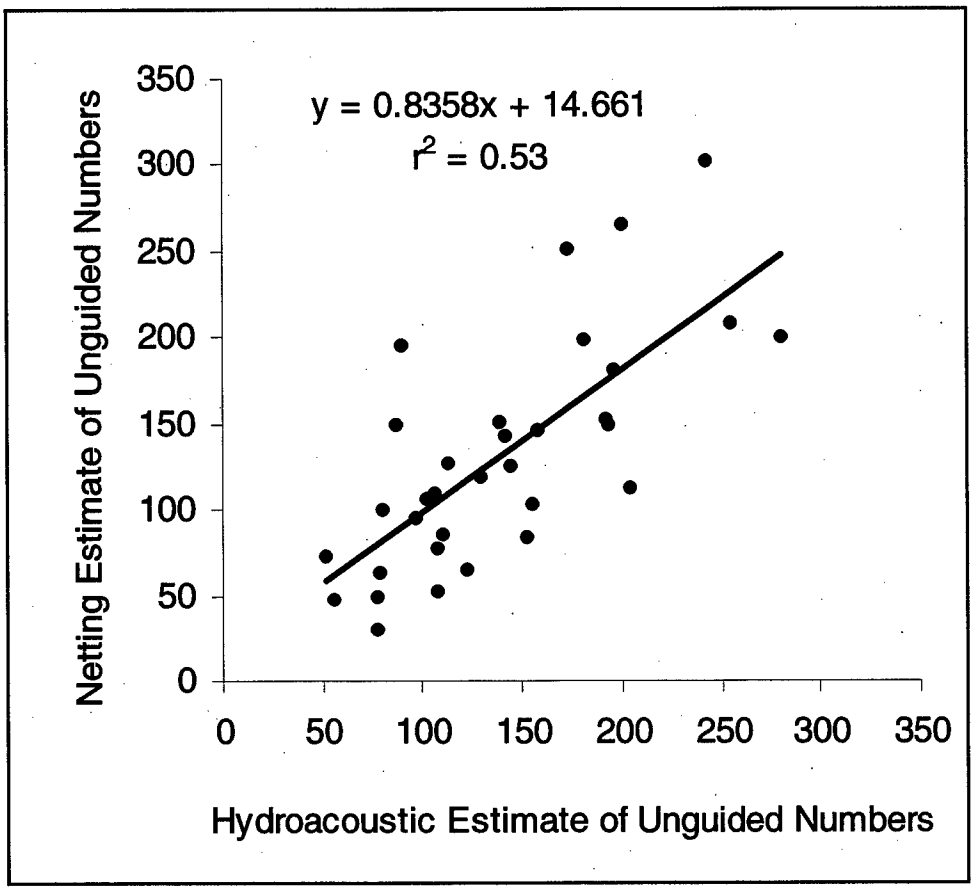

Figure 38. Correlation of fyke netting estimates of the number of fish passing under the ESBS at Unit 8 with hydroacoustic estimates

The correlation of netting and hydroacoustic estimates of FGE at Unit 8 also were highly significant (Figure 39). A single point in the figure (x and y coordinates 0.50, 0.24) seemed to be an obvious outlier for the correlation, but dropping it from the analysis could not be justified. Excluding that point from the correlation increased the r^2 value by only 3 percent, from 0.65 to 0.68. The r^2 for FGE estimates was 12 percent higher than corresponding statistics for numbers of guided and unguided fish.

Paired t-tests of paired observations indicated that hydroacoustic and netting estimates of FGE did not differ significantly in spring, but differences were significant in summer despite low sample sizes (Table 11). After pooling spring and summer observations, a t-test indicated that the means were significantly different, although they only differed by 3 percent.

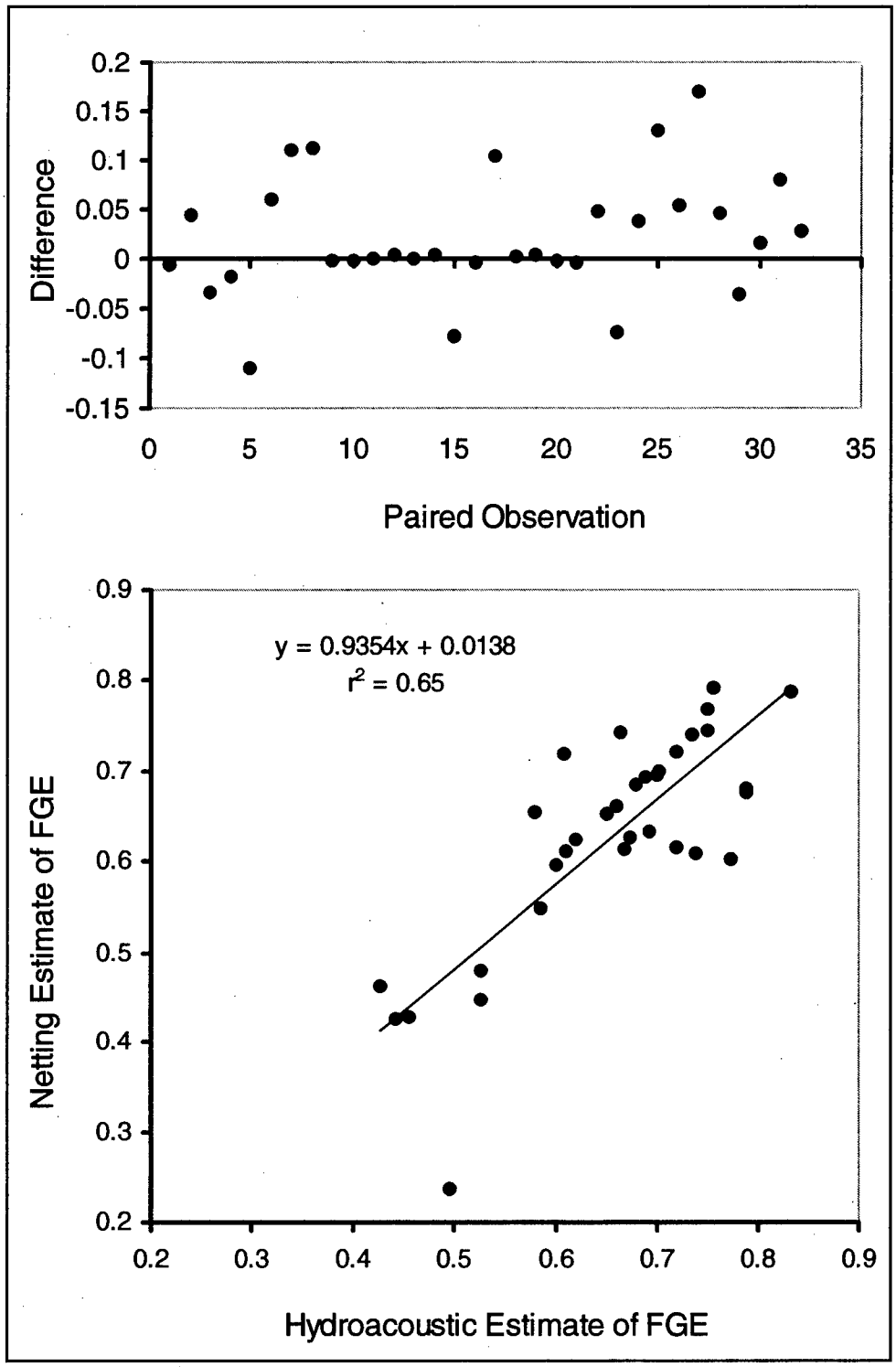

Figure 39. Plot of the difference in hydroacoustic and netting estimates of FGE for the ESBS in Unit 8 (top) and of the correlation of netting estimates of FGE at Unit 8 (bottom) with hydroacoustic estimates

Table 11
Paired t-Tests Comparing Mean Estimates of FGE by Hydroacoustics and Netting for the ESBS at Unit 8 in Spring, Summer, and Both Seasons

Statistics	Season					
	Spring		Summer		Both	
Statistics	Acoustic	Netting	Acoustic	Netting	Acoustic	Netting
Mean	0.7009316	0.6923437	0.5744144	0.5111946	0.6549254	0.6264713
Variance	0.0041179	0.0033514	0.0136211	0.0146673	0.0110757	0.0149674
Observations	21	21	12	12	33	33
Hypothesized Mean Difference	0		0		0	
df	20		11		32	
t Stat	0.7217173		2.4480456		2.2406703	
P(T<=t) two-tail	0.4788219		0.0323578		0.0321172	
t Critical two-tail	2.09		2.20		2.04	

4 Discussion

Hydroacoustic Detectability

The motivating force behind efforts to improve detectability modeling is the desire to provide hydroacoustic estimates that are quantitative as well as reliable relative indices to fish passage. Ratio estimators such as the FGE of the PSC, ESBSs, and STSs only require that hydroacoustic beams sampling guided and unguided fish have equal detectability so that ratios of counts, not necessarily the counts themselves, are accurate. Similarly, combining counts from different locations such as powerhouses and a spillway also requires equalization of detectability so that counts from different locations are comparable. Nevertheless, accurate counts estimated by proper expansion of detected fish have the potential to provide estimates with inherent quantitative value as well as providing acceptable relative estimates.

Expanded hydroacoustic counts of guided and unguided fish at Unit 8 were compared with estimates from netting by the NMFS to evaluate the reasonableness of our detectability modeling and the resulting spatial expansion factors. Preliminary hydroacoustic estimates of numbers of guided and unguided fish at Unit 8 were 3-5 times higher than NMFS netting estimates, and this suggested that the calculated effective beam angles were too narrow and spatial expansion factors were too large. On reviewing preliminary modeling efforts, it was found that average target strength had been input rather than a target strength converted from the average backscattering cross section of detected fish. This mistake caused the model to underestimate the hydroacoustic size of fish and effective beam angles. As a result, spatial expansion factors derived from fish detection ranges were overestimated. The use of revised target strength estimates calculated from the average backscattering cross section provided ratios of hydroacoustic and netting estimates that approached 1:1. These results demonstrate the value of using multiple sampling methods for calibration purposes. Ploskey and Carlson (1999) observed that hydroacoustic sampling only provides a relative index to fish passage unless calibrated against unbiased netting.

Quality Control on Automated Fish Tracking

Variability in human counts of fish traces

It was found that different individuals tend to have characteristic biases that manifest themselves in different counts of fish from the same hydroacoustic data sets. As in the last three seasons when the phenomenon of interpersonal bias in echogram counts of fish traces was investigated, it was found that some people tend to consistently track higher or lower numbers of fish traces than other people. This problem occurs even with experienced trackers. Human trackers were hired and trained as a group over about a month before the season started. Basic hydroacoustic theory and practice was taught, deployments were described, tracking criteria were carefully explained, data sets from previous years were tracked by all individuals, results were compared, and then problematic data were tracked again by the group. Considerable and consistent differences remained in fish counts from different people (Figures 8-10). Interpersonal bias is considered an important and persistent error that is often neglected in hydroacoustic data processing. This source of error is especially problematic because the differences among people tend to be consistently biased and are therefore additive over time (Table 8). Whenever human trackers are used to produce fish passage estimates, as is often done, or to calibrate an autotracker, as done here, this tendency for human bias should be considered.

If human trackers are used to provide counts for passage estimates, then the data should be distributed to them in such a way that the bias-induced differences are averaged over time. It is preferable that data are distributed so that each person tracks all systems and deployments for a given day, rather than one person specializing on a given system, deployment, or passage route. Personal biases will then be controlled over many days that have been tracked by the several different people. For example, a high tracking individual processing "guided" routes and a low tracking individual processing "unguided" routes would produce FGE estimates that were too high, whereas the opposite arrangement would produce incorrectly low FGE estimates.

Human vs. autotracker comparisons

The autotracker's performance is considered to be acceptably close to that of the mean human tracker and a much better approximation of the mean human fish count than are some of the more biased human trackers. The autotracker was found to produce fish counts that were close to the means of individual human fish counts on five "tracker calibration days" (Figures 8-10, Table 8), and for all of the days there was a very strong correlation between autotracker counts and the mean count by human trackers (Figure 11).

Major Passage Metrics — Project and Powerhouse FPE, Spill Efficiency, and Spill Effectiveness

Powerhouse 1 FPE declined by only about 6 percent from spring to summer, and the PSC was a major contributor in summer, when the FGE of in-turbine screens declined significantly. If the entire powerhouse had been as efficient as the PSC, Powerhouse 1 FPE in summer would have been about 22 percent higher than a hypothetical FPE provided by 10 turbines with screen efficiencies comparable to that of the ESBS in Unit 8. A full powerhouse PSC would have been about 42 percent more efficient than 10 turbines with STS efficiencies. These differences are highly significant.

Adjustment of PSC efficiency in spring and summer to compensate for not sampling center sluiceways in PSC units would increase mean PSC guidance efficiency to 83-84 percent and raise the PSC contribution to Powerhouse 1 FPE over STS contributions from 6 to 8 percent in spring and 12 to 15 percent in summer. According to radio-telemetry results, about 50 percent of tagged fish in the PSC passed through sluice gates in the center intakes of PSC units (Scott Evans, USGS, and Gary Johnson, BioAnalysts, Personal Communication) where they could not be sampled with hydroacoustics. If that 50 percent estimate held for run-of-the-river (untagged) fish, in-turbine sampling with hydroacoustics would have underestimated PSC efficiency by 15 percent. A correction for sluice passage would increase both spring and summer PSC efficiencies to 83-84 percent. However, adding one-half again as many fish to the PSC-guided category would further increase the southern skew in the Powerhouse 1 fish passage distribution (i.e., consider a 50 percent increase in the height of vertical bars for guided fish at PSC Units 1-6 in Figures 12 and 13). There is no doubt that many run-of-river fish passed through sluice openings at center PSC slots, but it is difficult to imagine 500,000-700,000 fish passing over each 21-ft wide weir with an average water depth of about 2 ft.

Conservative estimates of PSC performance indicate that it was a highly used route in 2000. The PSC guided an estimated 18 percent of the total Bonneville Dam passage (guided, unguided, and spilled fish combined) in spring and 21 percent of the total detected passage in summer (Table 12). These proportions are conservative in that they do not allow for any increments of shallow PSC passage that were undetected by our method, although radio-telemetry studies, as mentioned above, indicate that approximately 50 percent of radio-tagged fish passed through the center sluices inside PSC units.

Table 12
Proportions of All Fish Passing by Different Turbine and Non-turbine Passage Routes at Powerhouse 1 in Spring and Summer

Season	Non-turbine Routes	Turbine Routes
Spring	23% (PSC 18%)	12%
Summer	27% (PSC 21%)	17%

Spatial Aspect of Fish Passage Metrics

Horizontal distribution

Horizontal passage patterns at Powerhouse 1 were consistent between seasons, but the relative discharge through the primary passage routes was generally a poor indicator of the relative proportion of fish passage among those same routes. More fish passed through PSC units than through three of the four units north of the pier between Units 6 and 7 despite a relatively even distribution of flow.

Vertical distribution

The vertical distribution of fish in front of the PSC at Powerhouse 1 was conducive for successful surface collection with a deep slot configuration. Sample volumes 1-3 m upstream of the PSC detected 92 to 99 percent of fish in spring and from 85 to 96 percent in summer fish above the elevation of the PSC floor.

Temporal Trends in Fish Passage

Higher fish passage through the PSC than through Units 7, 8, and 10 in spring and summer and higher nighttime densities upstream and downstream of PSC slots suggest that fish may be accumulating at PSC units when daylight conditions permit them to search for preferred passage routes. The loss of visual position cues likely is responsible for increased fish passage into turbines just after sunset because smolt passage at turbine units is not a function of increased flow there. During the daytime when fish could orient by visual cues, densities upstream of PSC slots and the proportion guided by the PSC were both significantly higher than they were at night. The depth distribution of fish and associated exposure to ambient light conditions apparently have a pronounced effect on the diel distribution of fish passage through the PSC (Figure 26), through turbines (Figure 27), and on the number of fish detected upstream of PSC entrances

(Figures 28 and 29). Whereas fish are aware of changes in their body acceleration via their otolith organs (reviewed extensively in Fay and Popper 1999), for relatively continuous motions and gradual accelerations, visual orientation is important. Mammals have irises that can rapidly adapt their eyes to lower light levels, but fish rely on the migration of sensory cells and masking chemicals in the retina, a process that takes much longer than mammalian adaptation.

The temporal correspondence of major peaks in the daily proportion of fish passage as determined by physical capture methods and by hydroacoustics was reassuring. Correspondence was found between hydroacoustic estimates of the peak daily proportion of fish passing Powerhouse 1 and the daily proportion of smolt sampled in the Powerhouse 2 JBS. Passage of juvenile salmon through the Powerhouse 1 JBS could not be used for comparison because sampling there was qualitative to determine descaling rates. Daily netting and hydroacoustic estimates of passage at Unit 8 were correlated.

There are two reasons why Powerhouse 1 FPE did not decline precipitously in summer as did the FGE of turbines with screens (Units 7-10). First, the efficiency of the PSC did not decline in summer and contributed more to Powerhouse 1 FPE in late spring and summer than it did most of spring (Figure 24). Second, the proportion of fish relative to the proportion of water passed was relatively constant in spring and summer at the PSC.

Perhaps the most significant finding of this study was the summer decline in FGE of turbines with screens while the efficiency of the PSC remained high and relatively stable (Figure 24). Even the efficiency of the ESBS in Unit 8 was as poor as that of STSs in other turbines in late summer. Two factors may contribute to the continued success of the PSC in summer. First, the interception location of the PSC was upstream of the powerhouse; second, the PSC was open to the sky and passed relatively more fish during the day than at night. In contrast, most fish passage through Powerhouse 1 turbines occurred at night. We assume that willingness of fish to enter a collector during the daytime would be greater when ambient lighting does not change abruptly at the entrance. The success of the PSC also probably has a lot to do with depth (45 ft), entrance velocities, and upstream hydraulics. The diel pattern of smolt passage through Powerhouse 2 turbines was more crepuscular in spring and summer than it was nocturnal. It has been speculated that the peak in fish passage through turbines around sunset results from passage of individuals that have lost visual cues and the ability to hold in the upper water column. The daytime-dominated passage at the PSC suggests that fish will readily enter the PSC during the day, whereas they generally resist passing into turbines during the day and end up passing more at sunset.

Assuming that the performance of each fish-guidance structure would be the same if every unit had only one type, a 22 and 42 percent increase would be projected in Powerhouse FPE in summer with a full PSC instead of ESBSs or STSs, respectively (Figure 40). In spring, a full-powerhouse PSC might be expected to provide a 22 percent increase in Powerhouse FPE relative to that provided by STSs, although similar benefits would be expected from ESBSs and a full powerhouse PSC.

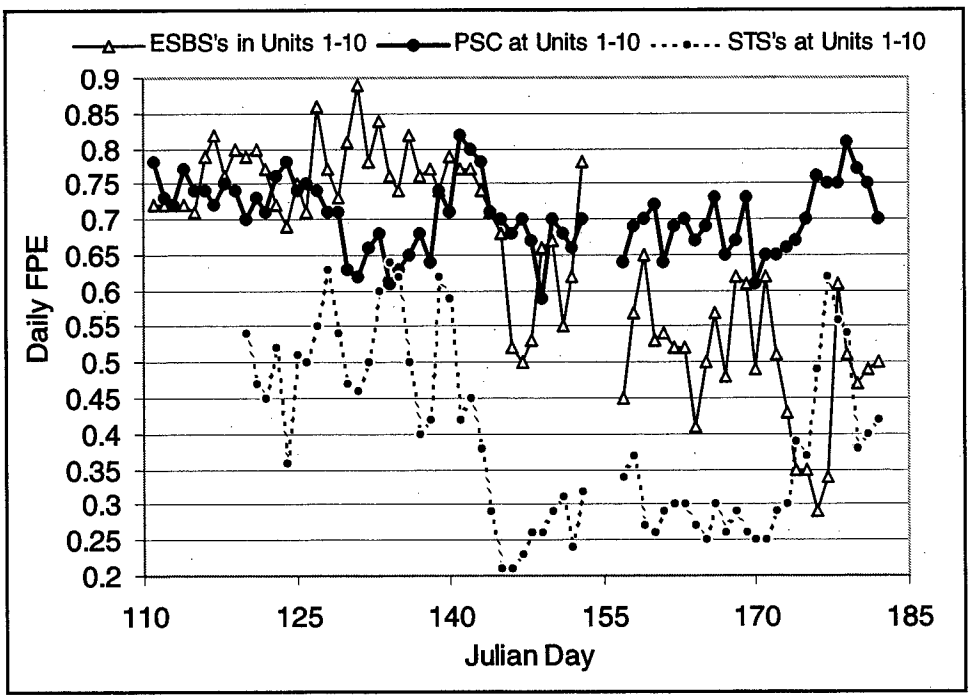

Figure 40. Temporal trends in Powerhouse 1 FPE assuming that all turbine units had only one type of fish guidance device and that the devices would be as efficient as the average efficiency observed for the respective devices in 2000

Fish Guidance Efficiencies

The most important contribution from this work on FGEs at Bonneville Dam is the high level of performance of Powerhouse 1's PSC, especially in summer. Summer passage has proven to be a serious challenge for smolt guidance at lower Columbia River dams, and sampling at Powerhouse 1 confirms that observation. The STSs performed worse than either the ESBS at Unit 8 or the PSC on Units 1-6 in spring. On Powerhouse 1 the PSC and the ESBS performed equally well in spring with estimated FGEs of 72 percent. The southernmost two units of the PSC performed best with FGEs of over 80 percent. In-turbine sampling shows that the PSC performed as well as the ESBS did in spring and much better than the ESBS or STSs in summer. In summer the average FGEs of STSs were 36 percent at Powerhouse 1 and the FGE of the ESBS in Unit 8 had dropped to 50 percent.

A large proportion of spring migrants and an even larger proportion of summer migrants passed south of the pier that extends upstream between Units 6 and 7, and most of those fish were guided by the PSC. So not only did the PSC have a higher efficiency than Units 7-10 in summer, but it also passed more fish.

Comparing FGE sampling methods for the PSC

No significant correlations were found between fish counts in turbine intakes downstream of the PSC with fish counts upstream of 20-ft wide PSC slots, unlike a significant correlation observed for a 5-ft wide slot in 1999. The most likely explanation for the differences is that the linear flow velocity at the 5-ft wide slot (5 fps) in 1999 was 39 percent higher than the velocity at the 20-ft wide slots in 2000 (3.5 fps). Given the wallowing of fish in split-beams immediately upstream of the 20-ft wide PSC slots, it seems logical that those fish were not committed to passing into the PSC and in fact may have been counted multiple times. By contrast, the probability of a fish in 5 fps flow passing into the PSC was likely significantly greater than it was for fish in the 3.5 fps flows observed in this study. If fish were not entrained or committed to passing into the 20-ft slot, they could be detected moving toward an entrance and still swim away after passing through the hydroacoustic beam. It is believed that differences in the probability of detected fish passing into the PSC may explain why significant correlations were found in 1999 but not in 2000. It also is possible that the model used to classify fish as passing into the PSC was not accurate. The acoustic screen model used to expand fish is best applied when the acoustic beams are between two structures or the flow through the beam is fast enough to preclude fish from being counted more than once.

Although counts from split-beam sampling upstream from the PSC were not correlated with the in-turbine single-beam counts, those data can still be used to evaluate the availability of fish for collection. Many more fish were found just upstream from the PSC face above the level of the PSC floor than below the level of the PSC floor in all hours of the day in summer. Expanded counts showed that there were twice as many fish above the level of the floor at night and an even higher proportion above the floor during the daytime hours. Even though the numbers of fish that actually entered the slots and passed through the PSC from those data cannot be confidently estimated, the data indicate that a large proportion of the fish were available to be collected by the PSC in summer.

By segregating range bins in forebay transducer beams, expanded estimates of fish abundance just upstream from the top halves and the bottom halves of the PSC slots were determined. During all hours of the day and particularly during daylight hours there were many more fish upstream of the top halves of the PSC slots than there were upstream of the bottom halves of the slots. Mobile hydroacoustics at Bonneville Dam (Ploskey et al. 1998; BioSonics Inc. 1998) have shown that upstream of the dam most fish are higher in the water column than screen FGEs would indicate. Current data suggest that, at the face of the surface collector, fish have not begun the descent that brings them under the screens and delivers them to the turbine intakes because the PSC intercepts fish before they are entrained.

Comparing FGE sampling methods for Unit 8

Netting and hydroacoustics both provide imperfect estimates of FGE because of gear and sampling limitations, and unexplained variability and bias adversely

affects the fit of correlations to these data. Nevertheless, comparison of sampling methods provides the opportunity to identify potential biases and highlights strengths and weaknesses of both methods. Bias cannot be measured with a single method and is, therefore, more insidious and difficult to quantify than sampling precision.

The correlation of hydroacoustic and netting estimates of FGE (r^2=0.65) was better than those for guided and unguided components of FGE because of compensating errors in the numerator and denominator of the ratio estimator during simultaneous hydroacoustic sampling of both FGE components. The assumption of equal detectability of guided and unguided smolts must have been reasonable most of the time given correlations between hydroacoustic and netting estimates of FGE with a correlation slope approaching 1. The near 1:1 ratio of numbers of guided fish netted in the gatewell to hydroacoustic counts above the ESBS and of numbers of unguided, fyke-netted fish to hydroacoustic counts below the ESBS was reassuring, despite substantial scatter in the correlation plots and r^2 = 0.53. The near 1:1 ratios for guided and unguided fish estimates by the two methods suggest that hydroacoustic detectability was not just equal but also relatively accurate, yielding appropriate expansion factors.

Many factors could contribute to scatter in the correlations, particularly when both the dependent and independent variables have error and potential bias associated with them. Both netting methods that were considered as a ground truth are less than 100 percent efficient, particularly for young salmon. Unless known numbers of fish were marked, introduced, and netted, the two types of nets were not calibrated and could have had different efficiencies. The assumption of equal net efficiencies may be incorrect and result in biased FGE estimates because the gatewell and turbine intake environments are dramatically different, as are the methods used to sample the two areas. Gessel et al. (1991) reported > 95 percent efficiency for gatewell dip-netting at Bonneville Dam. However, Steig and Ransom (1993) reported that many juvenile salmon guided by a bar screen at Rocky Reach Dam on the Columbia River were not sampled by a dip basket. They estimated that net-based FGE estimates would have more than doubled if net efficiency had been 100 percent. Fish also may remain in the gatewell slot before a test, may be lost through orifices during the test, or may be lost out the bottom of the gatewell during and particularly at the end of a test. Fish also may accumulate in an intake while the turbine is off and, depending upon their vertical distribution at startup, may bias estimates of numbers of guided or unguided fish.

Paired t-tests indicated that mean estimates of FGE by the two sampling methods did not differ significantly in spring, and although differences were significant for both seasons combined, means only differed by 3 percent and probably were biologically meaningless. In summer, the mean hydroacoustic estimate was 6 percent higher than the mean netting estimate, but even that difference is not too bothersome given problems encountered trying to exclude shad from the sample in summer.

Hydroacoustic sampling provides only a relative index to fish passage, unless correlated against unbiased physical capture estimates. However, significant correlations between hydroacoustic and netting estimates indicate that the

hydroacoustic data could be scaled by correlation coefficients to increase the accuracy of passage estimates. Ideally, nets would be calibrated to account for net efficiency bias. The significance of calibrating hydroacoustics to netting is that the nondestructive nature of hydroacoustic sampling permits it to be used much more extensively than netting.

Correlations between estimates of FGE derived from netting and hydroacoustic sampling are reassuring and useful because both methods have advantages that can be exploited to improve overall sampling effectiveness at a project. Netting can provide estimates of fish passage and guidance efficiency by species but is labor intensive, injures or kills fish, and cannot be used for more than a few hours per day at one or two intakes. This restriction to one or two intakes prevents biologists from evaluating spatial variation in fish passage and FGE among intakes. Hydroacoustic sampling can be applied to all turbine units, 24 h/day, without adversely affecting fish. However, hydroacoustic sampling cannot provide species-specific estimates without netting to determine species composition. If the goal is to determine the efficiency of many screens or other fish guidance structures during spring and summer runs, hydroacoustics can provide a meaningful index. Some netting should be required to calibrate hydroacoustic estimates, however, if FPEs are important or if species-specific estimates of FGE are desired.

Comparing PSC guidance efficiency by different methods

Average collection efficiency of the PSC was 83 percent in spring and 84 percent in summer after it was adjusted by radio-telemetry estimates of the proportion of smolts in the PSC that passed into the center-slot sluiceways, and the adjusted estimates agree favorably with estimates by other methods. Sluice gates in center slots of PSC Units 1-6 were open throughout spring and summer 2000 but could not be sampled with hydroacoustics. Nevertheless, radio-telemetry data indicated that approximately 50 percent of radio-tagged fish in the PSC passed through the sluiceway (Scott Evans, USGS, and Gary Johnson, BioAnalysts, Personal Communication). Therefore, hydroacoustic estimates of total passage at the PSC were at least 15 percent low in 2000. Radio-telemetry and acoustic-telemetry estimates of PSC efficiency for all species combined in spring 2000 were 83 and 92 percent, respectively (Johnson and Carlson 2000), and those estimates agree well with an 83-84 percent hydroacoustic estimate corrected for sluiceway passage. In 1998 hydroacoustic estimates of PSC collection efficiency for 20-ft slot openings in PSC Units 3 and 5 were 87.8 percent in spring and 92 percent in summer. A radio-telemetry estimate for 1998 was 97.5 percent for the 20-ft slot treatment. In 1999, hydroacoustic estimates for a 20-ft slot entrance at Unit 5 were 84.4 percent in spring and 75.2 percent in summer. Radio-telemetry studies in 1999 estimated 20-ft slot efficiency at 65 percent, the lowest of any estimates by any method (Johnson and Carlson 2000).

References

Bardy, D., Lindstrom, M., and Fechner, D. F. (1991). "Design of extended length submerged traveling screen and submerged bar screen fish guidance equipment." Pages 345-354 in *Proceedings of the Conference on Waterpower 91, Denver, Colorado*. American Society of Civil Engineers, New York, NY.

BioSonics, Incorporated. (1998). Hydroacoustic evaluation and studies at Bonneville Dam, Spring/Summer 1997. Contract Report to the U.S. Army Corps of Engineers District, Portland, OR.

Fay, R. R., and Popper, A. N., eds. (1999). *Comparative Hearing: Fish and Amphibians*. Springer-Verlag. New York, NY.

Gessel, M. H., Williams, J. G., Brege, D. A., and Krcma, R. F. (1991). "Juvenile salmonid guidance at the Bonneville Dam Second Powerhouse, Columbia River, 1983-1989." *North American Journal of Fisheries Management* 11:400-412.

Giorgi, A. E., and Stevenson, J. R. (1995). A review of biological investigations describing smolt passage behavior at Portland District Corps of Engineer Projects: implications in surface collection systems. Contract Report prepared by Don Chapman Consultants, Inc. for the U.S. Army Engineer District, Portland, OR.

Hawkes, L. A., Martinson, R. D., Absolon, R. F., and Killins, S. (1991). Monitoring of downstream salmon and steelhead at Federal hydroelectric facilities. Annual Report 1990 by the U.S. Dep. Commerce, NOAA, NMFS, ETSD, to the U.S. Dept. Energy, Bonneville Power Admin., Portland, OR.

Johnson, G. E., Johnson, R. L., Anglea, S. M., Abernathy, C. S., Blanton, S., Simmons, M., Kudera, E. A., Sullivan, C. M., and Skalski, J. R. (1998). Fixed location hydroacoustic evaluation of the prototype surface bypass and collector, spill efficiency, and fish guidance efficiency at Lower Granite Dam in spring and summer 1997. Final report submitted to U.S. Army Engineer District, Walla Walla, by the Pacific Northwest National Laboratory.

Johnson, L., and Schadt, T. (1986). Hydroacoustic evaluation of the fish guiding efficiency within turbine intakes, Contract Report, Parametrix, Incorporated, Bellevue, WA.

Johnson, L., Schadt, T., and Sullivan, R. (1987). Hydroacoustic evaluation of the fish guiding efficiency of submersible traveling screens at Little Goose Dam, Paper #58, International Symposium on Fisheries Hydroacoustics, Seattle, WA.

Johnson, G. E., and Carlson, T. J. (2000). Monitoring and evaluation of the prototype surface collector at Bonneville First Powerhouse in 2000: Synthesis of information on PSC Performance. U.S. Army Corps of Engineers Draft Report prepared by BioAnalysts, Inc. and Battelle.

Krcma, R. F., DeHart, D., Gessel, M., Long, C., and Sims, C. W. (1982). Evaluation of submersible traveling screens, passage of juvenile salmonids through the ice-trash sluiceway, and cycling of gatewell-orifice operations at the Bonneville first powerhouse, 1981. Final Report by the U.S. Dept. Commerce, NOAA, NMFS, Coastal Zone and Estuarine Studies Div. to the U.S. Army Engineer District, Portland, OR.

Love, R. H. (1977). "Target strength of an individual fish at any aspect." *Journal of the Acoustical Society of America* 62(6):1397-1403.

Magne, R., Stansell, R., and Nagy, W. (1989). A summary of hydroacoustic monitoring at the Bonneville Dam Second Powerhouse in 1988. U.S. Army Engineer District, Portland, OR.

Nestler, J., and Davidson, R. (1995). Imaging smolt behavior on an extended-length submerged traveling screen at The Dalles Dam in 1993. Technical Report EL-95-13 of the U.S. Army Engineer Waterways Experiment Station, Vicksburg, MS.

Ploskey, G. R., and Carlson, T. J. (1999). "Comparison of hydroacoustic and net estimates of fish guidance efficiency of an extended submersible bar screen at John Day Dam." *North American Journal of Fisheries Management* 19:1066-1079.

Ploskey, G. R., Johnson, P. N., Nagy, W. T., Burczinski, M. G., and Lawrence, L. R. (1998). Hydroacoustic evaluations of smolt passage at Bonneville Dam including surface collection simulations. U.S. Army Engineer Waterway Experiment Station Technical Report EL-98-4 prepared for the U.S. Army Engineer District, Portland, OR.

Raemhild, G., Steig, T., and Ransom, B. (1988). Hydroacoustic evaluation of juvenile salmon and steelhead movement past a bar screen deflector at Rock Island Dam Powerhouse No. 2 in 1988. Contract Report by hydroacoustic Technologies, Incorporated, Seattle, WA.

Ransom, B. H., Steig, T. W., and Nealson, P. A. (1996). "Comparison of hydroacoustic and net catch estimates of Pacific salmon smolt (*Onchorynchus* spp.) passage at hydropower dams in the Columbia River Basin, USA." *Journal of Marine Science* 53: 477-481.

Skalski, J. R., and Robson, D. S. (1992). *Techniques for wildlife investigations: Design and analysis of capture data.* Academic Press. San Diego, CA.

Stansell, R. J., Magne, R. A., Nagy, W. T., and Beck, L. M. (1990). Hydroacoustic monitoring of downstream migrant juvenile salmonids at Bonneville Dam, 1989. Fishery Field Unit, U.S. Army Engineer District, Portland, OR.

Steig, T. W. (1993). Hydroacoustic evaluation of juvenile salmon and steelhead approaching two bar screen deflectors at Rocky Reach Dam in 1992. Contract Report for Chelan County Public Utility District, Wenachee, WA, by Hydroacoustic Technology Incorporated, Seattle, WA.

Steig, T., and Ransom, B. (1989). Hydroacoustic evaluation of juvenile salmon and steelhead approaching a bar screen deflector at Rocky Reach Dam in 1989. Contract report by Hydroacoustic Technology Incorporated, Seattle, WA.

Steig, T. W., and Ransom, B. H. (1993). Long term hydroacoustic evaluations of a fixed in-turbine fish diversion screen at Rocky Reach Dam on the Columbia River, Washington. Pages 219-228 *in* Hall, D. W., ed., *Waterpower '93, Proceedings of the International Conference on Hydropower*, American Society of Civil Engineers, New York, NY.

Steig, T. W., and Nealson, P. A. (1994). Hydroacoustic evaluation of juvenile salmon and steelhead approaching a bar screen deflector at powerhouse No. 1 of Rock Island Dam in 1993. Contract Report for Chelan County Public Utility District, Wenachee, WA, by Hydroacoustic Technology Incorporated, Seattle, WA.

Steig, T., Raemhild, G., and Ransom, B. (1988). Hydroacoustic evaluation of juvenile salmon and steelhead approaching a submersible traveling screen at Rocky Reach Dam in 1988, Contract Report by Hydroacoustic Technology, Incorporated, Seattle, WA.

Steig, T. W., Iverson, T. K., and Adeniyi, R. (1995). Hydroacoustic evaluation of the behavior of juvenile salmon and steelhead approaching the powerhouse in the forebay of Rocky Reach Dam during 1994. Contract Report for Chelan County Public Utility District, Wenachee, WA, by Hydroacoustic Technology Incorporated, Seattle, WA.

Swan, G. A., Krcma, R. F., and Farr, W. E. (1979). "Dip basket for collecting juvenile salmon and trout in gatewells at hydroelectric dam." *Progressive Fish-Culturist* 41:48-49.

Thorne, R., and Kuehl, S. (1989). Evaluation of hydroacoustic techniques for assessment of juvenile fish passage at Bonneville Powerhouse I. Contract Report for the U.S. Army Engineer District, Portland, by BioSonics Incorporated, Seattle, WA.

Thorne, R., and Kuehl, S. (1990). Hydroacoustic evaluation of fish behavioral response to fixed bar screens at Lower Granite Dam in 1989. Contract Report for the U.S. Army Engineer District, Walla Walla, by BioSonics Incorporated, Seattle, WA.

Uremovich, B. L., Cramer, S. P., Willis, C. F., and Junge, C. O. (1980). Passage of juvenile salmonids through the ice-trash sluiceway and squawfish predation at Bonneville Dam, 1980. Oregon Dep. Fish. Wildl. Annual progress report prepared for the U.S. Army Engineer District, Portland, OR.

Willis, C. F., and Uremovich, B. L. (1981). Evaluation of the ice and trash sluiceway at Bonneville Dam as a bypass system for juvenile salmonids, 1981. Oregon Dept. Fish. Wildl. Annual progress report prepared for the U.S. Army Engineer District, Portland, OR.

Wood, L. A., Martinson, R. D., Graves, R. J., Carroll, D. R., and Killins, S. D. (1994). Monitoring of downstream salmon and steelhead at Federal hydroelectric facilities. Annual Report 1993 by the U.S. Dept. Commerce, NOAA, NMFS, ETSD to the U.S. Dept. Energy, Bonneville Power Admin., Portland, OR.

REPORT DOCUMENTATION PAGE

Form Approved
OMB No. 0704-0188

1. REPORT DATE *(DD-MM-YYYY)*	2. REPORT TYPE	3. DATES COVERED *(From - To)*
July 2002	Final report	

4. TITLE AND SUBTITLE

Hydroacoustic Evaluation of a Prototype Surface Collector and In-Turbine Screens at Bonneville Dam Powerhouse 1 in 2000

5a. CONTRACT NUMBER

5b. GRANT NUMBER

5c. PROGRAM ELEMENT NUMBER

6. AUTHOR(S)

Gene R. Ploskey, Carl R. Schilt, Michael E. Hanks, John R. Skalski, William T. Nagy, Peter N. Johnson, Deborah S. Patterson, Jina Kim, and Larry R. Lawrence

5d. PROJECT NUMBER

5e. TASK NUMBER

5f. WORK UNIT NUMBER

7. PERFORMING ORGANIZATION NAME(S) AND ADDRESS(ES)

See reverse.

8. PERFORMING ORGANIZATION REPORT NUMBER

ERDC/EL TR-02-15

9. SPONSORING / MONITORING AGENCY NAME(S) AND ADDRESS(ES)

U.S. Army Engineer District, Portland
Portland, OR 97208-2946

10. SPONSOR/MONITOR'S ACRONYM(S)

CENWP

11. SPONSOR/MONITOR'S REPORT NUMBER(S)

12. DISTRIBUTION / AVAILABILITY STATEMENT

Approved for public release; distribution is unlimited.

13. SUPPLEMENTARY NOTES

14. ABSTRACT

This study was one of many investigations of the U.S. Army Engineer District, Portland, to resolve critical uncertainties in the implementation of surface-collector technologies at Bonneville Dam. This research tested the efficiency of a six-unit version of the Prototype Surface Collector (PSC) and implementation of extended-length submersible bar screens at the dam's Powerhouse 1.

The PSC slot configuration for 2000 consisted of a constant 20-ft-wide slot width for all six PSC units. The primary effects evaluated were weekly changes throughout spring and summer in a variety of juvenile fish passage measures, including numbers passing into and under the PSC, efficiency, effectiveness, diel patterns, and horizontal and vertical patterns of distribution. Detailed statistical methods are presented.

15. SUBJECT TERMS

Bonneville Dam
Fish detection – Columbia River
Fish habitat improvement
Fishways
Underwater acoustics

16. SECURITY CLASSIFICATION OF:			17. LIMITATION OF ABSTRACT	18. NUMBER OF PAGES	19a. NAME OF RESPONSIBLE PERSON
a. REPORT	b. ABSTRACT	c. THIS PAGE			19b. TELEPHONE NUMBER *(include area code)*
UNCLASSIFIED	UNCLASSIFIED	UNCLASSIFIED		99	

9. (CONTINUED).

Pacific Northwest National Laboratory
902 Battelle Boulevard
Richland, WA 99352

Mevatec Corporation
1525 Perimeter Parkway
Huntsville, AL 35806

U.S. Army Engineer District, Portland
P.O. Box 2946
Portland, OR 97208-2946

DynTel Corporation
3530 Manor Drive, Suite 4
Vicksburg, MS 39180

U.S. Army Engineer Research and Development Center
Environmental Laboratory
3909 Halls Ferry Road
Vicksburg, MS 39180-6199